GEOCHEMISTRY

OF SELECTED ALKALINE GRANITES

A Thesis Submitted in conformity with
the requirements for the degree of

MASTER OF SCIENCE

By

© ABDEL-FATTAH MOSTAFA ABDEL-RAHMAN

in the

Department of Geology
UNIVERSITY OF TORONTO

1982

Acknowledgements

The author is deeply indebted to Prof. J. C. Rucklidge and Prof. J. Gittins, Department of Geology, University of Toronto for kind supervision and critical reading of the manuscript.

I would like to express thanks to Prof. M. Gorton for his encouragement in the course of the present work.

Dr. Sarah J. Barnes and Drs. R. Hancock and C. Cermignani were helpful in the aspects of neutron activation and microprobe analytical techniques.

The financial support from Prof. J.C. Rucklidge is deeply appreciated.

TABLE OF CONTENTS

		Page
CHAPTER I:	Introduction and Previous Work	1
II:	Geological Setting and Field Observations	8
A.	The Deloro pluton	8
B.	The Abu-Kharif Granitic Complex	16
CHAPTER III:	Petrography of the Granitic Rocks	29
a.	Petrography of the Abu-Kharif Granites	29
b.	Petrography of the Deloro Granites	40
CHAPTER IV:	Petrochemistry and Geochemistry of The Abu-Kharif and Deloro Granitic Rocks	61
-	Analytical Techniques	63
-	Petrochemistry	67
-	Geochemistry	86
	a. Major Elements	86
	b. Trace Elements	91
	c. Petrogenesis of the Granitic Rocks	120
CHAPTER V:	Geochemistry of the Abu-Kharif and Deloro Mafic Minerals	124
1.	Biotite	129
2.	Amphibole	136
3.	Alkali Amphibole	142
CHAPTER VI:	Summary and Conclusions	162
REFERENCES	.....	172

CHAPTER I

INTRODUCTION AND PREVIOUS WORK

CHAPTER I

INTRODUCTION AND PREVIOUS WORK

The present work has been performed on the petrochemistry and geochemistry of two granitic plutons emplaced in two different shields. The Deloro pluton is one of the many granitic bodies in the Grenville structural province of Ontario, Canada. The Abu-Kharif complex occurs in the Central, Eastern Desert of Egypt, which is a part of the Arabian Nubian Shield (see the location maps figures I.1 and I.2). The emplacement of Deloro pluton, along with its petrographic and mineralogical characteristics have been described in some detail by Saha (1957, 1959). Kuehnbaum (1973) studied the crystallization history of that granitic body. The geology of the Abu-Kharif complex have been thoroughly studied by Abdel-Rahman in 1979. The geochemistry of the different granitic phases of both plutons is the goal of the present study.

The Deloro pluton covers an area of about 35 sq. km. in Marmora and Madoc township, Hastings County (Fig. I.1). The pluton lies near the southern fringe of the Canadian Shield. It is composite, made up of a north-south elongated body of riebeckite granite and calcic syenite-granite (about 10.5 km. long, 3.5 km. wide), with an ESE trending projection, and an oval shaped body of granophyric granite, covering about 7 sq. km., in the eastern part of the pluton, (Kuehnbaum, 1973). The Abu-Kharif granitic complex covers

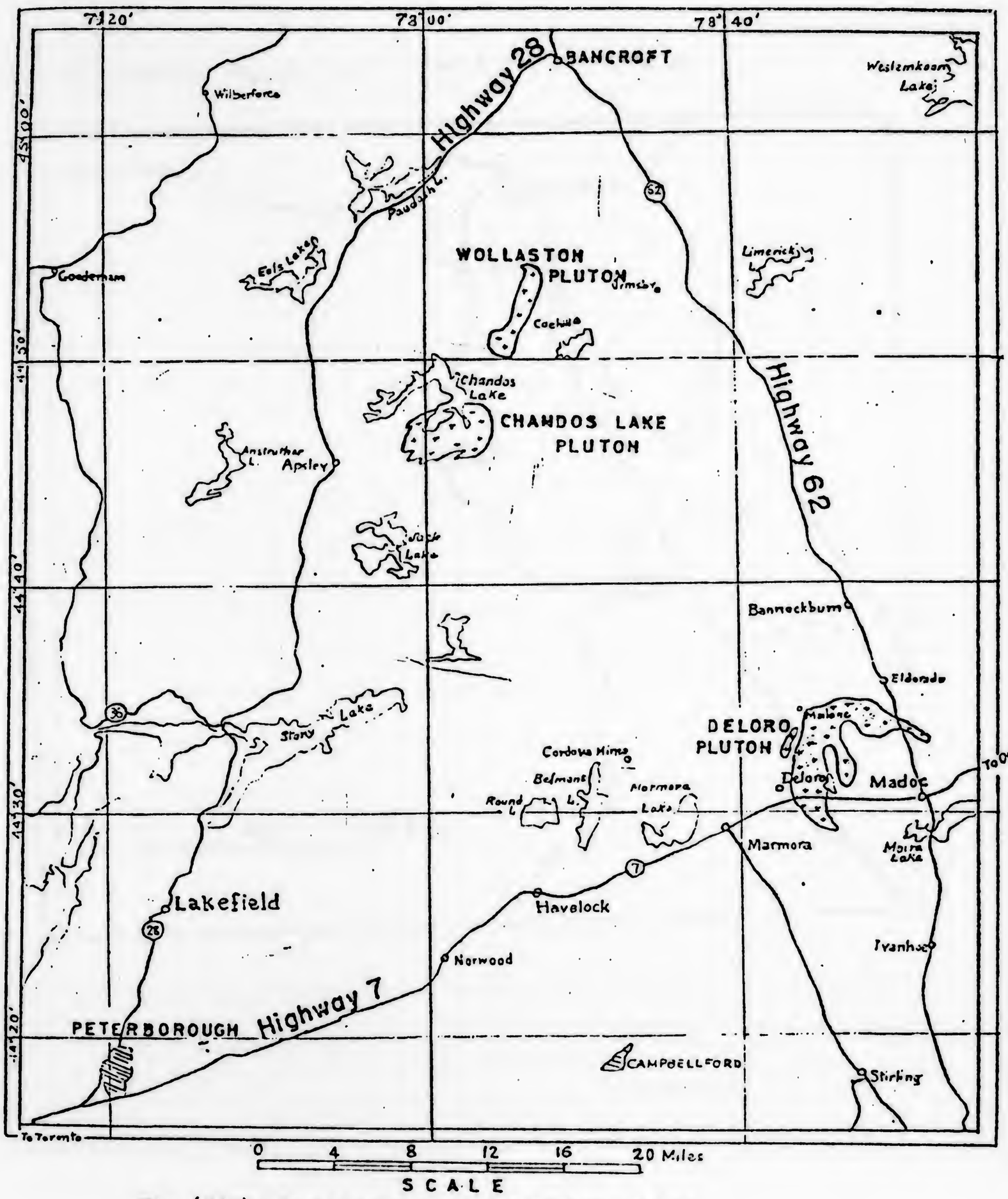

Fig.(I.1); Location map of the Deloro pluton

Fig.(I.2); Location map of the Abu-Kharif granitic complex

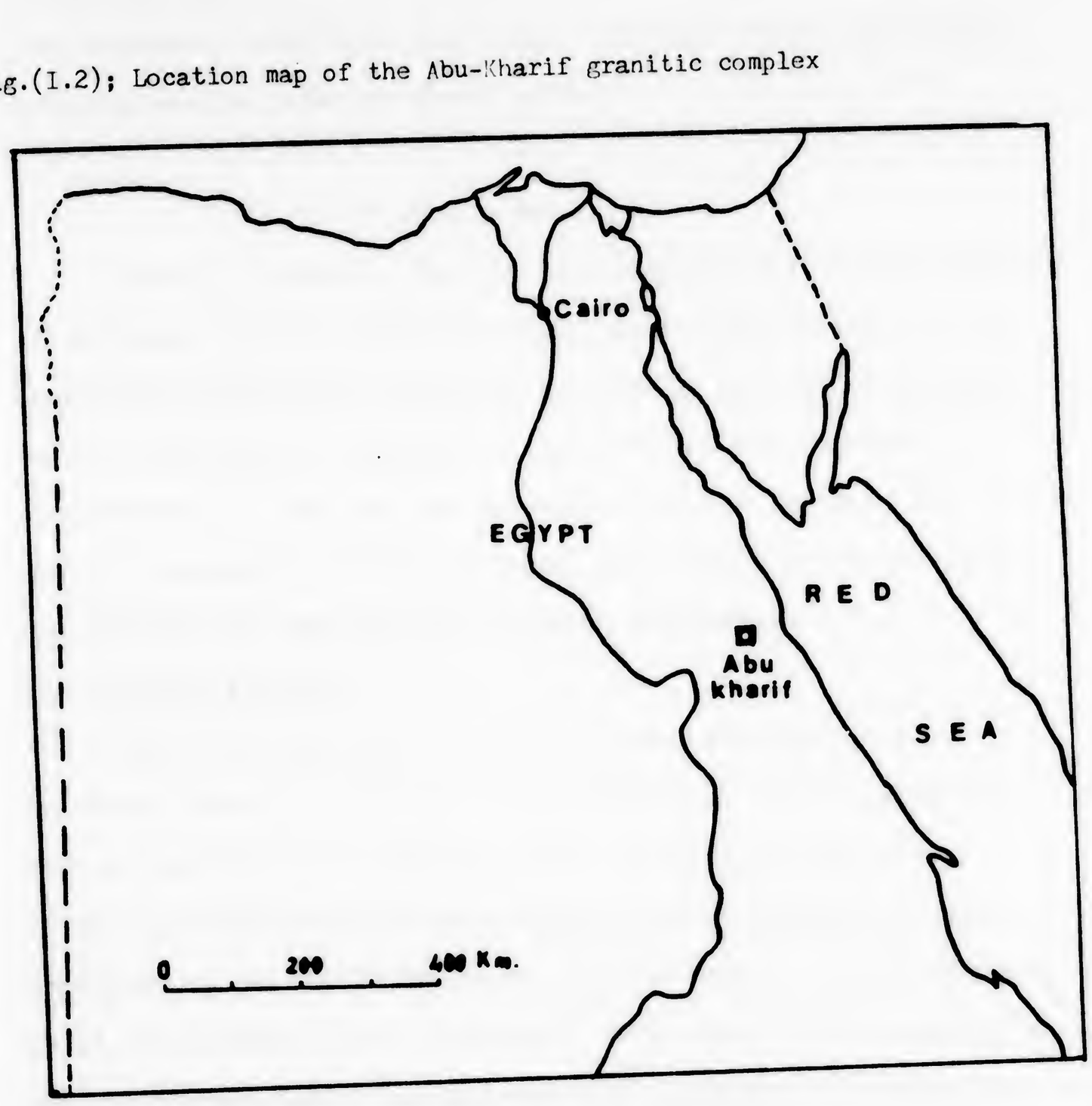

some 150 sq. km. near the port Safaga on the Red Sea. The Abu-Kharif granitic rocks are represented by syntectonic granodiorites, late-tectonic calcalkaline granites and post-tectonic alkaline granites. Several dykes and quartz veins traverse some of these rocks.

Previous Work

Fairly intensive geological mapping and investigations of economic mineral deposits have been carried out in the Granville structural province including the Deloro pluton. In the Abu-Kharif complex, a few workers had previously contributed to the geology of the granitic rocks. The following is a summary of the previous work carried out in both the Deloro and Abu-Kharif granitic complexes.

(1) Deloro Pluton:

The granitic bodies of the Grenville structural province have not received much attention until recently. Deloro granites and syenites were recognized by Wilson (1940) as being distinctive among similar bodies in the surrounding Grenville terrain, and he mapped them accordingly as a separate unit. Tuttle (1952) described a sample of Deloro granite as a typical perthite granite in which no recrystallization has taken place. Bown (1958) used feldspars from the "Madoc" granite to exemplify their hypersolvus types. The Ontario Department of Mines published, (1957)a, a compilation geological map of the Haliburton-Bancroft region on the scale 1(inch)= 2 miles.

Saha (1957) studied in some detail the mode of emplacement of the Deloro pluton and other granitic plutons in South-East Ontario. Saha (1957) concluded that the Deloro pluton was emplaced in two distinct stages:

a) An earlier, forceful intrusion of perthite granite, which grades to syenite to the western border due to assimilation of the gabbro-diabase country rocks.

b) An intrusion of more sodic and less mafic granophyric granite.

Recently, Kuehnbaum (1973) concluded that the sequence of emplacement was as follows: intrusion of gabbroic rocks, intrusion and fractionation in situ of the calcic suite (calcic syenite-granite), diapiric intrusion of the relatively dry peralkaline magma and finally the high level intrusion of granophyric granites.

2) Abu-Kharif complex:

The granitic rocks of Abu-Kharif complex, Red Sea hills of Egypt, were first recognized by Hume (1935), who stated that Gabel Abu-Kharif is composed of quartz diorite and coarse granite. He classified it among his coarse red Gattarian granites of the late precambrian. Schurman (1966) splits the Gattarian granites into two parts, separated by the Hammamat formation. He groups the riebeckite granites (never observed as boulders in Hammamat), collectively with part of the red pegmaticic granites, to the post Hammamat Gattarian granites. According to Schürman, these granites are traversed by the post granitic dikes. The Abu-Kharif

granitic complex is shown in the regional geological map of the basement complex of Egypt by El-Ramly (1972) as being formed of syntectonic to late-tectonic granites.

Zalata (1972) considered the alkaline riebeckite-granites collectively with other granitic rocks as late and post orogenic granites. All these granitic rocks were considered to be traversed by post-granitic dykes (see Abdel-Rahman 1979). Sabet et al. (1972) split the late and post orogenic granites of Zalata (1972) into three phases represented by adamellites, granites and alkaline-granites. He considered the so-called post-granitic dykes as representing the youngest Precambrian magmatization.

Recently, Abdel-Rahman (1979) has observed that the post-tectonic alkaline granites are not traversed by any kind of dykes, despite the fact that, they are forcefully intrude the so-called post granitic dykes.

These observations suggest that the different granitic phases of Abu-Kharif complex should be reclassified.

Purpose of Study

The main purposes of this study can be summarized in the following points:

(1) To study the petrochemistry of Deloro granitic rocks (an example from the Canadian Shield) in comparison to the Abu-Kharif granites (belonging to the Nubian-Arabian Shield).

(2) To determine the geochemical characteristics - both Major and Trace Elemenets including Rare Earth Elements - of the Abu-Kharif granitic rocks as well as of Deloro granites.

(3) To estimate the serial character (the presence of one or more granitic seris) within each granitic complex.

(4) To study the geochemistry of the mineral phases with special emphasis on the alkali amphiboles.

(5) To estimate the petrographic characters in each granitic phase.

(6) To use the geochemical data supported by the field observations in order to evaluate the possible genetic hypotheses relating to the rocks studied.

CHAPTER II

GEOLOGICAL SETTING AND FIELD OBSERVATIONS

CHAPTER II

GEOLOGICAL SETTING AND FIELD OBSERVATIONS

(a) Deloro Pluton

The Deloro pluton is one of the numerous granitic bodies in the southernmost exposed part of the Grenville Structural Province of the Canadian Shield. It is situated roughly between Madoc and Marmora, Ontario, Canada (Fig.I.1). Geologic mapping carried out by the Geological Survey of Canada and by Saha (1957) indicates that Deloro pluton is dominantly covered by gabbroic or dioritic rocks - commonly distributed on the west part of the body -, calcic syenite-granites, peralkaline riebeckite-bearing granites (formerly called "perthite granites" by Saha (1957), and granophyric granites (see the geologic map, Fig. II.1). Riebeckite bearing xenoliths of mafic syenitic and gabbroic (diabasic) material were recorded (Fig. II.2). Saha (1957) concluded that the granitic and syenitic rocks of the pluton are extremely massive, with the only macroscopic linear element being the occasional "parallel arrangement of small clots of inclusion". Metavolcanic dykes as well as thin riebeckite-bearing dykes were observed intruding the previous rock units (Fig. II.3). An elliptical, predominant, western portion and an easterly extending arm give a crescentic outline to the body (Kuehnbaum, 1973). Saha described that this body could not be regarded either as a cone-sheet or as a ring-dyke. Several workers have studied the tectonic aspects of

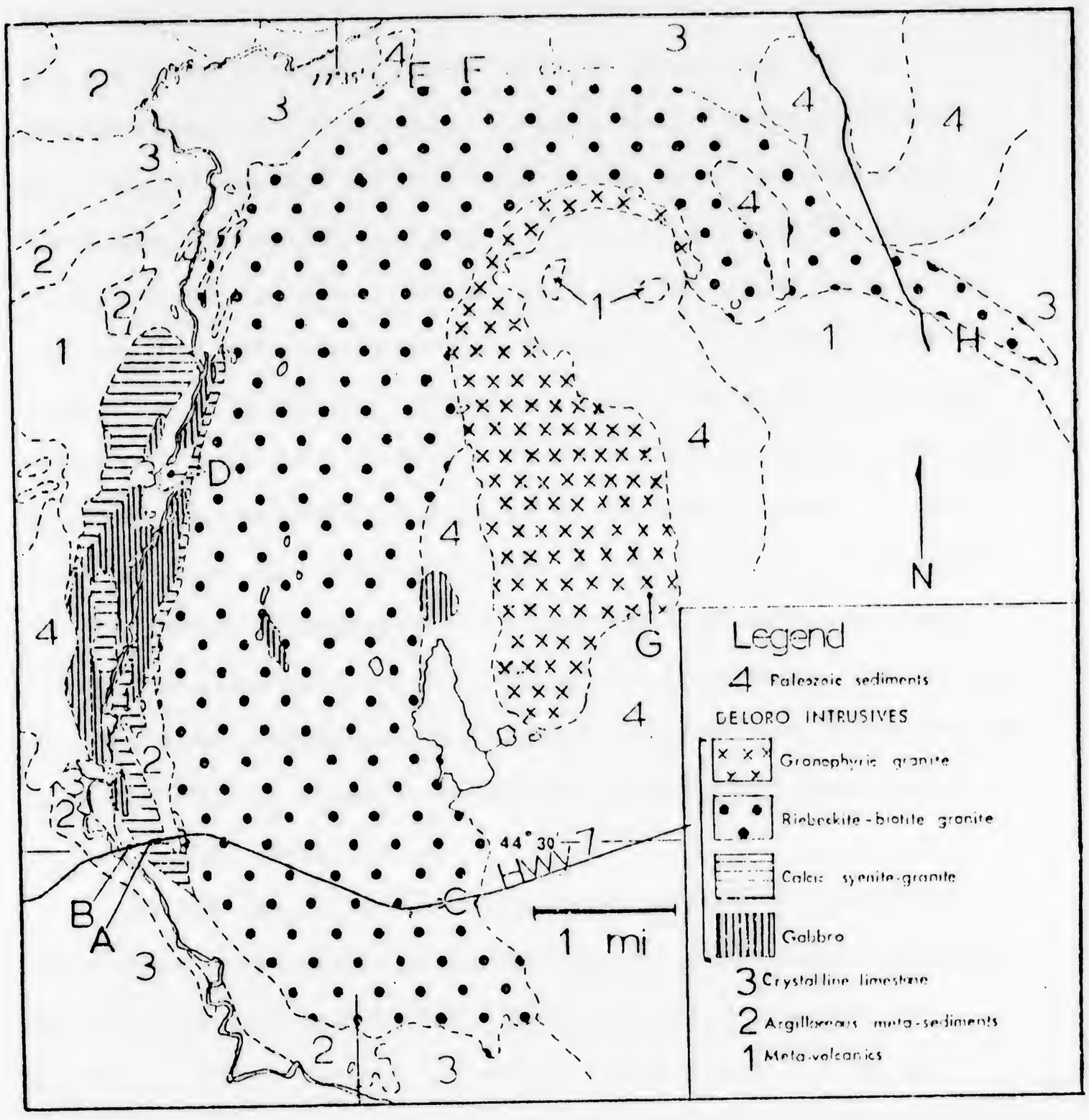

Fig.(II.1); Generalized map of the Deloro Pluton showing distribution of the major intrusive phases and country rocks. Letters indicate localities discussed in text. Units are modified from Wilson (1940), Saha (1957) and Hewitt (1968).

emplacement of the crescentic shaped granitic complexes in the Archean of Ontario. Between them, they concluded that the numerous crescentic granitoid plutons ranging in composition from diorite to granite were injected between dome-shaped, second-order diapirs and their supracrustal envelopes (Schwerdtner et al. 1979). The granitic complex of the Deloro pluton intrudes in a conformable fashion the surrounding metasediments and metavolcanic rocks of the Grenville Precambrian. Lumbers (1967) has dated the later suite of rocks as 1,350m.y. In 1979, Fyson et al. (in their study of the regional deformation and emplacement of granitoid plutons) had reach the conclusion that the development of flat-lying structures near granitoid plutons has been linked to modifications in regional strain above the bodies as they rose during two main phases of regional deformation. Such flat-lying structures are well-developed near the Deloro pluton (Fig. II.4).

As the peralkaline reibeckite granite is injected by thin veins and irregular injections of granophyric granite, Saha (1957) concluded that the granophyric granite is definitly the youngest granitic phase. The latter is generally finer grained towards the contact of the riebeckite-granite and tends to become coarser inwards from the contact. Saha in his study had considered that both the riebeckite-granite and the calcic syenite-granite were formed as a result of an earlier forceful intrusion of perthite granite which grades to syenite in the western border due to assimilation of the gabbroic rocks. In 1973, Kuehnbaum observed

Fig.(11.2); Fine grained, riebeckite-bearing xenoliths in peralkaline riebeckite granite of the Deloro pluton.

Fig.(II.3); Riebeckite-rich dykelet cutting the peralkaline riebeckite granite, Deloro pluton.

Fig.(II.4); The Unconformity where the paleozoic sediments overlie the Deloro granitic rocks. (Looking North, Hwy 7 roadcut).

that the contact relations between the riebeckite-granite and the calcic syenite-granite suite are obscured, he added, nowhere were there found to be dykes of either rock intersecting the other.

At the contact between the peralkaline riebeckite granite and the calcic syenite-granite (along Hwy. 7 roadcut), we observed that a three meter wide riebeckite granitic dyke cuts the calcic syenite granites. This observation leads to the conclusion that the riebeckite granitic phase represents a later episode. It seems also that the origin of the calcic syenite-granites are much more complex than the hypothesis of hybridization or assimilation of gabbroic rocks, suggested by Saha (1957, 1959) to explain their evolution. Meanwhile, Kuehnbaum (1973) mentioned that syenites are observed in contact with marbles where gabbroic rocks are entirely lacking.

The granitic rocks in the examined area show three types of joints; (i) vertical or steeply inclined joints, (ii) sheet or horizontal and (iii) oblique ones (Fig. II.5a, b and c). Red coloration in the riebeckite granites as well as in calcic syenite-granites is occasionally observed along joint planes.

Based on field observations, and as observed by Kuehnbaum (1973), the granitic rocks of the Deloro pluton are thought to be emplaced as follows:

(1) Intrusion and fractionation <u>in situ</u> of calcic syenite-granite, syenite complex.

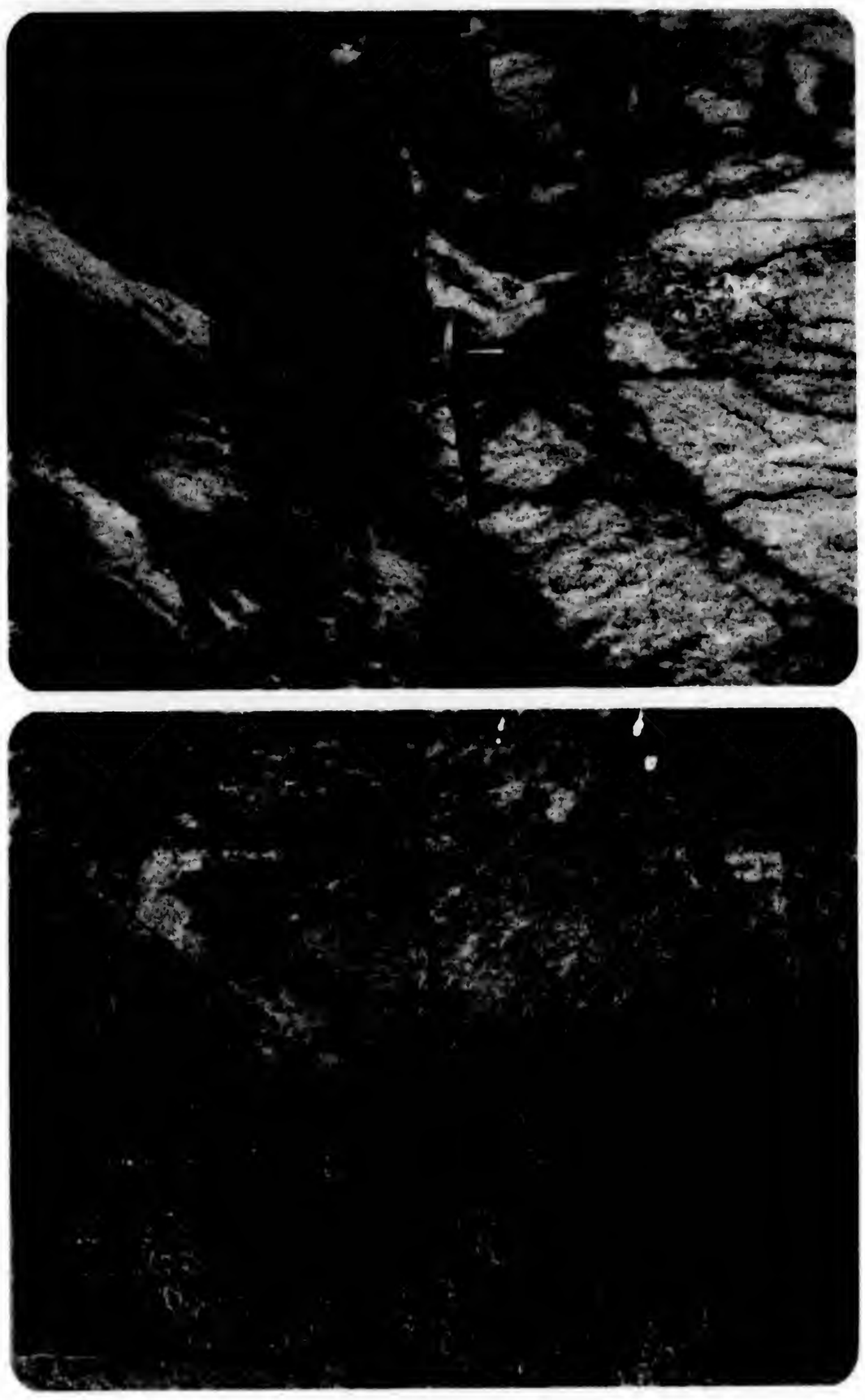

Fig.(II.5); (a) Oblique joint set in the Deloro granites.

(b) Vertical and horizontal master jointing in the Deloro peralkaline riebeckite granites. (Scale 1 :50)

Fig.(II.5c); Cross joints in the Deloro granites. (Looking North, Hwy 7 roadcut, scale 1 : 50).

(2) Intrusion of the riebeckite granite

(3) High level intrusion of water rich, less femic, granitic liquid forming the granophyric granites.

(b) Abu-Kharif granitic complex:

The detailed geological mapping (scale, 1:40,000), and field observations of Abu-Kharif granites carried out by Abdel-Rahman (1979) shows that the complex consists of syntectonic grey granites, late tectonic calc-alkaline granites and post tectonic alkaline granites. Metavolcanics as well as diorites are also mapped in the northern-eastern side of the examined area (Fig. II.6). The majority of these rocks are traversed by several dykes of basic, intermediate and acidic nature. The detailed field study reveals that the metavolcanics and diorites are intruded by the syntectonic grey-granites, of which several offshoots are also recorded within the diorite suite. The contacts between the low lying country rock, which is grey-granite and the moderately elevated pink granites are sharp and marked by intrusions of the pink into the grey. Both the grey granites and the calc-alkaline pink granites are traversed by numerous dykes where the alkaline granites intrude and represent the last manifestation of igneous activity in the area.

A brief summary of the three main granitic phases at Abu-Kharif complex is given below:-

Syntectonic grey-granites

The grey granites are composed essentially of plagioclase and quartz with subordinate amounts of alkali feldspars,

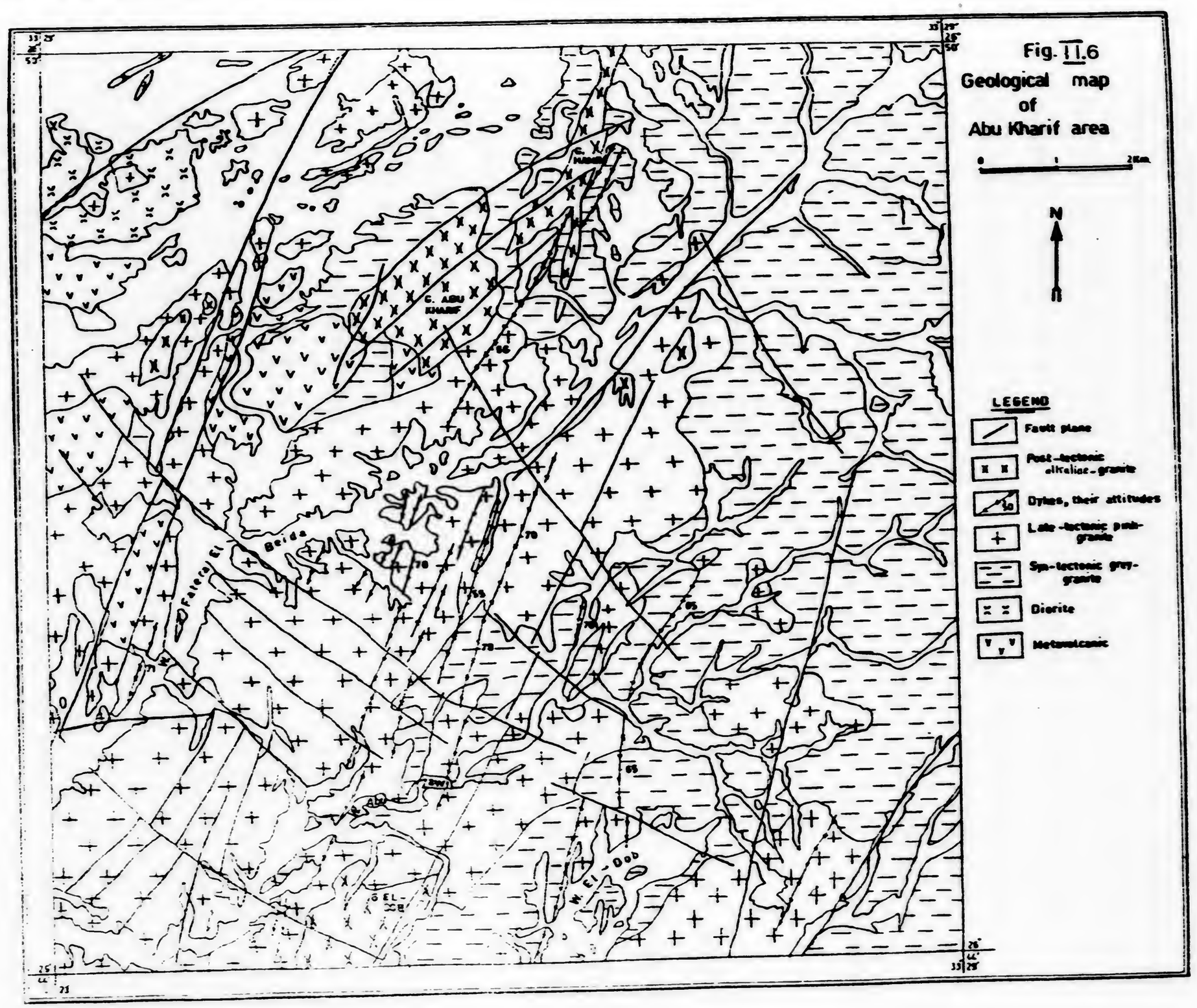
Fig. II.6
Geological map
of
Abu Kharif area
N
LEGEND
Fault plane
Post-tectonic alkaline-granite
Dykes, their attitudes
Late-tectonic peth-granite
Syn-tectonic gran-granite
Diorite
Metavolcanic

while biotite and hornblende are the predominant mafic minerals. Grey granites include several varieties exhibiting several colours such as pinkish-white, buff and grey. These varieties do not form mappable units. Red colouration in the grey granites is frequently observed along fracture planes. Abdel-Maksoud et al. (1979) concluded that the grey granites show sharp and intrusive contact with the metavolcanics which are occasionally caught up as xenoliths. They also intrude the diorites with several offshoots of granite in the diorite belt. The grey granites are intruded by the pink granites with markedly sharp contact.

Late tectonic pink-granites

Pink-granites form a moderately elevated country and exhibit a pink colour on the fresh surfaces, while a yellowish pink colour is usually seen on the weathered surfaces. Block type of weathering (Fig. II.7) is predominantly with the mass of pink granites. They are composed essentially of alkali feldspars, quartz with subordinate plagioclase, while biotite is the frequently recorded mafic mineral. The pink granites intrude the grey granites as well as diorites with sharp intrusive contacts. Several offshoots of pink granites are recorded in the grey granites (Fig.II.8). Numerous dykes are also recorded intersecting the pink granites.

Dykes

Basic, acidic and alkaline type of dykes include varieties such as andesites, dolerites, quartz, porphyries,

Fig.(II.7); Block weathering in the Abu-Kharif pink granites (Looking N.)

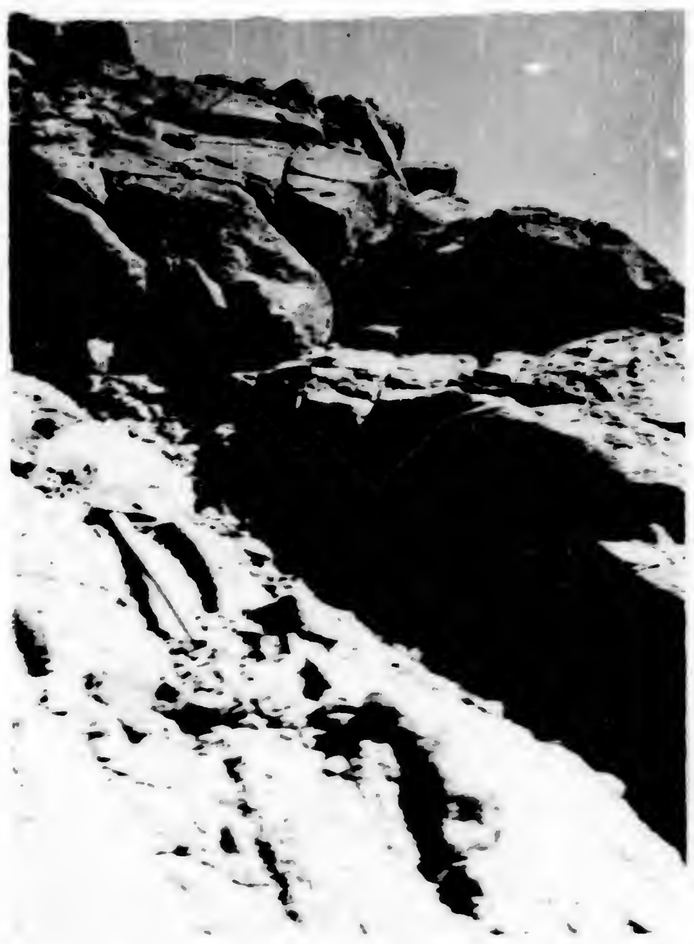

Fig.(II.8); Sharp contact between pink granite (P) and granodiorite (G)
(Looking NE).

bostonites and trachytes are recorded and cut all the previously mentioned country rocks (Fig. II.9). Chronologically, they are equivalent to the so-called post-granitic dykes frequently observed intruding the late tectonic pink granites in the basement complex of Egypt. Since the term post-granitic dykes was first developed by Amin, et al. (1953), all the workers on the basement complex of Egypt considered those dykes as being the youngest phase of igneous activity in the Egyptian basement complex (see for example Akaad 1966, and Sabet 1972, in their classification of the basement rocks of Egypt, tables II.1, and II.2). Field studies on Abu-Kharif area by Abdel-Rahman (1979) indicate that the alkaline granites, which form the highest peak of the area, forcefully intrude the dykes (Fig. II.10). The intensive upward movement of this major granitic mass causes the strike of a three meter thick doleritic dyke to change from N40E to N20W (Fig. II.11). That observation indicates, that the dykes are chronologically located between the late tectonic pink granites and the still younger alkaline granites. Accordingly, they cannot be regarded as post-granitic according to the popular model. Abdel Maksood et al.(1979) concluded that the traditional term "post-granitic" for dykes that traverse the late tectonic pink granites of the Eastern Desert, should be modified as the occurrence of a still younger period of granitic activity is now well established.

Fig.(II.9); A doleritic dyke (D) intruding the pink granite (P) and the quartz-porphry dyke (Q). Note that faulting in pink granite is evidenced by the displacement of a quartz-porphry dyke (Q) (Looking South, The Abu-Kharif complex).

Fig.(II.10); The alkaline granite forcefully intrude the dyke (D).
(Looking NW, Abu-Kharif complex).

Fig.(IIII); General view for a dyke intruded by the Abu-Kharif alkaline granite. Note the change in the strike of the dyke.

Post tectonic alkaline granites

The alkaline granite which form three main elongated masses aligned in a NE-SW direction contains the highest peaks of the area (about 1327m. high). They are hard, massive and pale yellowish white in colour. In hand specimen, the predominant mafic mineral, alkali amphibole, exhibits a characteristic blackish colour. The alkaline granites intrude both all the previously described rocks. Abdel-Rahman (1979) described that, to the north and south of the examined area they intrude both the grey-granites and the pink-granites (Fig. II.12), (where contacts are intrusive with several offshoots of the alkaline granites). They also intrude the dykes. This latter observation leads to the conclusion that the alkaline granites should be considered as the last manifestation of igneous activity in the Abu-Kharif area. They represent a separate granitic phase erupted after the intrusion of the dykes. The geo-chronological correlation of Abu-Kharif rocks, related to the other classifications of the basement rocks of Egypt, is represented at table (II.3). In general, Abu-Kharif granitic rocks are traversed by several strike slip faults. Faulting is evident by displacement of dykes, (see Fig. II.9), occurrence of shear zones as well as by the presence of slickensided surfaces, frequently observed on the fault planes.

Several authors relate the structural trends in the basement complex to those developed in the Red Sea graben. Based on linear analysis, Sabet (1961), El Etr et al. (1973) and Morcos (1977), distinguished several trends, which are correlated with the trends of the Red Sea graben. The rocks representing the alkaline granitic phase are traversed by faults formed, most probably, during the formation of the Red Sea graben. Consequently, from a stratigraphic point of view, this phase was considered as pre-rifting (Abdel-Maksood et al. (1979). Three types of joints, cross or vertical, sheet or horizontal, and conjugate or oblique have been observed in the granitic rocks. The first two groups resulted during the thermal modifications of the granitic masses, (Fig. II.13) while conjugate joints are formed comtemporaneously with faulting.

Fig.(II.12); The alkaline granite (A) intruding low land, highly weathered granodiorite (G). (Looking S, the Abu-Kharif area).

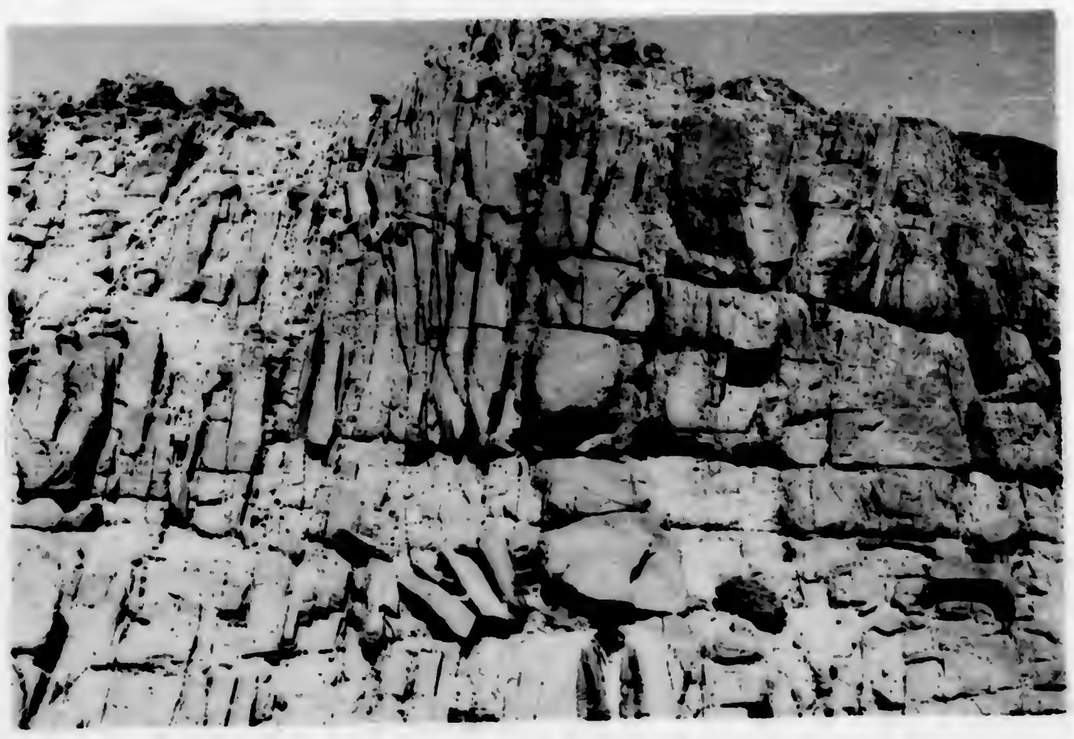

Fig.(II.13); Vertical and horizontal minor jointing in the Abu-Kharif calc-alkaline granite. (Looking W., scale, 1: 80).

Principal events		Rock units
Explosive volcanism of trachytic lavas		Trachyte plugs and breccias
Regional normal faulting		
Transgressive deposition of quartzose sandstones on stable shelf		Nubia sandstone
Prolonged quiescence, erosion and peneplanation		Regional unconformity
Intrusion of felsite bodies, sheets, plugs and breccia (field relations with Younger Granites uncertain)		Post-Hammamat felsites
Intrusion of acidic, minor alkaline and lamprophyre dykes in and around granite plutons		Post-granite dykes
Emplacement of granite plutons during later orogenic movements, effecting the folding and faulting of the Hammamat Group and older units		Younger Granites (Umm Hombos and Umm Had plutons)
Deposition of bedded dark grey greywackes	Hammamat Group	2. Shihimiya Formation (c) Umm Hassa Greywacke Member (b) Umm Had Conglomerate Member
Deposition of coarse conglomerate derived from all older rock units and reworked Igla Formation		
Uplift in source area		
Deposition of green-grey siltstones, minor subgreywacke and conglomerate		(a) Rasafa Siltstone Member
Deposition of purple haematitic siltstone, subgreywacke, minor arenite, conglomerate and intraformational breccia		1. Igla Formation
Prolonged erosion and peneplanation		Regional unconformity
Intrusion of porphyrites, andesites. Subaerial eruption of glassy agglomerates and tuffs. All rich in iron		Old Volcanics of Dokhan type (unmetamorphosed)
Regional fault and thrust movements		
Emplacement of granites directly after climax of early orogenic folding	Synorogenic Plutonites	Older Granites (Fawakhir and Abu Ziran plutons)
Emplacement of gabbroic plutons during climax of early orogenic folding and regional metamorphism affecting these and all older rock units		Metagabbro Complxes (Fawakhir, Sid, Fannani and Atalla)
Intrusion of concordant ultramafic bodies in hinge zones of incipient regional folds and heralding main phase of orogeny		Serpentinite Ranges (Muweilih, Saneyat, Fannani and Atalla)
Intrusion of andesits. Eruption of dacitic tuffs	DESERT SUPERGROUP	6. Umm Seleimat Formation
Intrusion of doleritic laccoliths and sills		5. Abu Mreiwa Formation
Deposition of siliceous mudstone, minor siltstone, aroksic greywacke, intraformational conglomerate and limestone		4. Atalla Formation
Deposition of alternating conglomerate and greywacke, minor siltstone, mudstone and intraformational breccia		3. Atud Formation
Uplift in source area		
Effusion of pillowed spilites, diabasic flows, spilitic crystal tuffs, epiclastic adinole, intrusive andesite	Abu Ziran Group (eugeosynclinal filling)	2. Muweilih Formation
Deposition of alternating shale and calcareous shale, minor siliceous limestone and carbonaceous chert		1. Hammuda Formation (c) Khors Schist Member (b) Umm Hombos Metapyroclastic Lentil (a) Umm Shagar Metagreywacke Member
Eruption of basic lapilli-, crystal- and lithic tuffs merging into epiclastics		
Deposition of alternating greywackes and mudstones, minor conglomerates and pelites		
Deposition of successive psammites, psammopelites, calcpelites, semipelites to lithic greywacke, lithologically transitional to geosynclinal (turbidite) facies		
Slow deposition of quartzose and feldspathic sandstones, minor shale and calde-shale in extensive notably stable basin	ARABIAN Meatiq Group	Abu Fannani Schists (Formation)
		Thick mature siliceous granulites and minor schists. Subdivision into formations in progress

Table (II.1); The Chronological Sequence of The Principal Events and Lithostratigraphy of The Hammamat-Umm Seleimat District,

TABLE (II.2) SABET (1972)

Orogenic Stage	Formation Name
	Post-granite dykes
	Igla Formation red conglomerates, greywackes purple and green slates with red granite boulders
Posterogenic Stage	
	Tectonisation
Late orogenic Stage	Yellow muscovite garnet granite (Gabal Mirifya)
	Red biotite poor pegmatitic granite (Sheik Salem)
	Pink granite (Kadabora, El-Atawi, Gattar and El-Sibai)
	Hammamat Formation, Green breccia, greywake and purple slates with some volcanics and clacarecus bands
Synorogenic Stage	Tonalite-Granodiorite-Adamellite group (Wadi Haria)
	Gabbro (Gabal Atud)
	Kariem Formation, red conglomerates, greywackes and purple slates (7000 m.) associated with acid volcanics
	Old volcanics (Dokhan)
	Epidiorite and dioritic rocks (Wadi Dubur)
Initial orogenic Stage	Serpentinites (Barramiya)
	Metavolcanics (Shadli, Atalla and Umm Gheig)
Geosynclinal Sedimentation	Ancient metasidements; schists, marble, metamudstones (Wadi Umm Luseifa, 8 Km.) and paragneiss and migmatites (Hafafit)

Table II.3 : Correlation of the Basement rocks of G. Abu Kharif area with other classifications. (Abdel-Rahman, 1979).

Major rock unit in the present area	Akaad and El Ramly (1960)	El Ghazly (1964)	Gabet (1972)
Post-tectonic riebeckite granite	--	--	--
Post-Gattarian granitic dykes	Post-granite dykes	Postorogenic volcanics	Post-granitic dy
		b- Post orogenic plutonites	
Late-tectonic pink granite		a- Late-orogenic plutonites	Pink granite
Syntectonic grey granite	Grey granites	Synorogenic plutonites	Tonalite-Granodi Adamellite group
Diorites	Gabbroid-dioritic rocks		Epidiorite and dioritic rocks
Metavolcanics	Serpentine and Barramiya rock Meta-volcanic group.	Main geosynclinal volcanics	Metavolcanics

CHAPTER III

PETROGRAPHY OF THE GRANITIC ROCKS

CHAPTER III

PETROGRAPNY OF THE GRANITIC ROCKS

In 1957, Saha gave a petrographic description of the granitic rock units of the Deloro pluton, and Keuhnbaum (1973) gave a more complete description. Abdel-Rahman (1979) has studied in some detail the petrography of the three granitic phases of the Abu-Kharif complex. A brief summary of the petrographic characteristics of the Abu-Kharif and Deloro granites is given here.

(A) Petrography of the Abu-Kharif granites

Field studies reveal that the granitic rocks comprise three main field types. Beginning with the oldest, these are; the syntectonic granodiorites, the late tectonic pink granites, and the post tectonic granites. In addition, such rocks can be subdivided on their mafic content.

In the following, the petrography of the different granitic varieties is given:

1. Syntectonic granodiorite

a) Hornblende granites:

Microscopically, these rocks show holocrystalline hypidiomorphic granular texture. They are composed mianly of quartz, plagioclase feldspars, alkalifeldspars and hornblende with accessory sphene and iron oxides.

Quartz crystals are almost xenomorphic, integranular and varying between 1.4 mm. and 2.2 mm. across. They are occasionally undulose and commonly contain inclusions of

zircon and iron oxides. They exhibit sharp contact against feldspar crystals.

Plagioclase forms euhedral to subhedral prismatic crystals, showing polysynthetic as well as simple twinning. The individual twin lamellae are variable in breadth and a single crystal may consist of up to 20 lamellae, (Fig. III.1). Plagioclase crystals, frequently show oscillatory zoning. The composition of the plagioclase is (An = 17), i.e. oligoclase.

Alkalifeldspars are represented either by perthite with orthoclase host and albite inclusions or microcline with poorly developed cross-hatch twinning. Perthite crystals range from 0.6 mm. to 2.5 mm. across. They are partially altered.

Hornblende forms green subhedral to anhedral twinned, strongly pleochroic crystals, with x = yellow and Y=Z=Green. The Z^c angle ranges from 18 to 25 degrees. Hornblende crystals are sieved and usually enclose biotite, zircon, magnetite, and quartz granules. Accessory sphene forms rhombohedral crystals. Iron oxides form either skeletal patches or granules.

Some varieties are biotite-bearing. Biotite forms green and/or brown euhedral to subhedral occasionally twinned crystals. Both green and brown varieties are strongly pleochroic. They also exist moulding around feldspar terminates showing a subophitic relationship.

b) Biotite granite:

Biotite granite consist essentially of quartz, plagioclase, alkalifeldspars and biotite. Sphene and magnetite are detected as accessories.

Quartz forms anhedral crystals, ranging from 0.9 mm. to 1.3 mm. across and displaying sharp contact against feldspar and mica and occasionally enclosed by them.

Plagioclase is present in the form of euhedral to subhedral twinned prismatic crystals. The anorthite content is (An = 15), i.e. oligoclase. Occasionally, plagioclase crystals enclose smaller corroded plagioclase. This may indicate two periods of crystallization separated by a period of magmatic corrosion.

Alkalifeldspar form anhedral crystals ranging from 1.0 mm. to 3.9 mm. across. They are represented by microcline and perthite. Perthite crystals have corroded margins and are highly altered. Microcline exhibits poorly developed cross-hatch twinning.

Biotite is green and/or brown subhedral and occasionally twinned. Brown biotite may appear surrounding green ones, with chlorite inner zone. The greenish variety is pleochroic according to the scheme z = yellow and X=Y=green, while the brown variety shows, Z=yellowish brown and x=Y=brown. Biotite crystals have crenulated margins and are charged with iron oxides along cleavage planes.

Rhombic sphene crystals are observed as accessories. They exist either surrounded by biotite crystals or as inclusions in them.

2. Late tectonic calc-alkaline granites

a) Biotite granite:

Under the microscope, these rocks are holocrystalline with hypidiomorphic granular texture. They are composed essentially of quartz, alkalifeldspar, plagioclase and biotite with accessory iron oxides and sphene.

Quartz develops anhedral crystals, varying in diameter between 0.6 mm. and 2.6 mm., and fill the intervening spaces between the feldspar crystals.

Alkalifeldspars are represented by perthite. They form anhedral crystals, varying between 1.1 mm. and 3.4 mm. across. Replacement, vein, and patch perthites are recorded. Perthite crystals are frequently twinned on the Baveno law, and rarely the Carlsbad law. Two phases of prthitic crystallization may be suggested, where perthite crystals enclose smaller ones.

Plagioclase exists in subordinate amount, forming subhedral crystals. Zoning of oscillatory type is scarcely observed (Fig. III.2). Most of the plagioclase crystals have oligoclase composition (An = 13). They exhibit myrmekitic texture with quartz and frequently enclose quartz fragments, iron oxides and euhedral sphene crystals. Plagioclase may exhibit the "convolute zoning described by

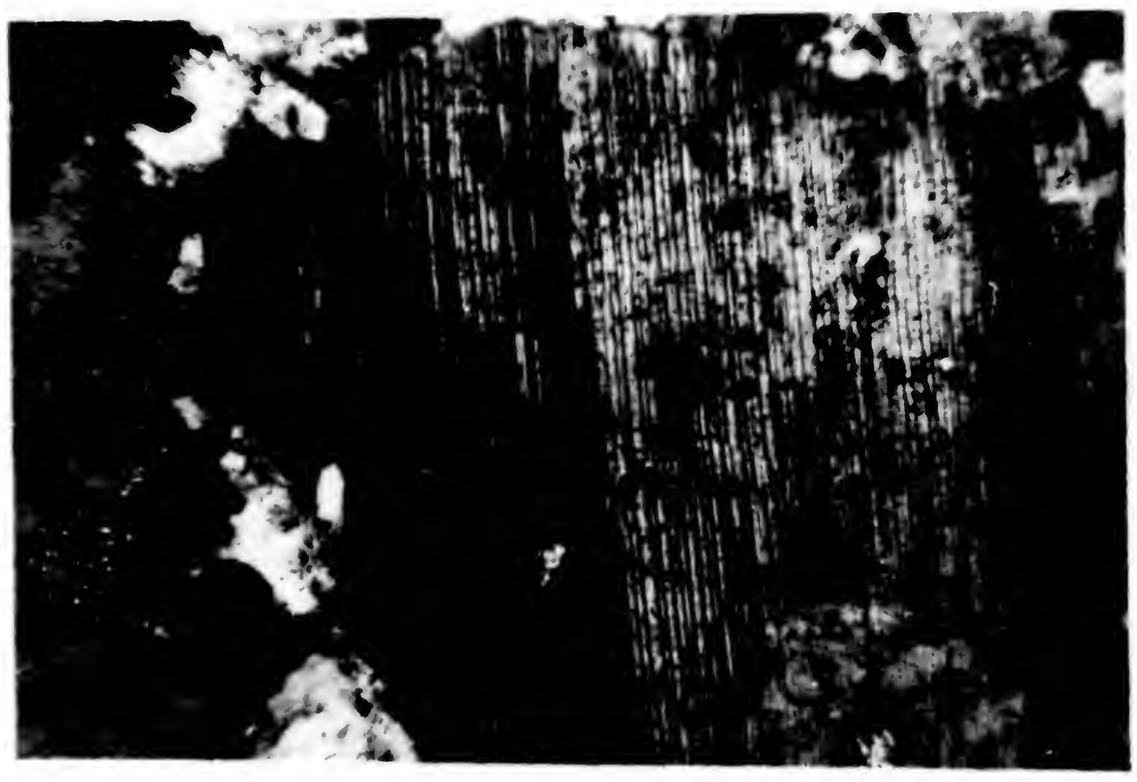

Fig.(III.1); Plagioclase crystal showing multiple twinning of more than 20 lamellae. C.... X10.

Fig.(III.2); Oscillatory zoning in plagioclase. Note the core alteration of the plagioclase. C.... X4.

Blackerby (1968). Convolutions are shown where the phenocrysts have apparently been embayed magmatically.

Biotite occurs in green and/or brown subhedral to anhedral crystals with crenulated margins (Fig. III.3). Green biotite crystals are pleochroic according to the scheme Z = pale yellow and X=Y=reddish brown. Biotite is frequently moulded around the terminations of feldspar crystals recalling a sub-ophitic relationship.

Quartz and zircon crystals are sometimes found as inclusions exhibiting with biotite a sieve-like texture. Sphene crystals are frequently observed filling the interstitial spaces.

Some varieties are hornblende-bearing where specks of hornblende are recorded in associateion with biotite. Hornblende specks are slightly pleochroic and show sharp contact against biotite.

b) Biotite muscovite granite:

Biotite muscovite granite consists essentially of quartz, alkalifeldspars, plagioclase, biotite and muscovite with accessory iron oxides.

Quartz forms anhedral crystals, ranging from 0.7 mm. to 3.5 mm. across enclosing minute crystals of zircon, muscovite and biotite.

Perthite forms subhedral to anhedral crystals ranging in length from 0.9 mm. to 1.7 mm. and in breadth from 0.4 mm. to 0.9 mm. They are microcline and orthoclase perthites of the compound type. Perthite crystals may enclose corroded plagioclase crystals. This may indicate a period of magmatic

corrosion that affected the early formed plagioclase crystals. Thereafter, conditions were favourable for the precipitation of a perthitic phase around the plagioclase. Occasionally, perthite crystals exhibit a myrmekitic texture. Microcline occurs either as separate crystals or in perthitic intergrowth with albite.

Plagioclase forms rarely zoned crystals of albite, composition (An = 10). They exhibit albite-twinning, and more than 20 lamellae in individual crystal may be observed.

Biotite forms green and/or brown subhedral to anhedral crystals. Both green and brown varieties are strongly pleochroic, and interlaminated with muscovite. Not uncommonly, they recall a subophitic relationship with feldspar crystals.

Muscovite forms subhedral to unhedral crystals. They may form irregular flakes charged with magnetite granules along cleavage planes. Microprobe analysis and classification of biotites are presented in Chapter V.

Iron oxides are represented either by magnetite or hematite. Magnetite forms either separate patches or inclusions in biotite, muscovite and quartz crystals. Hematitic materials are observed along cleavage in the feldspar crystals.

3. Post tectonic alkaline granites

a) Arfvedsonite granite

These rocks show holocrystalline hypidiomorphic granular texture. They are composed essentially of quartz, alkali-

feldspars, plagioclase, and arfvedsonite. Iron oxides occur in accessory amount.

Quartz forms anhedral crystals, ranging from 1.7 mm. to 3.2 mm. across, which fill the interstitial spaces between feldspars but are occasionally enclosed in them.

Alkalifeldspars are represented by perthite (and rarely by antiperthite). They are subhedral to anhedral occasionally twinned crystals, ranging in length from 1.3 mm. to 4.3 mm. and in breadth from 0.6 mm. to 1.7 mm. String and flame-perthites, (Fig. III.4) are the predominant types of intergrowth. Antiperthitic intergrwoth is also recognised with microcline host and albite inclusions. Perthite crystals show both Carlsbad- and Baveno-Twinning.

Plagioclase is present in a relatively small amount, forming subhedral to anhedral crystals. They are of oligoclase composition (An = 15). Plagioclase crystals are accumulated in the intervening spaces. They may be partially or wholly enclosed within the perthite crystals.

Arfvedsonite forms anhedral crystals (1.7 mm. and 2.4 mm. diameter) of deep blue colour. They may appear moulded around feldspar terminations recalling a subophitic relationship. Some arfvedsonite grains are highly charged with iron oxides (Fig. III.5). Geochemistry of arfvedsonite is presented in Chapter V.

Iron oxides are represented by magnetite granules, frequently associated with mafics particularly with the arfvedsonite.

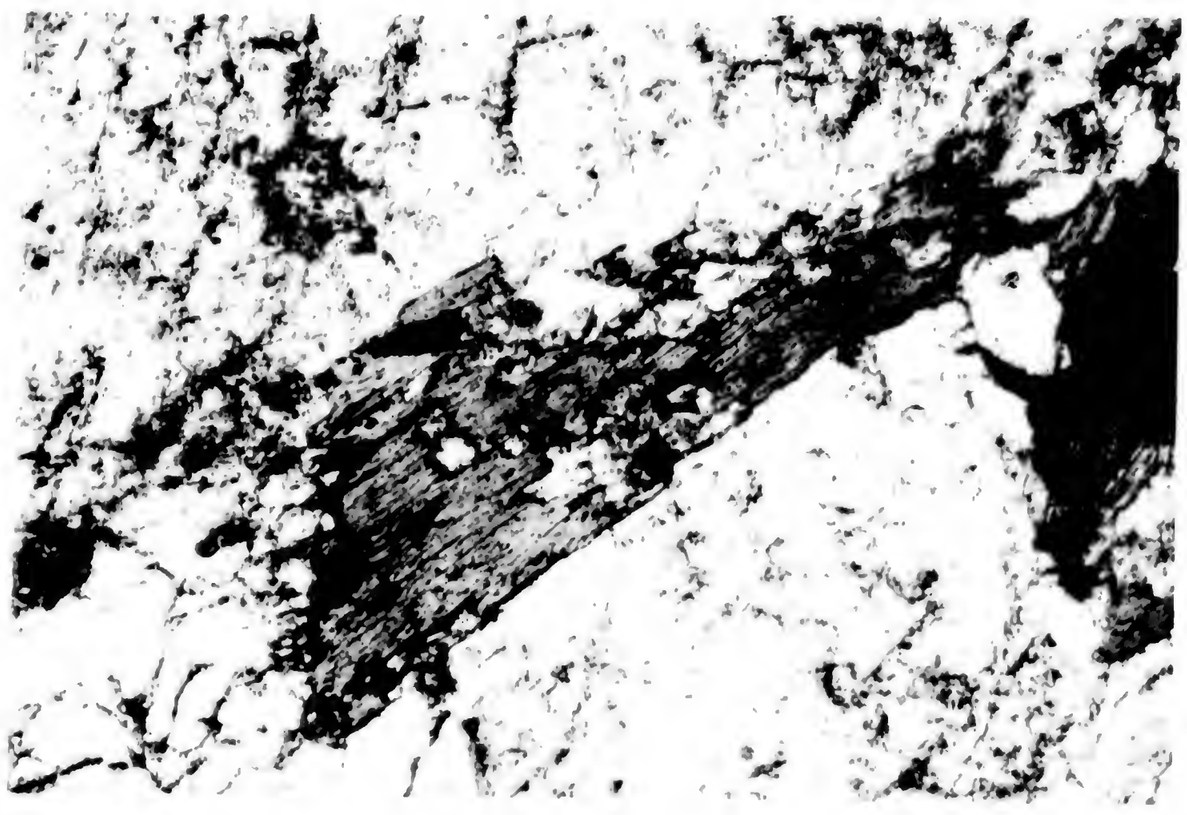

[illegible] crystal, with [illegible] margins and [illegible] [illegible] [illegible]. [illegible] X.

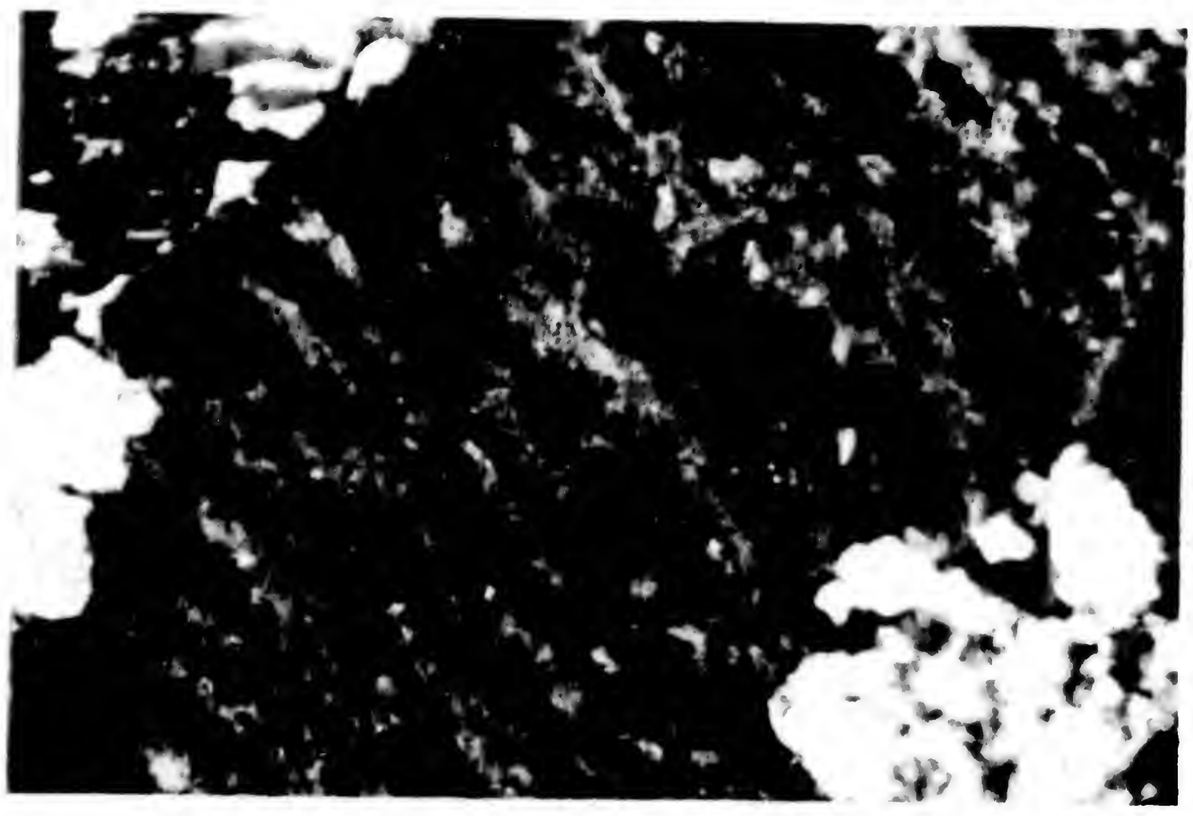

[illegible] [illegible] [illegible]. [illegible]

b) Arfvedsonite-biotite granite:

These rocks are holocrystalline with hypidiomorphic granular texture. They are composed essentially of quartz, alkalifeldspars, plagioclase, arfvedsonite and biotite, with accessory iron oxides.

Quartz forms anhedral crystals of average diameter 1.3 mm. They show mass extinction and fill the interstitial spaces between the feldspar crystals.

Alkalifeldspars are exclusively perthite. They form subhedral to anhedral, occasionally twinned crystals, ranging from 2.2 mm. to 6.7 mm. in length and from 1.1 mm. to 2.8 mm. in breadth. Vein, rod and patch perthite are recorded. Perthite crystals exhibit Carlsbad and Baveno types of twinning (Fig. III.6). A complex intergrwoth is observed, in which the quartz rods penetrate the perthite crystals.

Plagioclase forms euhedral to subhedral prismatic crystals. They show albite twinning. The anorthite content of the plagioclase is (An = 13), i.e. oligoclase.

Arfvedsonite is deep blue with slight pleochroism. It exhibits sharp contact with feldspar crystals.

Biotite occurs as subhedral to anhedral crystals, frequently associated with alkali amphiboles, and with crenulated margins.

Sphene crystals exist in rhombohedral form, enclosed either in feldspars or mafic crystals.

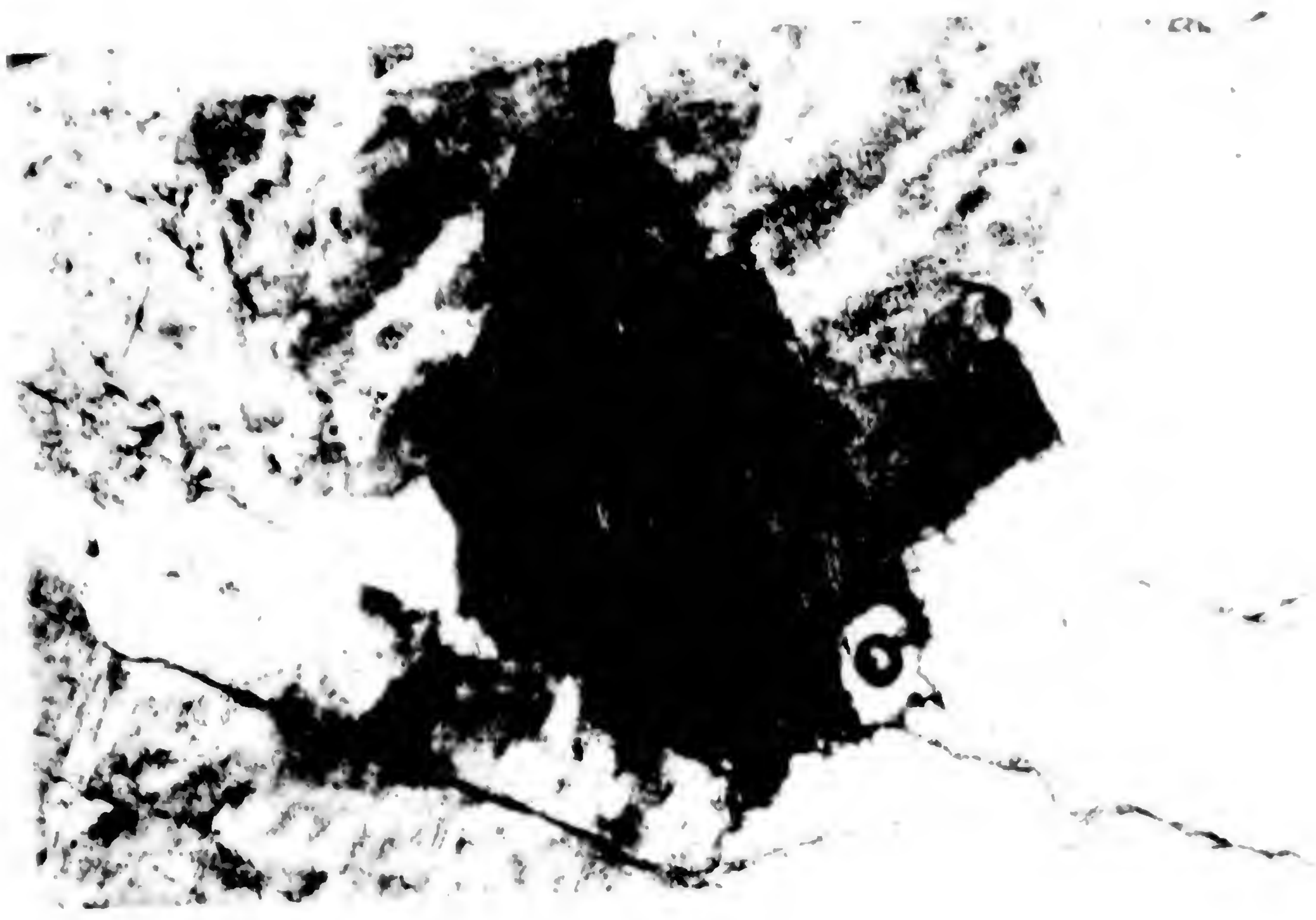

[illegible] : An [illegible] grain, highly charged with iron oxides. [illegible]

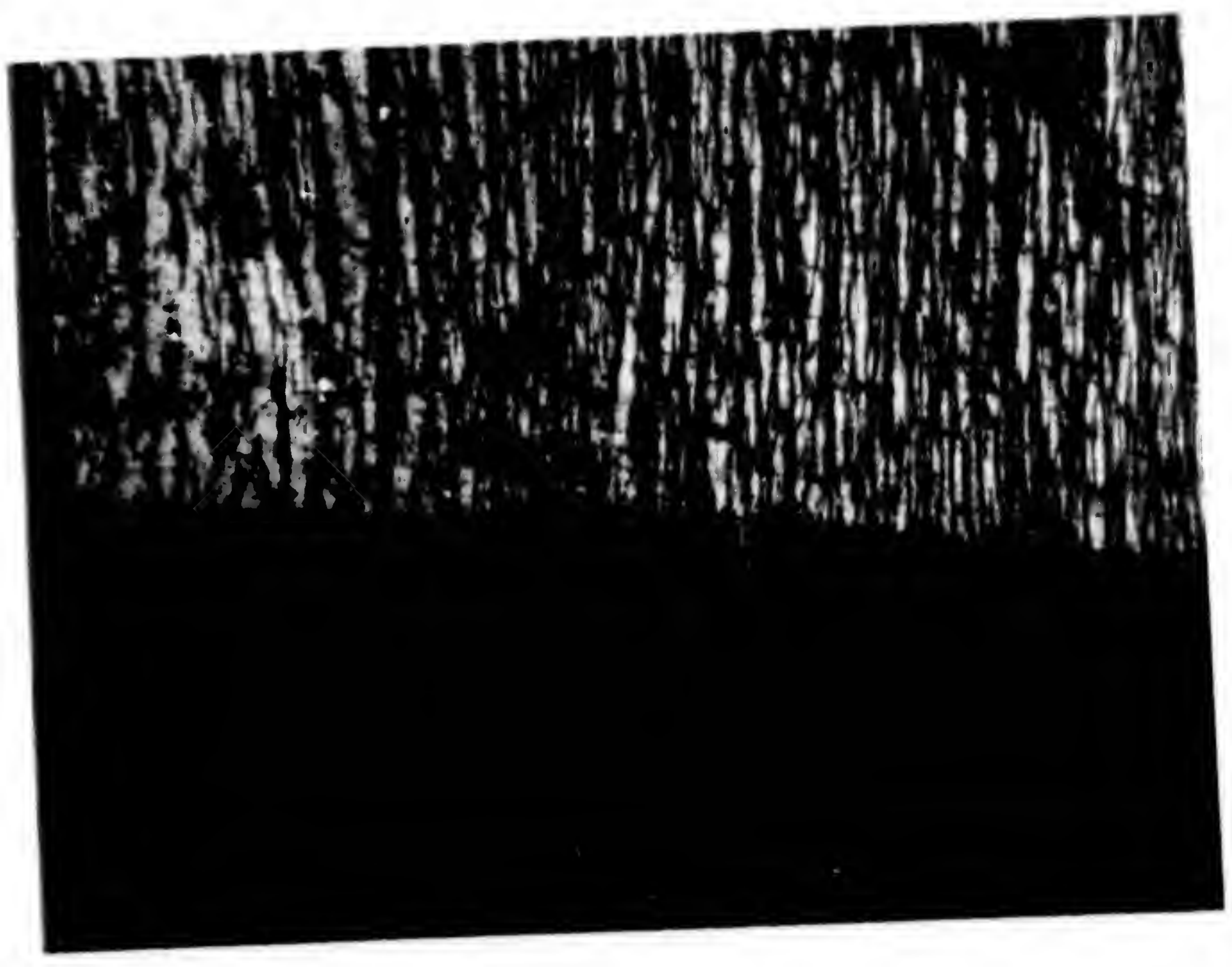

[illegible] : [illegible] twin in [illegible]. [illegible]

c) Leucocratic granite:

Leucocratic granite is composed essentially of quartz, alkalifeldspars, and plagioclase. They are devoid of mafics.

Quartz forms anhedral crystals ranging from 1.2 mm. to 2.4 mm. across. They occur intruding alkalifeldspar crystals.

Alkalifeldspars are mainly represented by perthitic intergrowth between orthoclase or microcline host and albite inclusions. Perthite crystals, range from 2.6 mm. to 5.0 mm. in length and from 1.1 mm. to 2.0 mm. in breadth.

Three types of perthitic intergrowths are recorded in these rocks, ribbon perthite, patch perthite and replacement perthite. Two phases of perthite are recorded, where perthite crystals are observed enclosing smaller corroded ones.

Plagioclase is present in the form of euhedral to subhedral twinned prismatic crystals. It has anorthite content An = 10, i.e. albite. Plagioclase crystals are magmatically corroded and frequently enclose quartz and magnetite granules. They also show the well developed myrmekitic texture.

The composition of the feldspars is presented in Table (III.1), which include the microprobe analyses of the Abu-Kharif and Deloro feldspars.

B) Petrography of the Deloro granitic rocks

The Deloro pluton consists of three main granitic phases: calcic syenite-granite, peralkaline riebeckite granite, and granophyric granite. Among the three granitic

units, several petrographic varieties have been identified. The petrography of the different granitic varieties is given in the following:

1. Calcic syenite-granite

The complex assemblages of mafic minerals associated with this suite, particularly the amphiboles, have been ascribed by Kuehnbaum (1973) to the multiple intrusive history of the calcic suite in which earlier phases have been thermally metamorphosed by the more differentiated later varieties.

The present petrographic investigations of the calcic syenite-granites has revealed the presence of an aenigmatite-bearing variety (Fig. III.7), in addition to those previously recognized. Calcic amphiboles are the main mafic constituents. Rocks containing two, three or four different calciferous amphiboles are characterized by varieties generally containing patchy replacement perthite or plagioclase frequently saussuritized.

Microprobe analyses of the calcic amphiboles as well as its classification are given in Chapter (V).

It is found that the main mafic constituent of the calcic syenite-granites are calcic amphiboles covering a broad compositional range extending from ferro-actinolite to hastingsite. Aenigmatite is found only in two specimens (P8-145 and P8-142), where it forms long prismatic red crystals characterized by high absorption that mask the interference

colour. Hastingsite occur in subhedral to euhedral greenish yellow crystals and it is characteristically associated with epidote. Compositional zoning is well developed in some crystals (Fig. III.8). Long prismatic, unrimmed, actinolitic hornblende is also observed (Fig. III.9). The calcic amphiboles are occasionally sieved by inclusions of quartz and apatite with occasional ilmenite, sphene, calcite or fluorite.

Age relations between coexisting aluminous amphiboles may be obscured by a high degree of intergrowth of the two or more phases. These mixtures can occur as large patches (1 mm.), probably representing the breakdown of a once-homogeneous phase, and original grain outlines may be preserved (Kuehnbaum, 1973).

Feldspars establish subhedral to anhedral coarse grain size crystals (2 to 3 mm.), with fine-grained material appearing in some of the more granulated specimens. Heterogeneity of the feldspar types in this suite is related to the complexity of the calcic amphiboles. Kuehnbaum (1973) pointed out that estimates of bulk composition range from mesoperthitic (microcline slightly greater than albite) to virtually pure albite. Feldspar type may vary from albite to antiperthite, to string mesoperthite and microcline perthites. Presence of interperthitic albite rinds imply similarities of formation with the peralkaline riebeckite granites. Lamellar varieties or exsolution are infrequent; however, patchy to braid perthites predominate, specially in rocks with a high

Fig.(III.7); Dark red crystal of aenigmatite, showing high absorption.

P.L. 44.

Fig.(III.8): Compositional zoning in calcic amphibole (hastingsite).

P.N. X10.

albite/microcline ratio, suggesting that these types might be due to replacement combined with exsolution.

Carlsbad- or Manebach twinned perthitic albite zoned to patchy antiperthite confirm an original high-temperature phase (Kuehnbaum, 1973). Inclusions of random or oriented needles of amphibole, apatite, chlorite, biotite and zircon are recorded in the feldspars, while hematization is observed quite frequently along its cleavage planes.

2. Peralkaline riebeckite granite

Three petrographic varieties have been identified within the peralkaline granitic phase. These are riebeckite biotite granite, riebeckite granite and leucocratic granite. A summary of the petrographic characteristics of each petrographic variety is given below:

a) Riebeckite biotite granite

The riebeckite biotite granite is holocrystalline with hypidiomorphic granular texture. It is composed essentially of quartz, alkali feldspars, alkali amphiboles, biotite and ilmenite with accessory zircon, hematite, calcite, fluorite, chlorite, pyrite and sphene.

Quartz forms xenomorphic crystals with sharp contacts against feldspar and mica crystals, and are occasionally enclosed in them. Granophyric intergrowths are occasionally observed.

...matic crystal of actinolitic hornblende.

...ing the actinolitic hornblende.

Alkali feldspars are mainly microcline perthite, as subhedral to anhedral crystals. String and rod perthites are the most common types of perthitic intergrowths (Fig. III.10). Alkali feldspars frequently enclose tiny grains of quartz zircon, biotite and riebeckite. Only in rocks where there exists obvious, intense surface weathering does sericitization occur (Kuehnbaum, 1973). Although the entire albite component of the examined granites may be within perthite, thin rims of secondary albite between perthite are widespread (Fig. III.11). The composition of the feldspars is listed in Table (III.1).

Riebeckite occurs in deep grennish blue, subhedral, slightly poikilitic crystals. In some of the more massive grains of the alkali amphiboles, a fine dusting of oxides has developed specially along cleavage planes.

Biotite occurs in brown subhedral to euhedral crystals. Feldspar crystals are sometimes found as inclusions within biotite exhibiting a sieve-like texture. However, biotite is occasionally moulded around the terminations of feldspar crystals recalling a sub-ophitic relationship. Alteration of biotite to a pale yellowish green penninitic chlorite is widespread, preferentially over the attack of the riebeckite. Biotite most commonly forms on the exterior portion of the riebeckite grains, and the distinctive reaction relationship is not apparent. Saha (1959) has suggested that the biotite is late stage hydrothermal in crystallization and that it grew by reaction with the riebeckite.

In 1973, Kuehnbaum observed, in some thin sections, that acicular grains fringe large plates of biotite or massive riebeckite may entirely envelop several rather leached-looking biotites. He assumed, accordingly, that both are generally in mutual equilibrium and that crystallization was essentially simultaneous.

Microprobe analyses and the classification of the biotites and the alkali amphiboles are presented in Chapter (V).

Ilmenite, zircon, fluorite, sphene and calcite are the predominant accessory minerals. Microprobe analyses of ilmenite is listed in Table (III.2).

b) Riebeckite-granite

Riebeckite is the only essential mafic mineral in some specimens (P8-122 and P8-136, and others), of the peralkaline granites. That petrographic variety (riebeckite granite) is composed essentially of quartz, feldspars and riebeckite with accessory ilmenite, zircon and fluorite.

Quartz develops anhedral crystals filling the intervening spaces between the feldspar crystals. It shows mass extinction and occasionally contains inclusions of iron oxides. Feldspars are mainly represented by microcline perthite as well as secondary albite. Both ribbon and string perthite are the predominant perthitic types (Fig. III.11).

Two phases of perthitic intergrowth are recorded where perthite crystals are observed enclosing smaller corroded

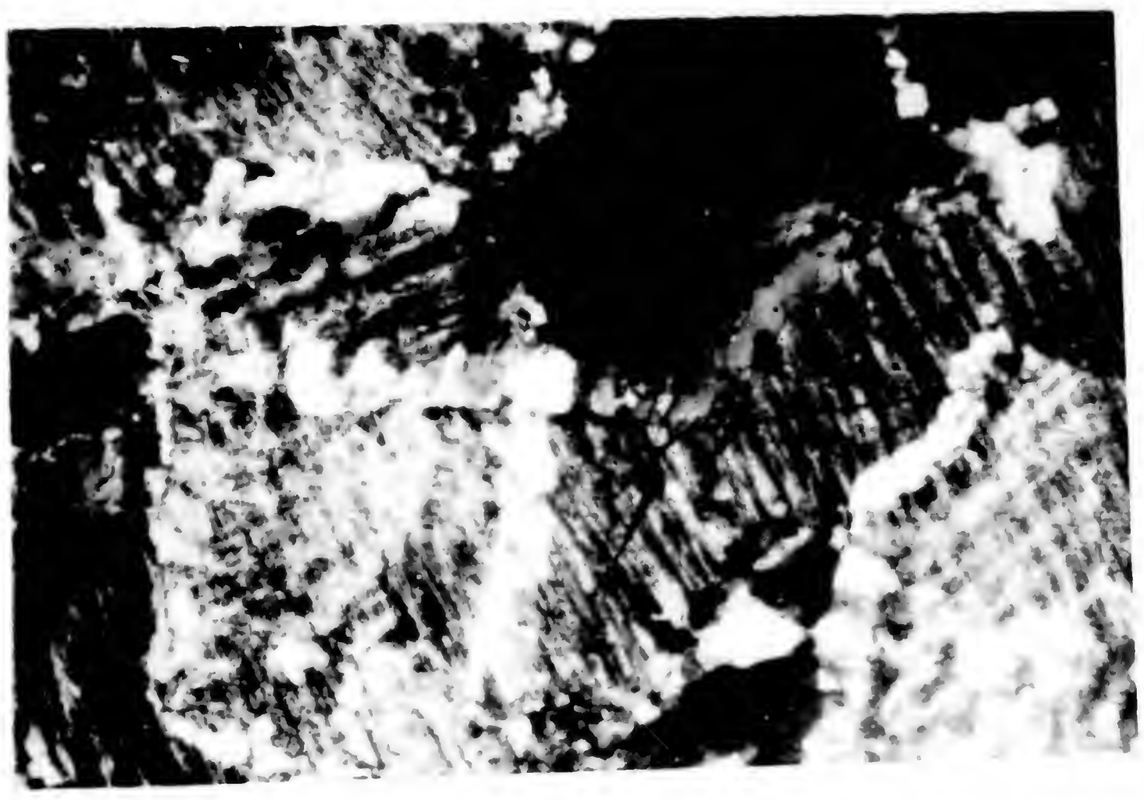

Fi . . . .11); . . . rims of secondary albite developed between perthite
. rains (ribbon perthite). C.N. 42.5.

Fi .(. . . .); . . . secondary albite cutting a perthite . rain.
. . . . .

ones. Carlsbad twinning is frequent and gives rise to the familiar "herringbone" pattern observed in many epizonal granitic intrusions (Toulmin, 1960, Jacobson et al. (1958). Acicular needles of riebeckite as well as quartz grains are observed as inclusions in perthites.

Several stages of recrystallization of the rocks can be traced using the feldspars as indicators of the process (Saha, 1957). Thin rims of albite between perthites are widespread (Fig. III.11). The "free" albite in this case is in optical continuity with the albite of the perthite.

The next stage (2) according to Saha (1957), is recognized by fine, granular, clear albite in different orientations from the albite in the perthite. In 1973, Kuehnbaum pointed out that the development of two rows of albite granules is restricted to perthite-perthite margins, whereby one row of albite is optically continuous with the albite of the perthite separated from its corresponding free albite by the second row. This exsolved albite is untwinned. Ramberg (1962) has discussed this feature in detail. Quartz may also be present in these rinds.

Large crystals of twinned albite (up to 2 mm.) form by the third stage (Saha, 1957). At this point, albite still forms only at perthite-perthite margins, and never at perthite-quartz interfaces. Veins of albite, with or without quartz or calcite may cut the perthites at this stage (Fig. III.12). Lastly, perthites with sutured margins sit in a mesostasis composed of

relatively fine-grained quartz, albite and often microcline, all the feldspars are well-twinned (Kuehnbaum, 1973).

Ramberg (1962) has concluded that the intergranular precipitation of albite in deep-seated rocks must be due to the unmixing of Na-k feldspars, due to low nucleation energy of albite at feldspar-feldspar margins.

In 1976, Martin and Bonin considered the albite that borders perthite grains - in their case study -, to be of hydrothermal origin.

The amount of "free albite", in the peralkaline riebeckite granite has been correlated by Saha (1957), to the amount of microcline present in the rock. He concluded that the "secondary albite" of these rocks is due to a state of late-stage stress with granulation assisting the exsolution of albite from the perthitic feldspars. The granulation is accompanied by a progressive reduction in the grain size of quartz.

Both riebeckite and crooidolite,fibrous variety of riebeckite, are recorded. Riebeckite occurs in subhedral to anhedral, poikilitic, ragged, inclusion-filled grains. The ragged nature of this type gives the impression that the amphibole crystallized late and has digested its way into surrounding feldspar and possibly quartz (Kuehnbaum, 1973). Such grains may partially or completely enclose quartz or feldspar crystal giving rise to sub-ophitic or ophitic textures (Fig. III.13). In the poikilitic grains, inclusions

are ilmenite, fluorite, zircon, quartz, feldspar and sphene. Riebeckite is usually deep greenish blue in colour and shows high pleochroism. It is pleochroic according to the scheme:

x = deep dark blue

y = dirty green, bluish green, greyish blue

x = greenish yellow, beige

In the centres of some of the larger, more massive grains of alkali amphibole, a fine dusting of oxides has developed, the border remaining clear, this feature may possibly indicate increasing oxidation with crystallizations (Kuehnbaum, 1973).

c) Leucocratic granite

Leucocratic peralkaline granite is made up essentially of quartz and feldspars. Accessory minerals are mainly represented by ilmenite, zircon, chlorite, iron oxides and sphene.

Quartz forms anhedral crystals filling the interstitial spaces between feldspars, and occasionally enclosed in them.

Feldspars are exclusively microcline perthites. Saha (1957) has indicated that the lamellae plane is nearly parallel to (100) of the albite phase, but occasionally braided perthite, showing two directions of exsolution, has irrational lamella orientation. The absence of discrete, primary, albite grains reflect the hypersolvus nature of the examined granites. Secondary albite is developed mainly along perthite margins. Braided and string perthites are

the predominant perthitic types (Fig. III.14). Both Carlsbad and Baveno twinning (Fig. III.15) are recorded. Alterations even in cases where mafic minerals have been heavily attacked, are uncommon, but hematization, however, is present in many specimens. Rarely does it reach a heavy state and may be accounted for by oxidation of Fe held in solid solution in the original high-temperature feldspars. The perthitic crystals frequently enclose chlorite, ilmenite, zircon and iron oxides.

Microprobe analyses of feldspars are listed in Table (III.1).

3. Granophyric granite

The quartz feldspar intergrwoths (Fig. III.16), as well as the lack of peralkalinity in this phase are the predominant criteria for the separation of the unit. Kuehnbaum (1973) pointed out that the alteration of mafic minerals is predominant, but the feldspars have remained remarkably fresh. Solution pits of pyrite and hematite are common.

Normal granophyre as well as a fine grain size variety with the development of intergrown patches of quartz and alkalifeldspars, often giving rise to radiating, spherulitic aggregates, have been recognized (Fig. III.17).

Quartz forms xenomorphic crystals and occur either as individual crystals or in graphic intergrwoth with feldspars.

Fig.(III.14); Riebeckite enclose perthite crystal recalling ophitic texture. C.N. X2.5.

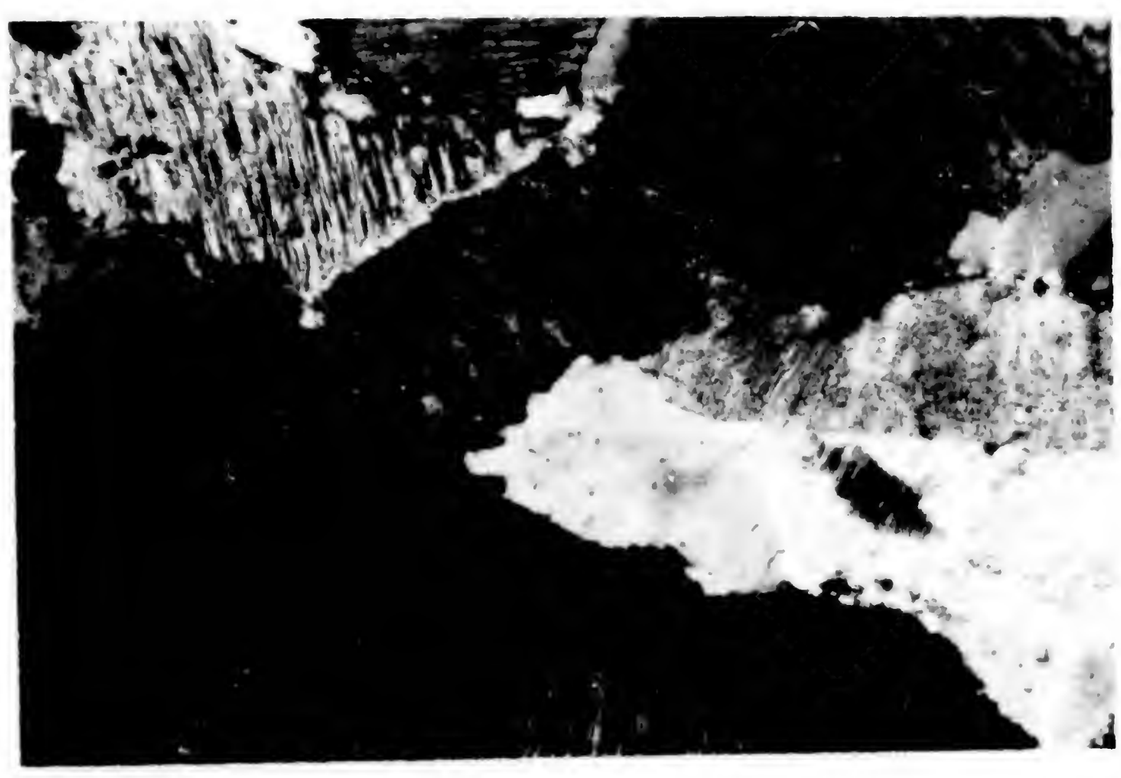

Fig.(III.15); Typical perthitic intergrowth (string perthite), in the upper olvus peralkaline granite. C.N. X-.

Fig.(III.15); Compound Baveno twinning. C.N. X4.

This type of intergrowth varies from wormy granophyric in texture, through to micrographic in which triangular quartz grains are common (Kuehnbaum, 1973). The feldspars are complex in character and type. Microcline microperthite is the predominant feldspar within the quartz-feldspar intergrowth, with cryptoperthitic (rarely microperthitic) albite forming phenocrysts up to 1.5 mm. across (Saha, 1957). Fine, subhedral crystals of muscovite with crenulated margins are recorded. Not uncommonly they are altered to chlorite and iron oxides.

The accessory minerals are mainly represented by muscovite, magnetite, pyrite euhedra, hematite and chlorite (as alteration products), as well as biotite, fluorite, zircon and calcite.

Fig.(III.16); Coarse region of micrographic intergrowth and medium region of the same intergrowth surrounding perthite phenocryst.C.N.X4

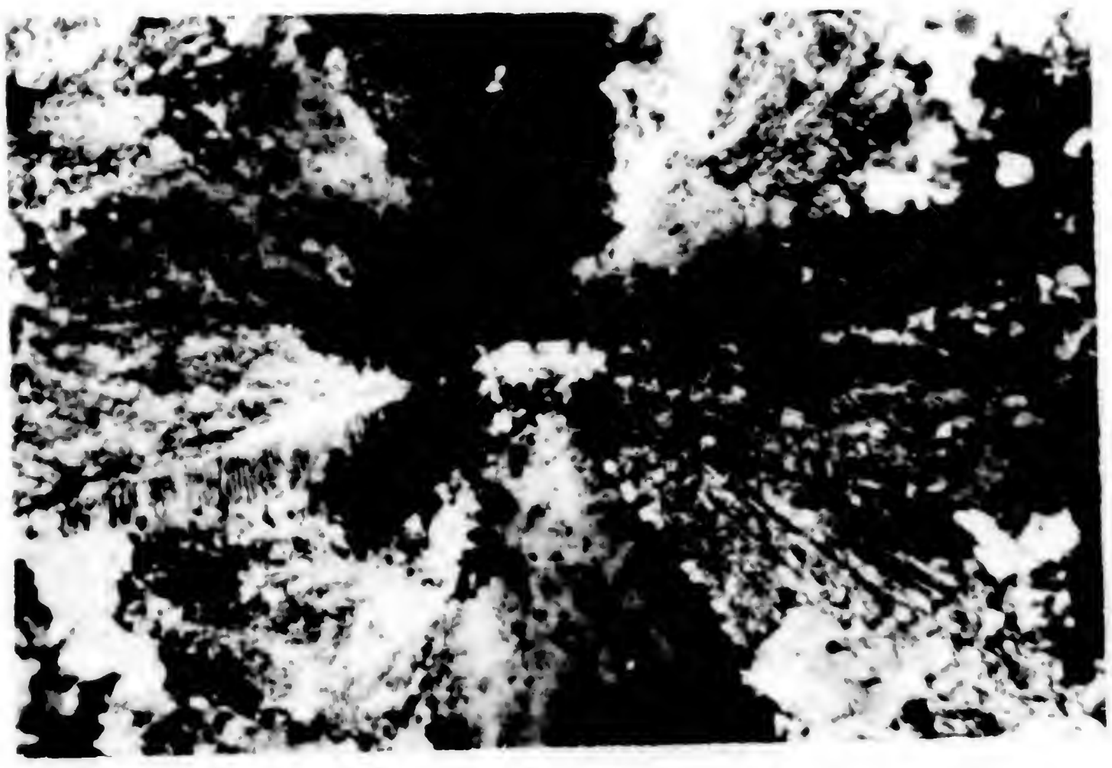

Fig.(III.17); Fine grained spherulitic aggregate in granophyric granite. C.N. X4.

Table(III.1); Microprobe analysis of the Abu-Kharif and Deloro feldspars

WEIGHT PERCENT	1	2	3	4	5	6	7	8	9	10
SIO2	60.93	61.36	60.21	60.85	65.50	65.99	65.67	66.08	66.24	69.72
AL2O3	24.54	24.61	24.54	24.20	18.64	18.32	18.78	20.41	18.50	18.14
FEO	0.20	0.13			0.13					
CAO	5.58	5.40	5.47	5.35				1.26		0.39
NA2O	7.86	8.39	8.27	8.24	1.10		0.60	10.84	0.63	18.75
BAO					0.73		0.85			
K2O	0.21	0.22	0.16	0.27	14.20	16.45	14.95	0.12	15.32	
SUM	99.32	100.11	98.65	98.91	100.30	100.67	100.85	98.73	100.69	99.06
ATOMIC PROPORTIONS										
SI	10.883	10.864	10.837	10.916	12.013	12.071	12.008	11.734	12.073	12.235
AL	5.167	5.146	5.206	5.117	4.030	3.956	4.048	4.272	3.975	3.752
FE2+	0.030	0.000			0.020					
CA	1.068	1.026	1.055	1.028				0.244		0.073
NA	2.722	2.886	2.886	2.876	3.391		0.213	3.703	0.223	3.653
BA					0.052		0.061			
K	0.048	0.050	0.037	0.062	3.323	3.847	3.488	0.027	3.562	
O	32.000	32.000	32.000	32.000	32.000	32.000	32.000	32.000	32.000	32.000
CATSL	19.918	19.992	20.021	19.990	19.825	19.875	19.816	20.010	19.832	19.718

Table(III.1) Continued ...

WEIGHT PERCENT	11	12	13	14	15	16	17	18	
SIO2	65.01	65.22	66.07	64.30	66.23	65.12	67.97	65.09	SIO2
AL2O3	18.09	18.20	17.30	18.19	18.54	18.22	19.25	18.43	AL2O3
FE2O3		0.20	0.17	0.26		0.15			FE2O3
FEO	0.18					0.11			FEO
CAO		7.46					0.10		CAO
NA2O					2.35	0.83	13.86	1.01	NA2O
K2O	16.25	7.66	15.32	15.81	13.68	15.72		15.44	K2O
SUM	99.53	98.74	98.86	98.56	100.80	100.16	101.18	99.97	SUM

ATOMIC PROPORTIONS

SI	12.058	11.932	12.246	12.028	12.025	12.007	11.852	11.998	SI
AL	3.955	3.923	3.780	4.011	3.966	3.960	3.957	4.007	AL
FE3+		0.028	0.026	0.041		0.021			FE3+
FE2+	0.029					0.017			FE2+
CA		2.647					0.019		CA
NA					0.827	0.297	4.686	0.361	NA
K	3.846	1.788	3.623	3.773	3.169	3.698		3.531	K
O	32.000	32.000	32.000	32.000	32.000	32.000	32.000	32.000	O
CATSUM	19.887	20.292	19.675	19.853	19.969	20.000	20.513	19.995	CATSUM

Table(III.1) Continued ...

WEIGHT PERCENT	19	20	21	22	23	24	25	26	27	
SIO2	64.57	64.63	65.20	65.74	65.10	66.87	65.30	64.95	65.13	SIO2
AL2O3	18.30	18.02	18.16	18.34	18.40	19.13	18.32	18.09	18.41	AL2O3
FE2O3	0.29	0.22	0.26	0.23	0.15	1.42				FE2O3
FEO										FEO
CAO	1.26	0.79	0.87	1.73		12.39				CAO
NA2O							0.51		1.50	NA2O
K2O	15.41	15.51	15.98	15.25	16.39	5.10	16.41	16.61	14.96	K2O
SUM	99.83	99.27	100.49	101.29	100.04	105.41	100.54	99.65	100.00	SUM
ATOMIC PROPORTIONS										
SI	11.958	12.022	12.006	11.986	12.020	11.598	12.012	12.050	11.991	SI
AL	3.995	3.951	3.942	3.942	4.005	3.911	3.973	3.956	3.995	AL
FE3+	0.000	0.034	0.000	0.000	0.023	0.000				FE3+
FE2+										FE2+
CA	0.452	0.295	0.311	0.612		4.335				CA
NA							0.182		0.536	NA
K	3.641	3.705	3.754	3.548	3.861	1.129	3.851	3.932	3.514	K
O	32.000	32.000	32.000	32.000	32.000	32.000	32.000	32.000	32.000	O
CATSUM	20.046	19.997	20.013	20.087	19.908	20.972	20.018	19.938	20.036	CATSUM

The Abu-Kharif samples

From 1 to 4 ; granodiorites

5 to 10; calc-alkaline granites

11 to 14; alkaline granites

The Deloro samples

From 15 to 18; calcic syenite-granites

19 to 24; peralkaline granites

25 to 27; granophyric granites

Table(III.2); Microprobe analysis of ilmenites from the Deloro pluton.

WEIGHT PERCENT	1	2	3	4	5	6	7	8	9	
SIO2	0.64	0.59	0.65	0.63	0.58	0.62	0.61	0.58	0.57	SIO2
TIO2	48.40	50.35	49.12	49.59	51.74	48.10	50.30	50.34	50.22	TIO2
FE203	4.03	2.83	4.50	3.22		3.31	0.43	1.49	1.42	FE203
FEO	37.24	37.39	35.65	36.49	40.08	38.80	39.72	40.38	40.84	FEO
MNO	6.96	8.49	9.18	8.75	5.37	5.13	6.16	5.51	4.94	MNO
SUM	97.27	99.64	99.10	98.67	97.77	95.96	97.22	98.30	97.99	SUM
ATOMIC PROPORTIONS										
SI	0.133	0.119	0.132	0.129	0.119	0.130	0.126	0.119	0.117	SI
TI	7.552	7.665	7.523	7.624	7.978	7.688	7.840	7.766	7.773	TI
FE3+	0.630	0.431	0.689	0.495		0.524	0.067	0.229	0.220	FE3+
FE2+	6.462	6.329	6.072	6.238	6.873	6.824	6.885	6.928	7.029	FE2+
MN	1.223	1.456	1.584	1.515	0.933	0.914	1.081	0.957	0.861	MN
O	24.000	24.000	24.000	24.000	24.000	24.000	24.000	24.000	24.000	O
CATSUM	16.000	16.000	16.000	16.000	15.903	16.000	16.000	16.000	16.000	CATSUM

CHAPTER IV

PETROCHEMISTRY AND GEOCHEMISTRY OF THE ABU-KHARIF AND DELORO GRANITIC ROCKS

CHAPTER IV

PETROCHEMISTRY AND GEOCHEMISTRY OF THE ABU-KHARIF AND DELORO GRANITIC ROCKS

Introduction

The granitic rocks of the Abu-Kharif and Deloro complexes belong to two different Shields: the Nubian Arabian Shield and the Canadian Shield, respectively. Much field and petrographic work has been done, but few geochemical investigations have been completed and published on these granites.

The petrochemistry and geochemistry of the different granitic phases as well as the resulting behavior of the trace elements in the genetic processes of the two granitic complexes are the target of this study. The abundance and distributions of selected Rare Earth Elements (REE), Rb, Sr, Ba, Cs, Cr, Sc, Co, Zr, Hf, Ta, Y, U and Th were determined for six granitic rock units. This being the first attempt to undertake such study of the Abu-Kharif and Deloro complexes.

Goldschmidt (1954) assumed that no significant degree of relative fractionation can be observed among the REE. It is well known by now that this assumption is incorrect and that fractionation among the REE is very common in igneous rocks (Haskin et al. 1966, Strong et al. 1982).

The last decade has been marked by an extensive use of trace elements in petrogenetic problems. The use of such studies has been restricted almost exclusively to basalts

and related rocks with fewer studies on acidic and particularly granitic rocks.

A number of significant problems concerning these plutons can be resolved by use of trace elements. Such problems as contrasting crystallization histories, whether or not certain plutons are co-magmatic, and the ultimate origin of the granitic magma can all be illuminated by trace element studies (Tauson, 1967).

29 chemical analyses representing 11 different types of Abu-Kharif granitic rocks and 18 samples of Deloro granitic rock types are shown in Table (IV.2). These results are compared with the world's average as given by Nockolds (1954). In addition, the average of some analysis of Egyptian granites as well as some Canadian granites are given in Table (IV.3) for purpose of comparison.

Rare Earth Elements as well as Rb, Ba, Cs, Cr, Sc, Co, Hf and Ta were analysed in twenty new samples from both the Abu-Kharif and Deloro granitic rocks by using the Neutron Activation-Technique. Zr, Sr, Y, U and Th for the same samples were also analysed by the author using X-ray fluroescence on pure powder rock pellets. The results of the trace element analyses are shown in Table (IV.6).

Analytical Techniques

(1) Neutron activation analysis

The neutron activation analysis has been done using the Slowpoke-2 nuclear reactor at the University of Toronto.

The irradiation of samples was done in a thermal neutron flux of 2.5 x 10" $n/cm^2.S.$ at a power of 5 kw. The gamma-ray detection system consisted of an Intrinsic-Germanium detector coupled to a 8192-channel pulse - height analyser (Canberra Series 80), and printer. Counting for short-lived radioactive species (half lives 1 to 11 days) was usually carried out a week after irradiation, while counting for the longer-lived ones (half lives, few days to 13.2 years) was done 30 to 40 days after irradiation.

The Canberra multi-channel analyser produced net peak areas and counting statistical data. The trace element concentrations were calculated by comparing the areas of the sample peaks with those of the rock standard (UTB1), whose trace element composition is well known, after having corrected these areas for such factors as interference, difference in sample weight and time elapsed after irradiation.

Preparation of samples and standards for irradiation: About 0.2 gm. of very finely powdered rock sample or standard (size of about 200 mesh) were accurately weighted and put

in 20 x 14 mm. plastic sheets, and closed perfectly by sealing along the borders.

For mineral separates (biotite, amphibole and alkali amphibole), a weight of about 0.5 gm. of the fine powder was used in order to compensate the expected low REE concentrations in such minerals.

About 12 such sample bags with one bag of the standard (UTB1) - for which the trace element composition is well known, were placed in polyethelyne capsules. The capsules were irradiated for 16 hours in the Slow Poke-2 reactor. The samples and standards were allowed to cool for 5 days after the end of irradiation and then counted after a 7-day and a 40-day intervals.

Rare Earth Elemennts and other trace elements (e.g. Rb, Ba, Hf, Ta, Cs, Sc, Co,----) for 20 new rock samples and eleven new mineral separates from both the Abu-Kharif and Deloro rocks have been analysed in this way.

The γ-ray energies of the REE used for the present study are shown in Table (IV.1).

TABLE (IV.1); γ-ray energies of REE, used for the present study.

Radio-nuclide Produced	Stable Nuclide	Half life of radioisotope	γ-ray energy used (Kev)
^{140}La	^{139}La	40.30 h	1595.40
^{144}Ce	^{140}Ce	35.50 d	145.40
^{147}Nd	^{146}Nd	10.98 d	91.03
^{153}Sm	^{152}Sm	46.44 h	103.20
^{152}Eu	^{151}Eu	13.20 y	1408.02
^{160}Tb	^{159}Tb	72.10 d	298.58
^{175}Yb	^{174}Yb	4.21 d	282.52
^{177}Lu	^{176}Lu	6.71 d	208.40

(2) X-ray Fluorescence

X-ray fluorescence spectrometry used to determine the concentrations of the following elements Zr, Sr, Y, Th and U at the ppm level.

The procedure included the preparation of pressed pellets, in which about 3 gm. of each sample was partially encapsulated with Boric acid at a ram pressure of about 5 tons per square inch.

The pellets were loaded 8 at a time into a computer controlled Siemens SRS, XRF spectrometer. The other two positions were occupied by standards UTB1 and SRO.

The operating conditions were:
Molybdenum x-ray tube excited at 60 kv. and current of 50 m.A at the power of 3 Kw.

Counting periods were 200 sec. (for peaks) and 100 sec. (for the background).

Each rock sample was run in duplicate against a secondary standard (UTB1), extensively used at University of Toronto.

The technique used for absorption corrections was based on background measurements with a precision of about 5%.

Petrochemistry
of the Abu-Kharif and Deloro granitic rocks

The results of chemical analysis of Abu-Kharif and Deloro granitic rocks (carried out by Abdel-Rahman, 1979 and Kuehnbaum, 1973 respectively) are compared with the world's average granite of Nockold's (1954) as well as the average of some Egyptian and Canadian granites (see Table IV.2 and IV.3).

A survey of the chemical analysis of the granitic rocks of Abu-Kharif and Deloro complexes, clearly shows that the majority of these granitic rocks compare rather well with the average results of the Egyptian granites (Geological Survey of Egypt, 1976) and the average of some Canadian granites (Strong and Dupuy, 1982), as well as those of Nockald's (1954).

Bulk chemical analysis have been recalculated to show molecular norms (Table IV.4) and Niggli values (Table IV.5).

Some petrochemical characters of the examined rocks will be dealt with in the following:

(1) Normative composition:

Normative minerals of Abu-Kharif and Deloro granitic rocks calculated on the basis of the chemical analysis, are shown in Table (IV.4). The normative albite, orthoclase and quartz are recalculated to 100% and are plotted on the ternary diagram Ab-Or-Qz, the "residua diagram" of Tuttle and Bowen (1958).

TABLE (IV.2) Chemical analyses (weight percent) of the Abu-Kharif and Deloro granites

No.	1 AK 10	2 AK 66	3 AK 26	4 AK 40	5 AK 80	6 AK 99	7 AK 18	8 AK 62	9 AK113	10 AK108	11 AK 33	12 P8-141	13 P8-142	14 P8-143	15 P8-147
SiO_2	69.05	70.94	69.6	71.61	72.47	74.49	75.46	74.81	74.23	74.34	73.99	57.41	57.93	59.31	68.93
TiO_2	0.34	0.21	0.26	0.14	0.20	0.11	0.09	0.11	0.20	0.15	0.16	1.08	1.01	1.14	0.37
Al_2O_3	15.07	14.33	14.60	14.62	14.16	13.77	13.06	13.45	11.01	11.12	11.03	12.57	13.59	13.62	13.23
Fe_2O_3	1.57	1.72	1.44	0.57	0.86	0.72	0.64	0.44	1.00	1.10	1.11	5.29	3.72	2.22	1.77
FeO	2.74	1.28	2.32	1.23	1.89	0.99	0.76	0.90	2.36	1.75	2.03	8.59	7.49	8.25	3.52
MnO	0.09	0.07	0.10	0.07	0.09	0.07	0.05	0.05	0.12	0.08	0.09	0.47	0.22	0.28	0.13
MgO	1.97	1.82	2.48	1.90	0.71	0.33	0.25	0.26	0.25	0.20	0.41	0.90	1.22	0.94	0.07
CaO	2.13	1.90	2.06	1.83	1.79	1.73	1.22	1.38	1.27	1.28	0.92	3.79	3.55	3.84	1.95
Na_2O	3.86	3.96	3.79	4.50	3.78	3.54	3.41	3.77	5.03	5.18	4.87	4.97	6.05	5.73	4.66
K_2O	2.43	3.05	2.45	3.54	3.72	3.85	4.23	4.01	4.04	4.32	4.68	3.23	3.55	3.40	4.44
H_2O^-	0.53	0.48	0.49	0.55	0.27	0.49	0.13	0.38	0.06	0.16	0.18	-	-	-	-
H_2O^+	0.11	0.11	0.11	0.15	0.09	0.10	0.07	0.11	0.09	0.09	0.06	0.63	0.85	0.72	0.49
TOTAL	99.89	99.87	99.70	99.72	100.04	100.19	99.37	99.67	99.66	99.87	99.53	98.95	98.98	99.45	98.56

TABLE (IV.2) Continued..

Sample No.	16 P8-148	17 P8-149	18 P8-154	19 P8-163	20 P8-114	21 P8-116	22 P8-117	23 P8-118	24 P8-119	25 P8-121	26 P8-127	27 P8-144	28 P8-139	29 P8-140
SiO_2	63.60	58.91	58.38	65.79	77.74	73.52	75.49	76.09	75.90	74.11	74.13	75.09	75.54	74.19
TiO_2	0.58	1.07	1.08	0.42	0.04	0.08	0.10	0.07	0.07	0.16	0.01	0.21	0.07	0.11
Al_2O_3	13.95	12.94	13.44	15.68	11.05	12.43	11.64	11.88	11.54	11.99	10.61	10.67	12.53	12.49
Fe_2O_3	3.89	4.12	3.50	1.41	0.08	0.61	0.49	0.31	0.52	0.46	2.34	2.10	0.39	1.96
FeO	3.08	7.79	8.19	2.75	1.55	1.57	1.96	1.64	1.77	1.90	2.82	2.63	0.58	1.01
MnO	0.15	0.31	0.24	0.08	0.03	0.07	0.07	0.06	0.06	0.06	0.10	0.15	0.03	0.02
MgO	0.42	1.12	1.19	0.70	0.03	0.09	0.24	0.18	0.04	0.05	0.03	0.14	0.07	0.12
CaO	3.20	3.04	3.09	0.93	0.38	0.49	0.40	0.39	0.36	0.56	0.06	1.58	0.64	0.40
Na_2O	4.99	5.00	5.99	6.35	4.18	4.72	4.45	5.06	4.33	4.62	5.32	4.10	3.98	5.19
K_2O	4.13	3.68	3.21	4.15	4.24	4.69	4.49	4.57	4.58	4.42	3.04	2.78	4.89	3.52
H_2O^-	-	-	-	-	-	-	-	-	-	-	-	-	-	-
H_2O^+	0.50	0.75	0.74	0.57	0.30	0.32	0.21	0.31	0.21	0.28	0.41	0.39	0.51	0.44
TOTAL	99.49	98.73	99.05	98.83	99.69	98.59	99.54	100.56	99.38	98.61	98.87	99.84	99.23	99.45

Abu-Kharif Complex

from 1 to 3 syntectonic granodiorites
4 to 8 late tectonic calc-alkaline granites
9 to 11 post tectonic alkaline granites

Deloro pluton

from 12 to 19 calcic syenite-granite
20 to 27 peralkaline granite
28 to 29 granophyric granite

TABLE IV.3: Selected averages of some chemical analysis of granites at several areas.

%	Strong and Dupuy (1982) Newfoundland, Canada		Average of the geological survey of Egypt (1976)		Average of Nockold's (1954)		
	Grano-diorites	Granites	Grey granites	Gattarian* granites	Grano-diorites	calc alkaline granites	Alkali granites
SiO_2	67.60	73.80	71.44	75.23	66.88	72.08	73.86
TiO_2	0.70	0.25	0.30	0.06	0.57	0.37	0.20
Al_2O_3	14.20	13.40	13.90	13.08	15.66	13.86	13.75
Fe_2O_3	2.22	0.90	1.04	0.69	1.33	0.86	0.78
FeO	3.47	1.21	1.53	0.24	2.59	1.67	1.13
MnO	0.15	0.05	0.10	-	0.07	0.06	0.05
MgO	1.92	0.38	0.86	0.47	1.57	0.52	0.26
CaO	2.57	0.50	2.38	0.92	3.56	1.33	0.72
Na_2O	3.04	3.72	3.98	4.45	3.84	3.08	3.51
K_2O	2.55	5.27	4.22	4.28	3.07	5.46	5.13
P_2O_5	0.13	0.01	0.09	0.01	0.21	0.18	0.14
L.O.I.	0.0	0.90	0.52	0.72	0.65	0.53	0.47
TOTAL	98.55	100.39	99.96	100.18	100.00	100.00	100.00

*Late tectonic granites.

From that diagram (Fig. IV.1), it is obvious that both Abu-Kharif and Deloro granitic samples fall within the area of maximum concentration of analyses of granites from several localities around the world. According to Tuttle and Bowen (1958), "The concentration of the analyses near the centre of the diagram is readily explained if a magmatic history is involved in the origin of most granites."

Accordingly, the granitic rocks of Abu-Kharif and Deloro complexes are considered to possess a magmatic history.

(2) Niggli values:

The calculated Niggli values of the Abu-Kharif and Deloro granitic rocks are given in Tables (IV.5). The calculations were carried out according to the well-known method of Niggli (see for example Barth, 1962), in which the chemical analysis of the rock is the basis for such calculations.

The relatively high values of alk, k and si as well as the low values of c and fm of the examined rocks are due to the relatively high percentage of silica and alkalis and low values of calcium and magnesium. The calcic syenite granites of the Deloro pluton have relatively higher c values. It can be seen that samples of the alkaline granites of the two complexes have alk more than al.

According to Niggli (1939), if alk > al, the excess alk with high si content of the rock usually goes into riebeckite or aegirine. Petrographic studies (Chapter III), have shown that the sole mafic minerals in the alkaline

TABLE (IV.4) Molecular Norm of Abu-Kharif and Deloro granitic rocks

Sample #	1 AK 10	2 AK 26	3 AK 66	4 AK 18	5 AK 40	6 AK 62	7 AK 80	8 AK 99	9 AK 33	10 AK 108	11 AK 113	12 P8-141	13 P8-142
Q	26.61	27.29	27.02	22.47	28.29	32.39	34.12	31.71	27.71	27.39	27.45	29.44	26.86
Or	14.55	18.25	14.70	20.80	22.25	23.10	25.50	24.10	24.10	25.70	27.95	11.50	11.90
Ab	35.15	35.95	34.50	40.20	34.35	32.25	31.25	34.40	36.65	35.40	32.95	26.95	32.70
An	10.70	9.55	10.35	9.05	9.00	8.70	6.20	6.95	-	-	-	1.48	0.05
C	2.47	1.16	2.18	0.06	0.72	0.71	0.72	0.45	-	-	-	-	-
En	5.52	5.08	6.94	5.22	1.98	0.92	0.70	0.74	0.70	0.56	1.14	3.00	4.06
Fs	2.84	0.60	2.24	1.40	2.20	1.00	0.70	1.02	3.62	2.62	3.10	10.68	9.56
Mt	1.67	1.82	1.53	0.60	0.92	0.77	0.69	0.47	-	-	-	6.68	4.70
Il	0.48	0.30	0.36	0.20	0.28	0.16	0.12	0.16	0.28	0.22	0.22	1.8	1.70
Ac	-	-	-	-	-	-	-	-	2.80	3.08	3.12	-	-
Wo	-	-	-	-	-	-	-	-	2.44	2.76	1.84	8.48	8.46
Na meta-silicate	-	-	-	-	-	-	-	-	1.68	2.27	2.22	-	-
TOTAL	100.00	100.00	100.00	100.00	100.00	100.00	100.00	100.00	99.98	100.00	99.99	100.01	99.99
*D.I.	76.31	81.49	76.22	83.47	84.89	87.74	90.87	90.21	88.46	88.49	88.35	67.89	71.46

* D.I.: Differentiation index of Thornton and Tuttle (1960).

TABLE (IV.4) Continued..

Sample #	14 P8-147	15 P8-148	16 P8-149	17 P8-154	18 P8-114	19 P8-117	20 P8-118	21 P8-121	22 P8-139	23 P8-140
Q	20.65	15.85	31.14	27.62	36.94	31.99	31.26	29.32	32.89	30.33
Or	26.18	24.35	13.19	11.4	25.92	26.52	26.97	26.08	28.86	20.79
Ab	39.35	42.18	27.15	32.35	33.22	34.85	35.63	37.05	33.64	43.86
An	2.09	3.48	1.2	0.20	-	-	-	-	0.86	-
C	0.31	3.18	-	-	-	-	-	-	0.38	0.14
En	0.17	1.04	2.75	3.96	0.07	0.6	0.45	0.12	0.17	0.30
Fs	4.64	1.77	9.90	10.96	2.85	3.58	3.02	3.34	0.69	0.09
Mt	2.55	5.64	5.21	4.41	-	-	-	-	-.56	2.85
Il	0.70	1.09	1.8	1.80	0.08	0.20	0.14	0.30	0.14	0.21
Ac	-	-	-	-	0.23	1.43	0.87	1.34	-	-
Wo	2.12	-	6.80	7.30	-	-	-	-	-	-
Na meta-silicate	-	-	-	-	0.43	0.27	1.43	0.12	-	-
TOTAL	98.77	98.58	99.04	100.00	98.84	99.44	99.77	97.67	98.19	98.57
D.I.	86.19	82.38	71.39	71.37	95.18	93.36	93.86	92.45	95.39	94.98

Abu-Kharif complex

From 1 to 3 granodiorite
4 to 8 calc-alkaline granite
9 to 11 alkaline granite

Deloro Pluton

From 12 to 17 calcic syenite-granite
18 to 21 peralkaline granite
22 to 23 granophyric granite

08 37

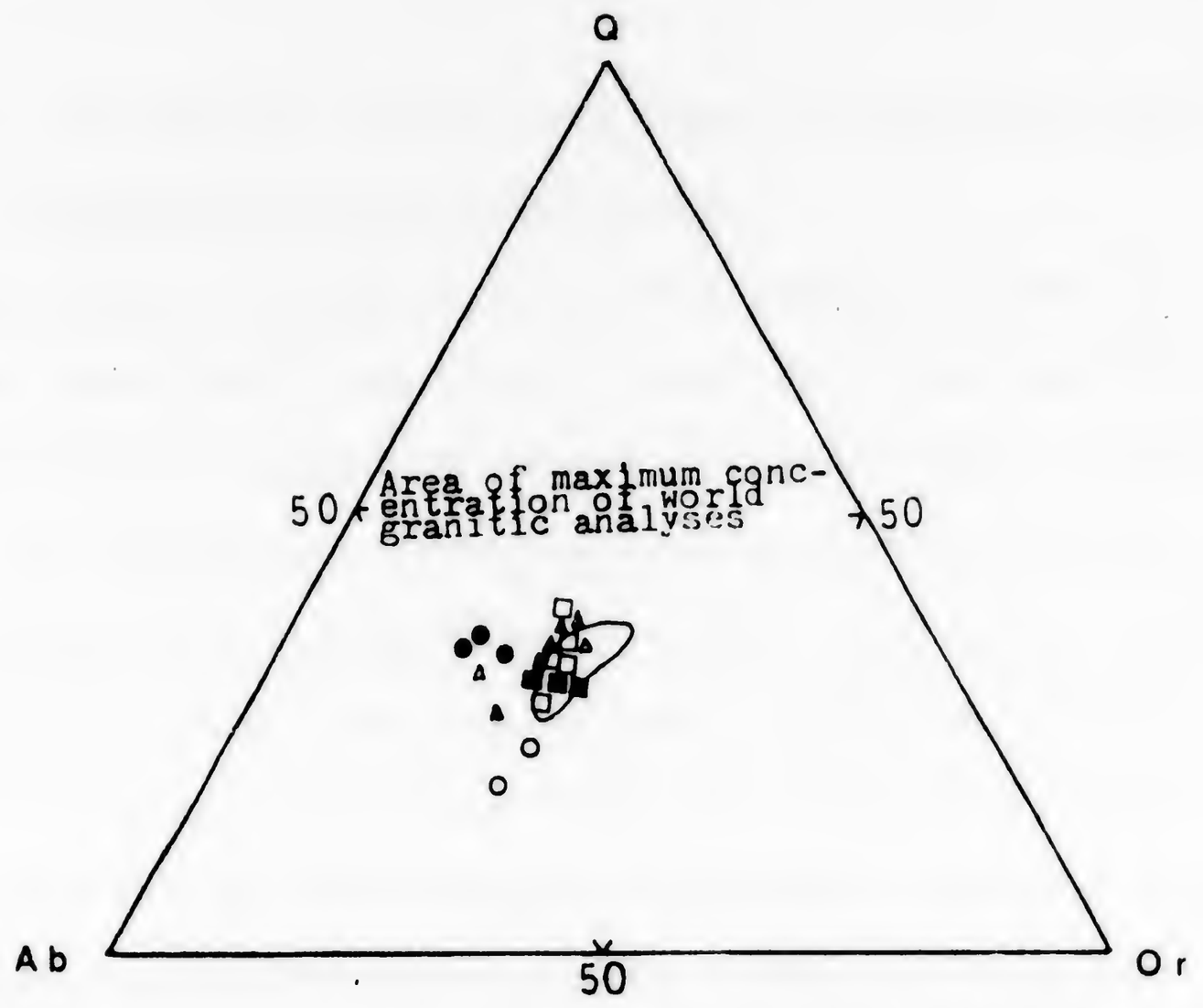

Fig.(IV.1); Orthoclase Quartz-Albite "residua diagram" of the Abu-Kharif and Deloro granitic rocks

SYMBOLS :-

Abu-Kharif granites;

- ● Syntectonic granodiorite
- ▲ Late tectonic calc-alkaline granite
- ■ Post tectonic alkaline granite

Deloro granites;

- o Calcic syenite-granite
- □ Peralkaline riebeckite granite
- △ Granophyric granite

granites at Abu-Kharif complex and some of the Deloro granitic rocks are riebeckites and arfvedsonites.

The relative proportions of the Niggli-values fm, c and alk for Abu-Kharif and Deloro rocks are shown in Fig. (IV.2). The plotted Niggli-values of Deloro granites show a continuous variation in composition from the calcic syenite-granite to the peralkaline and granophyric granites. The plots of the Egyptian rocks, apart from the separate alkaline granite, display a continuous variation from the syntectonic grano-diorites through the calc-alkaline granites. El-Gaby (1975) in his study to the Egyptian granites came to a similar conclusion.

Fig. (IV.3) shows the values of k plotted against values of fm. From this figure, it is clear that most of these rocks have alkaline-potassic tendencies. Deloro granitic rocks show extremely low mg values. The relation-ship between al and fm is shown in Burri and Niggli's diagram (1945) in Fig. (IV.4). It is obvious that the character of both Abu-Kharif and Deloro magmas are salic. The calcic syenite-granites of Deloro pluton are concentrated near the semi-femic field while the Egyptian syntectonic grey granites seem to concentrate near the semi-salic field.

The si values are plotted against the al, alk and fm values of Niggli, in Fig. (IV. 5a,b and c). These figures show that al and alk values increase proportionally with si in both Deloro and Abu-Kharif granitic rocks and reveal more or less parallel trends. The fm values of all

TABLE (IV.5) Niggli Values of the Abu-Kharif and Deloro granitic rocks

Sample No.	1 AK 10	2 AK 66	3 AK 26	4 AK 40	5 AK 80	6 AK 99	7 AK 18	8 AK 63	9 AK 113	10 AK 108	11 AK 33	12 P8-141	13 P8-142	14 P8-143	15 P8-147
si	301.02	331.40	304.59	332.40	368.47	419.05	456.29	436.73	401.22	402.60	451.89	183.80	187.60	197.24	317.35
al	38.71	39.46	37.65	39.99	42.42	45.65	46.43	46.27	35.07	35.49	35.30	23.71	25.94	26.69	35.89
fm	28.27	24.00	29.78	80.19	17.13	10.81	9.26	8.84	17.30	14.39	17.49	41.28	35.86	33.95	20.65
c	9.95	9.51	9.66	9.10	9.75	10.43	7.90	8.63	7.36	8.01	5.36	12.99	12.30	13.69	9.63
alk	23.07	27.03	22.92	30.73	30.29	33.12	36.30	36.27	40.28	42.12	41.85	22.02	25.90	25.67	33.83
ti	1.12	0.74	0.85	0.49	0.76	0.47	0.41	0.48	0.81	0.61	0.65	2.59	2.47	2.85	1.29
k	0.29	0.34	0.30	0.34	0.39	0.42	0.45	0.41	0.35	0.35	0.39	0.30	0.27	0.28	0.39
mg	0.45	0.53	0.54	0.65	0.31	0.26	0.24	0.26	0.12	0.11	0.19	0.10	0.16	0.14	0.02
c/fm	0.35	0.40	0.32	0.45	0.57	0.96	0.85	0.98	0.43	0.56	0.31	0.31	0.34	0.40	0.47
qz	+108.7	+123.4	+112.9	+109.5	+145.7	+186.6	+211.1	+191.7	+140.1	+134.1	+134.5	-4.3	-15.98	-5.44	+82.03
*	1.52	1.76	1.46	2.26	1.91	1.83	1.80	1.90	2.63	2.88	2.94	4.67	5.92	3.11	3.18

TABLE (IV.5) Continued...

Sample No	16 P8-148	17 P8-149	18 P8-154	19 P8-163	20 P8-114	21 P8-116	22 P8-117	23 P8-118	24 P8-119	25 P8-121	26 P8-127	27 P8-144	28 P8-139	29 P8-140
si	250.74	198.88	191.13	280.00	515.23	423.16	447.27	443.30	466.37	435.65	419.86	421.05	473.52	422.11
al	32.40	25.74	25.93	39.34	43.13	42.15	40.60	40.77	41.78	41.53	35.40	35.27	46.29	41.88
fm	24.65	38.98	37.53	19.02	9.45	11.26	14.33	11.25	12.13	12.06	24.05	23.03	5.67	14.31
c	13.51	10.99	10.83	4.21	2.68	3.03	2.52	2.44	2.35	3.53	0.36	9.50	4.31	2.41
alk	29.44	24.29	25.70	37.43	44.73	43.55	42.55	45.55	43.73	42.89	40.19	32.20	43.73	41.39
ti	1.72	2.72	2.65	1.35	0.20	0.01	0.44	0.31	0.32	0.69	0.01	0.88	0.33	0.47
k	0.35	0.33	0.26	0.30	0.40	0.40	0.40	0.37	0.41	0.39	0.27	0.31	0.45	0.31
mg	0.10	0.14	0.16	0.23	0.03	0.06	0.15	0.14	0.03	0.04	0.01	0.05	0.11	0.07
c/fm	0.55	0.28	0.29	0.22	0.28	0.27	0.18	0.22	0.19	0.29	0.01	0.41	0.76	0.17
qz	+32.98	+1.72	-11.67	+30.28	+236.3	+148.96	+177.1	+161.1	+191.45	+164.09	+159.10	+192.25	+198.6	+159.55
* б	4.03	4.73	5.50	4.83	2.03	2.90	2.46	2.80	2.40	2.62	2.24	2.14	2.41	2.43

sample numbers are the same as in Table (IV.2)

* Rittmann alkali index (б)

Fig.(IV.2); Ternary diagram showing the relative proportions of the Niggli-values fm,c and alk.
Symbols as in fig.(IV.1).

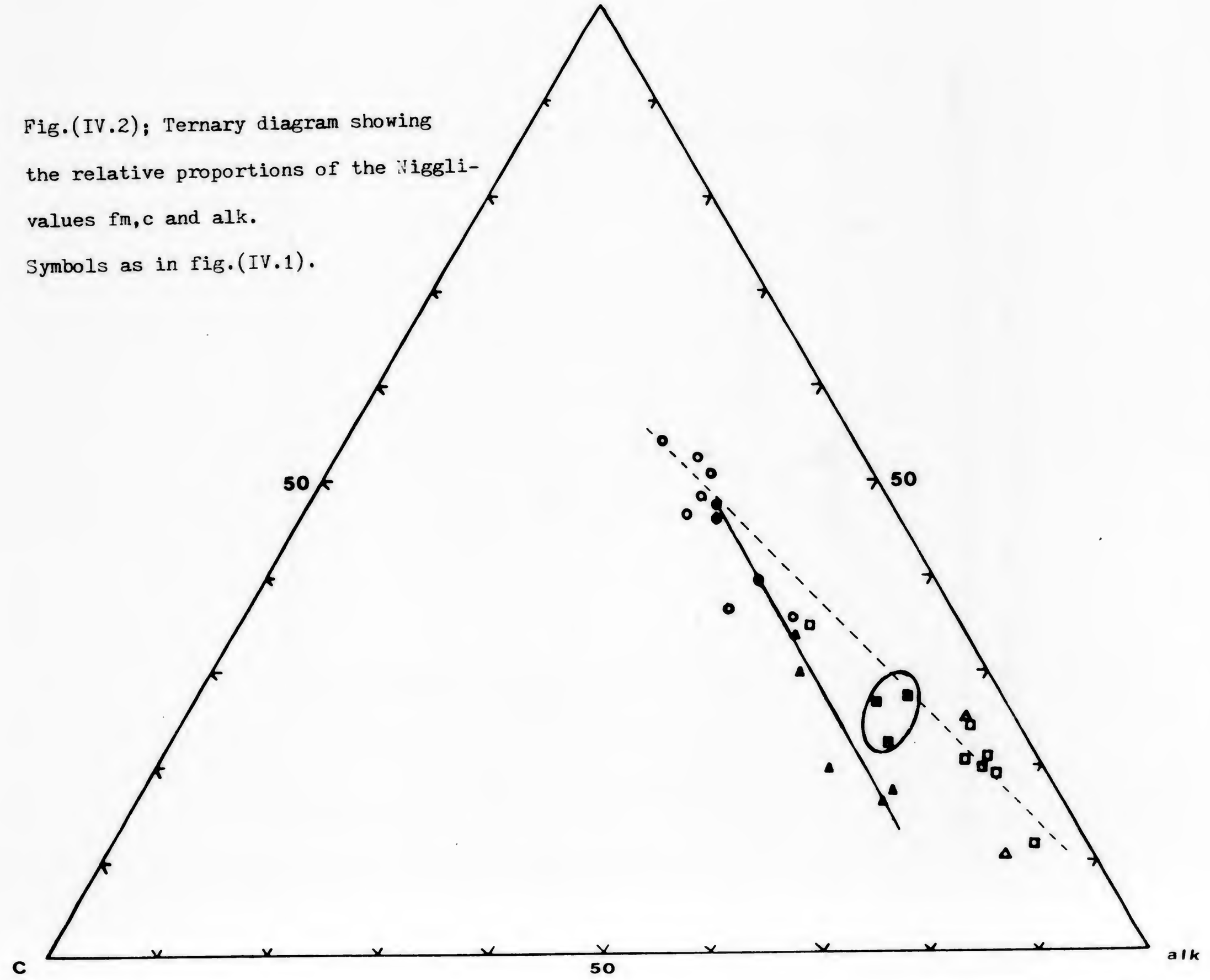

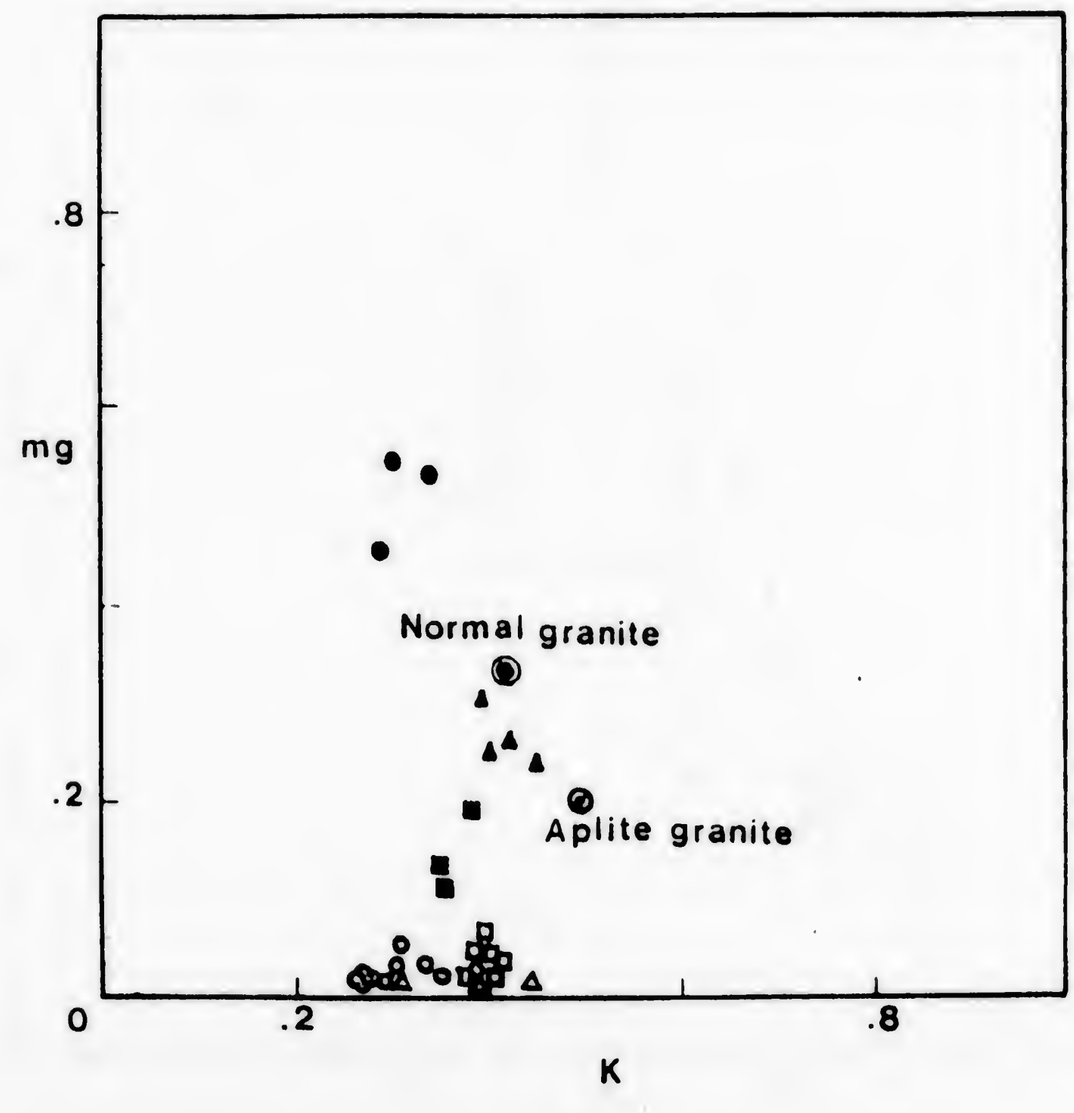

Fig.(IV.3); The k-mg relationships in the Deloro and the Abu-Kharif granitic rocks. Symbols as in fig.(IV.1).

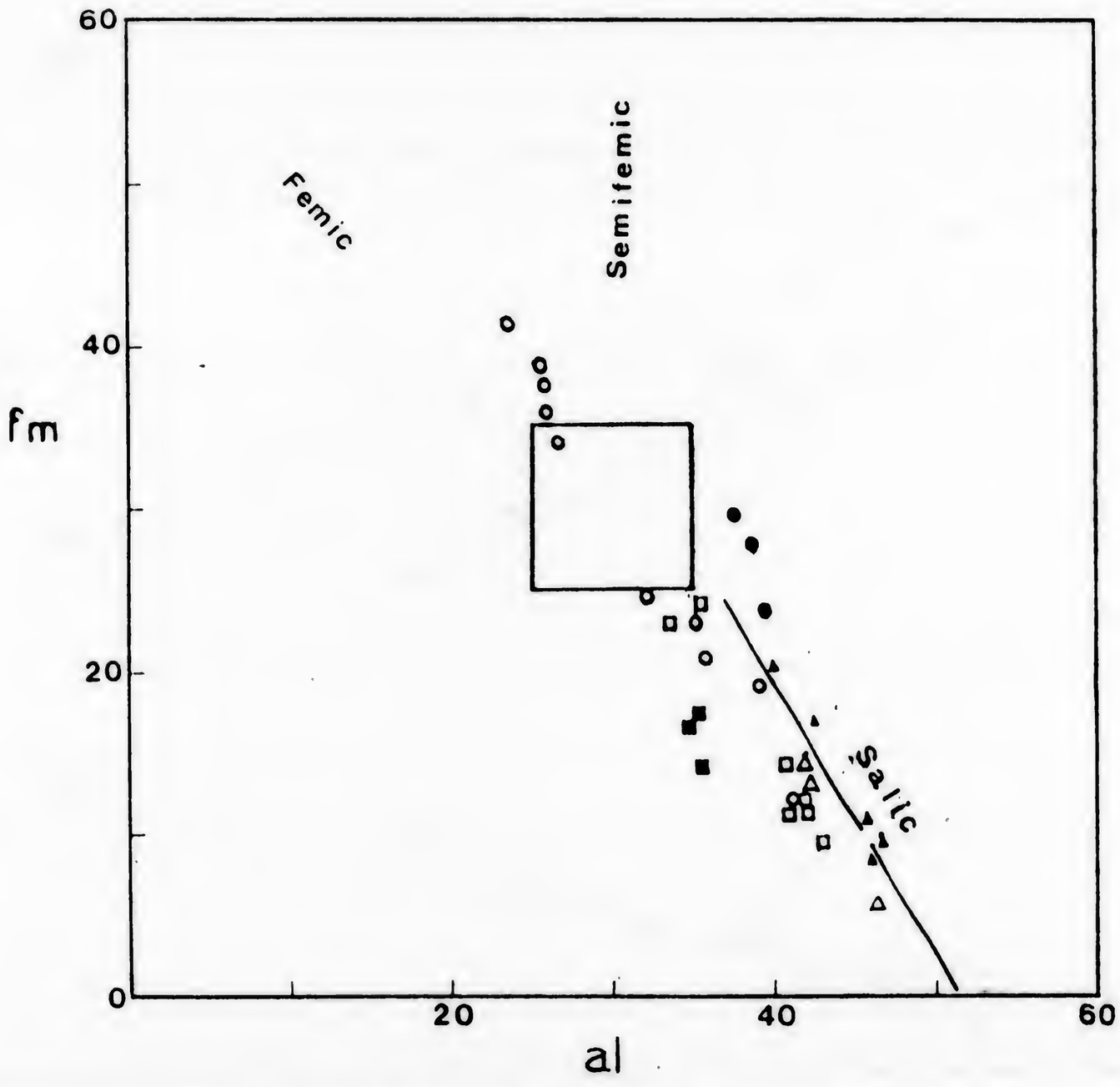

Fig.(IV.4); Relationships of al and fm in the studied granitic samples.

Symbols as in fig.(IV.1).

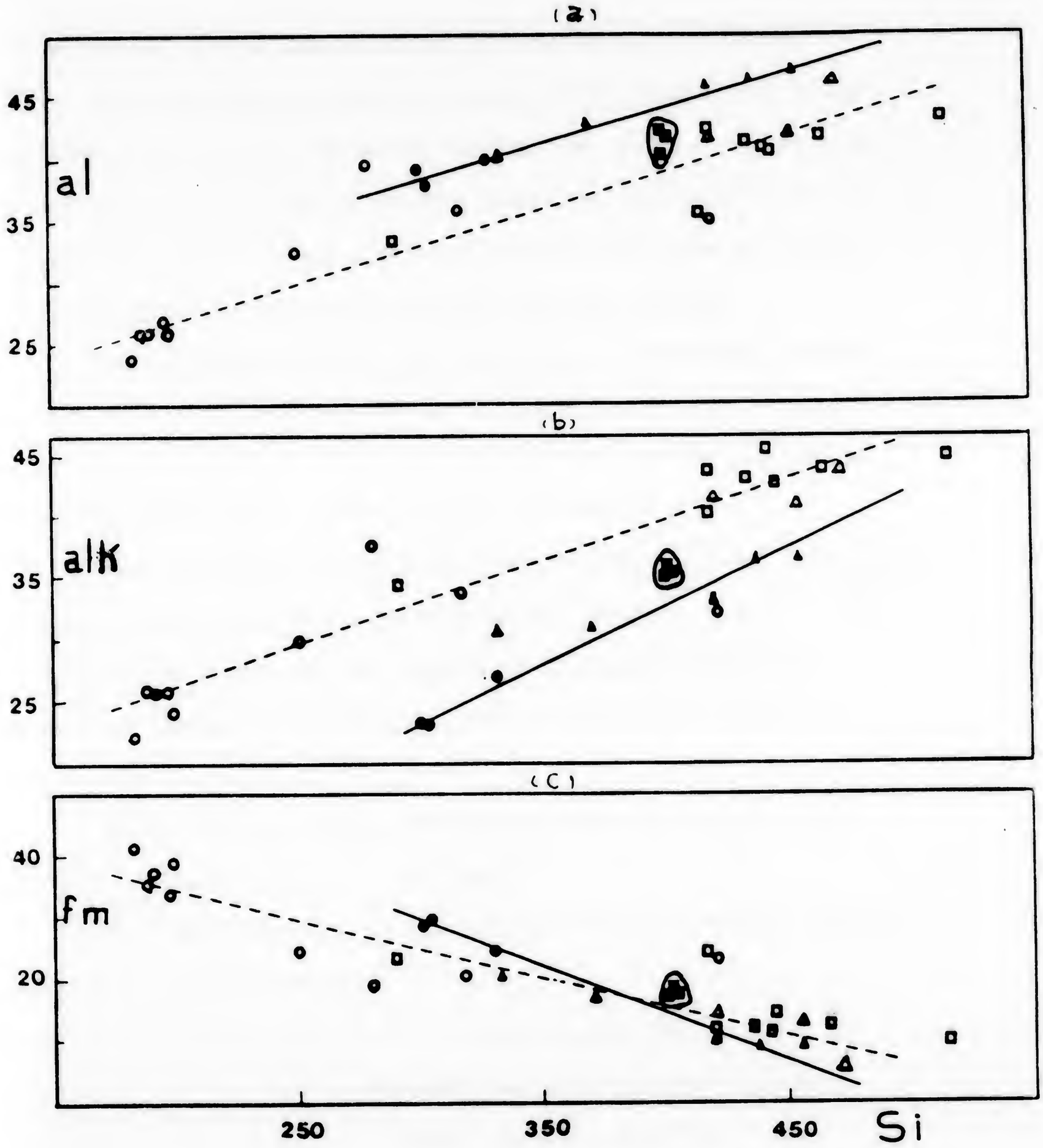

Fig.(IV.5); Relations of Si versus al, alk and fm in the Abu-Kharif and Deloro granites. Symbols as in fig.(IV.1)

the examined rocks decrease with increasing si values.

The Abu-Kharif granitic rocks show higher al values and lower alk values relative to Deloro rocks. It is clear that the Egyptian post-tectonic alkaline granites plot in a separate field either above or below the general trend.

(3) The serial character of the granitic rocks:

The alkali content has long been recognized as one of the more significant chemical characteristics used to determine the serial character of igneous rocks, which is revealed from alkali index (ϭ) of Rittman (1957).

The plotting of alkalies ($Na_2O + K_2O$, wt.%), against silica of the examined rocks is shown in Fig. (IV.6). In this diagram, most of the curves follow approximately parabolic trends and point toward a focus that lies at SiO_2 = 43%.

Table (IV.5) shows the calculated (ϭ values) for samples of both granitic complexes.

The quantitative subdivisions of the Rittman alkali index (ϭ) is cited below:

ϭ	Rock Character
< 1	Extreme pacific (super-calcic)
1 to 1.8	Strong pacific (calcic)
1.8 to 3	Medium pacific (calc-alkalic)
3 to 4	Weak pacific (sub calc-alkalic)

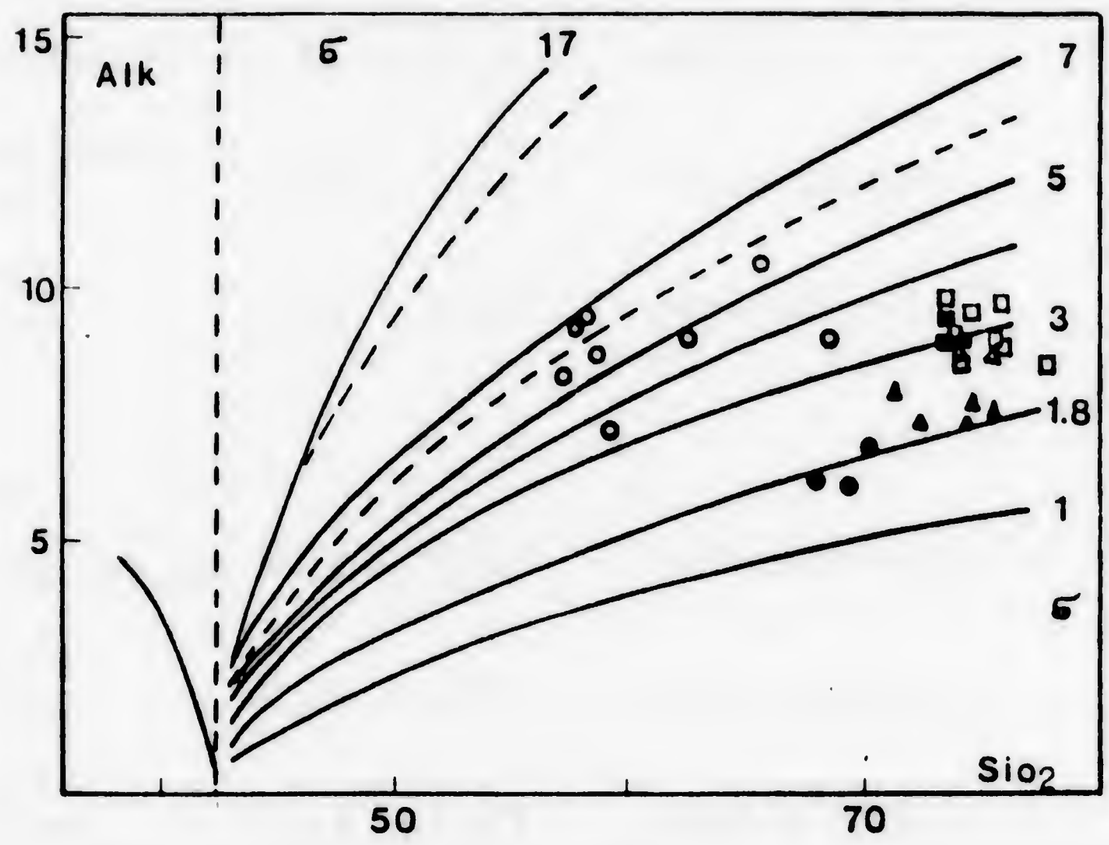

Fig.(IV.6); The alkali-index σ diagram of Rittmann (1962), for the studied granitic rocks. The parabolic curves are loci of constant σ -values. Symbols as in fig.(IV.1).

On the average, the petrochemical characters of Abu-Kharif and Deloro granitic rocks are as follows:

Rock Type	σ values	Rock Character
Abu-Kharif granites		
granodiorites	1.46 - 1.76	calcic
calc-alkaline granites	1.80 - 2.26	calc-alkalic
alkaline granites	2.63 - 2.94	calc-alkalic
Deloro granites		
syenite-granites	3.11 - 5.92	sub-calc-alkalic
riebeckite granites	2.03 - 2.9	calc-alkalic
granophyric granites	2.41 - 2.43	calc-alkalic

(4) Differentiation of the granitic rocks:

The differentiation index is a measure of the leucocratic nature of the rock. During the early course of differentiation of a silicate melt, the mafic minerals tend to crystallize out first, whereas enrichment takes place in quartz, albite and k-felspar compositions in the melt.

Thornton and Tuttle (1960) defined the differentiation index (D.I.) as the sum of normative quartz + albite + orthoclase. They also used Daly's data for average composition of igneous rocks to compute the following D.I. values; alkali granites 93, granite 80, and granodiorite 67.

The D.I. calculated for both Abu-Kharif and Deloro granitic rocks are given in Table (IV.4). The D.I. for Abu-Kharif granitic rocks ranges between 76.2 and 90.9, indicating a highly differentiated magma for the granitic rocks. Deloro granitic rocks have D.I. values as follows:

calcic syenite-granite	ranged between 67.9 and 86.2
peralkaline granite	ranged between 92.5 and 95.2
granophyric granite	ranged between 94.9 and 95.4

It is clear the the leucocratic nature of granophyric granites is more than that of the peralkaline granite, however, calcic syenite-granite is relatively less differentiated. Values of D.I. suggest also that both peralkaline granite and granophyric granites of Deloro pluton are more differentiated than Abu-Kharif alkaline granites. Variation diagrams of D.I. versus major elements, Trace elements and some of the REE for the examined rocks will be dealt with in the following section on geochemistry.

Geochemistry
of the Abu-Kharif and Deloro granitic rocks

The elemental abundances of the major elements were calculated from the chemical analyses given in Table (IV.2). The concentrations of the determined trace elements for the examined granitic rocks of both Abu-Kharif and Deloro plutons are given in Table (IV.6).

From the obtained data, the variation diagram showing the relationship between the ionic weight percentage Ca, Na and k is given in Fig. (IV.7). Apart from the Abu-Kharif alkaline granite, which plots separately, a continous variation is well displayed in both granitic rocks of the two plutons. A general trend of variation can be perceived which is markedly convex towards the k apex. Other diagrams illustrating the behaviour of the major and some of the trace elements including REE's are also constructed.

The variation of these elements with the differentation index will also be discussed.

(A) Major Elements

Silicon and Aluminium

Silicon is the most abundant element - after oxygen - in the studied granitic rocks. Variation diagrams of the major elements versus D.I. are given in Fig. (IV.8). The plots of SiO_2 against D.I. indicate that in both Abu-Kharif and Deloro granitic rocks, SiO_2 increases with increase of the differentiation index.

94

Fig.(IV.7); Variation diagram showing variation in relative proportions of Ca, Na and K. Symbols as in fig.(IV.1).

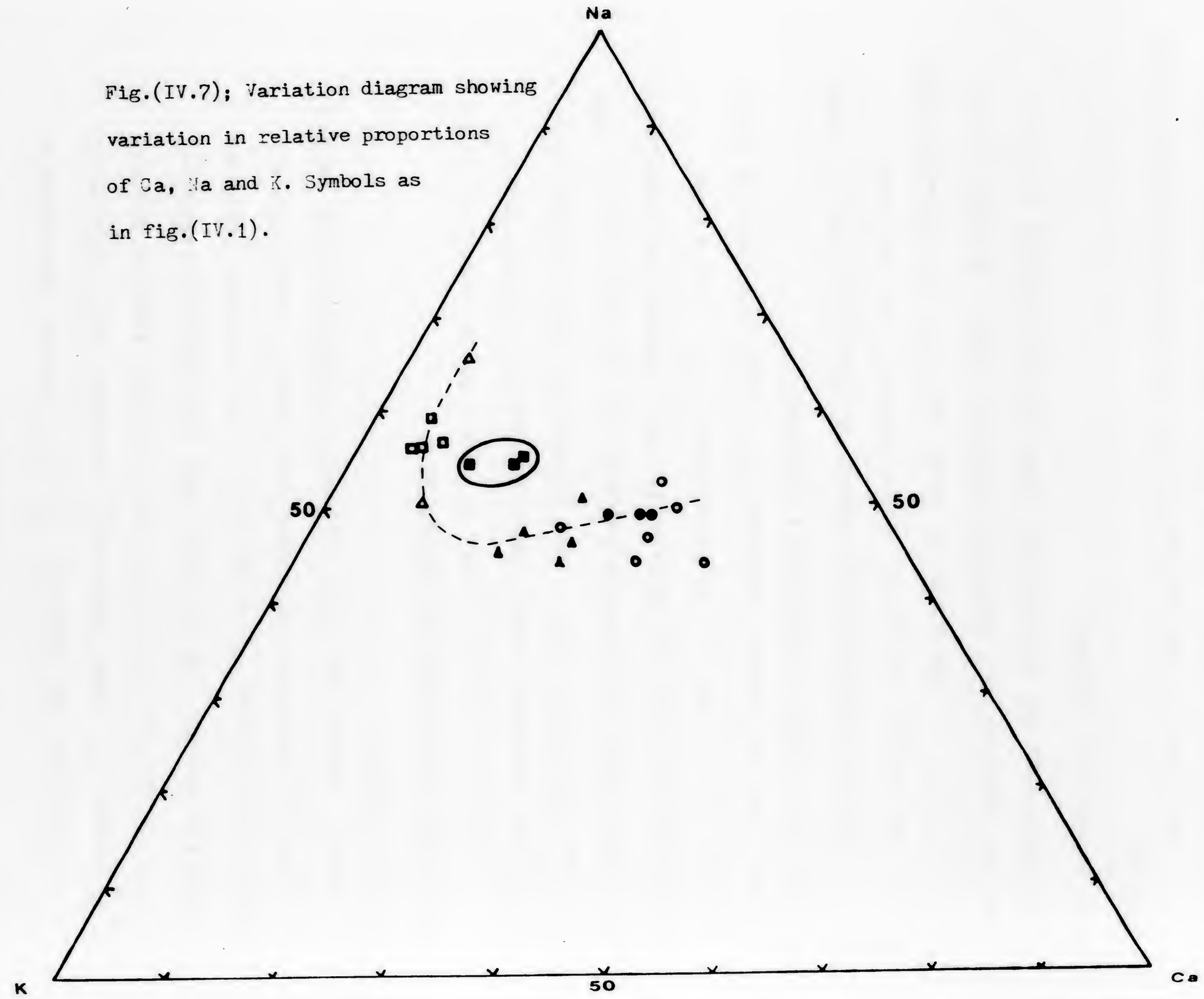

Excluding the Egyptian alkaline granite, the plots of Al_2O_3 versus D.I. show that Al_2O_3 increases with decreasing of D.I. in Abu-Kharif granites while Deloro samples display a parallel trends. It is clear that the Egyptian alkaline granite which occurs in a separate field is highly depleted in Aluminium, however, the other two granitic varieties of Abu-Kharif complex are more enriched in Aluminium than Deloro granitic rocks.

Total iron, Magnesium and Manganese

From the chemical point of view, Deloro granitic rocks are highly depleted in MgO contents relative to Abu-Kharif granites (see Table IV.2). The content of femic oxides (Fe_2O_3+ FeO + MnO + MgO) are plotted against D.I. in Fig. (IV.8). The plots indicate that the content of femic oxides show continuous decrease toward the more differentiated end. It is also obvious that the Deloro granites have higher contents of femic oxides than those of Abu-Kharif granites.

Deloro granitic plots exhibit a continuous smooth trend. Due to the higher content of mafic oxides in the Egyptian alkaline granite, the plots of these granites lie somewhat above the grey granite-calc alkaline granitic trend. El-Gaby (1975) concluded that the peralkaline rocks differ markedly in their high total iron content.

Calcium

The plots of CaO versus D.I. of the studied granitic rocks is shown in Fig. (IV.8). It is clear that the calcium content decreases with increase of D.I. in Deloro granites. With the exception of the alkaline granite of Abu-Kharif granitic com-

plex which has relatively low CaO content, the plots of CaO versus D.I. show a similar trend, i.e., CaO decreases with increasing D.I.

In general, Deloro syenite-granite exhibit the highest CaO contents of all the rocks studied.

Sodium and Potassium

The Deloro granitic rocks, in comparison, are markedly enirched in their sodium and potassium contents with respect to Abu-Kharif granites.

The plots of sodium and potassium versus the D.I. are shown in Fig. (IV.8). Within the granitic rocks of the Abu-Kharif complex, Sodium is constant in both granodiorites and calc-alkaline granites. The alkaline granites, again, lie in a separate field with higher Sodium content. The plots of Deloro granites show a very slight decrease in Na_2O content with the increase in the D.I. due to the predominance of Na-amphibole in both syenite-granite and peralkaline granite.

The plots of Potassium in the Deloro granites show that K_2O increases with D.I.. The plots of Abu-Kharif syntectonic granodiorites and late tectonic calc-alkaline granites exhibit a continuous increase in K_2O with differentiation, however, the post tectonic alkaline granites lie somewhat above the main trend.

In summary, it is obvious that, with the exception of the Egyptian alkaline granite, the SiO_2 and K_2O of the studied granitic rocks increase with the increase of differentiation.

The Al_2O_3, femic oxides and CaO decrease with D.I..
The Na_2O is constant within Abu-Kharif samples and decreases slightly with differentiation in the Deloro rocks.

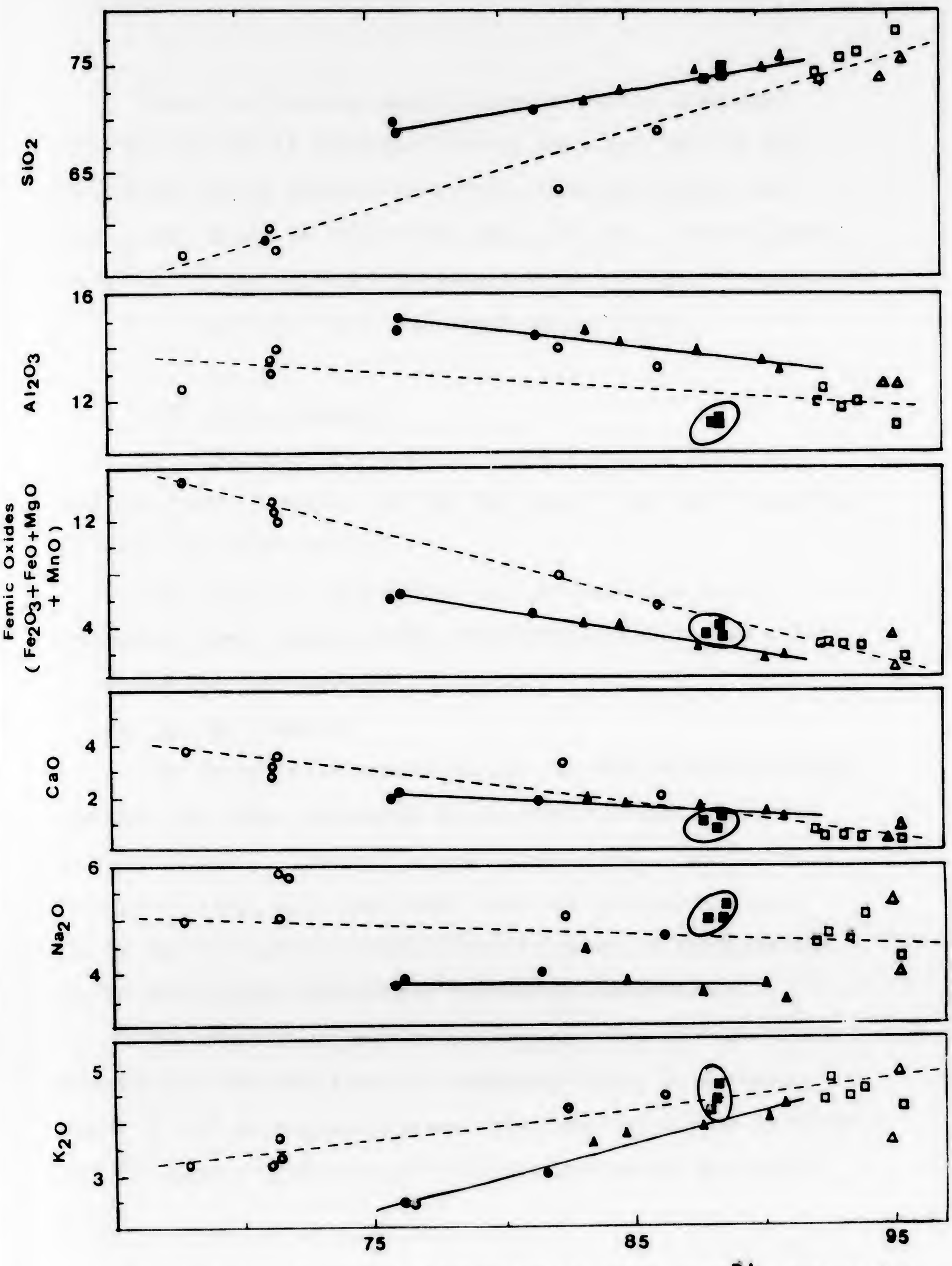

Fig.(IV.8); Variation diagram of major oxides (in weight persent), against D.I. for the Abu-Kharif and Deloro granitic rocks. Symbols as in fig.(IV.1)

From the previous description it can be concluded that the Abu-Kharif alkaline granite does not fall on the continuous smooth trend of the other granitic types, but lies either above or below that smooth trend. This suggests there may be two different populations or groups, a conclusion that is in agreement with our field observations.

(B) Trace Elements

The abundance (in ppm) of trace elements for the studied granitic samples of the Abu-Kharif and Deloro plutons are given in Table (IV.6).

The elemental abundances and the behavior of the determined trace elements may conveniently be studied under the following five groups.

1. Ba, Sr, Rb, and Cs

The large ion elements Rb, Sr, Ba and Cs are discussed together for their abundance is generally directly related to the feldspars. Nockold's and Allen (1953), Berlin and Henderson (1969) have concluded that the greater part of the Sr and Ba content of the granitic rocks is concentrated in the plagioclase and potash feldspars respectively.

The results of this study reveals that the more basic varieties of the two granitic complexes have, in general, higher Sr and Ba concentrations, and lower Rb and Cs contents than the more differentiated granitic varieties (see Table IV.6).

TABLE (IV.6) Trace-elements concentrations (ppm) in whole rock samples from the Abu-Kharif and Deloro granitic rocks

No.	1 AK 10	2 AK 26	3 AK 66	4 AK 18	5 AK 40	6 AK 62	7 AK 80	8 AK 99	9 AK 33	10 AK 108	11 AK 113	12 P8-141
Rb	21.36	29.86	38.22	88.32	104.95	52.9	101.90	98.06	56.27	64.87	40.45	37.18
Sr	578.81	502.85	425.69	36.30	302.31	26.16	217.44	230.50	19.26	20.90	25.97	112.65
Ba	455.10	516.17	547.64	198.94	906.7	538.20	477.43	689.20	264.70	312.70	347.59	826.70
Cs	0.40	0.21	0.42	0.80	1.20	0.69	1.30	1.02	0.33	0.43	0.42	0.64
Cr	33.62	25.88	13.45	7.60	11.70	9.99	36.66	19.22	11.91	10.93	12.43	37.81
Sc	12.73	10.49	5.16	1.52	2.13	1.57	2.23	1.46	0.77	0.82	1.23	7.23
Co	11.53	7.54	4.32	1.26	3.15	1.42	4.39	2.56	2.23	2.21	1.96	5.65
Zr	179.63	133.83	292.74	158.45	287.84	229.90	273.16	157.67	737.04	1103.48	1118.26	505.40
Hf	5.11	4.39	10.16	8.44	8.77	18.69	9.39	6.26	17.44	23.90	21.77	10.87
Ta	0.66	0.51	0.66	3.57	1.85	7.59	1.51	1.87	3.81	5.19	3.66	1.03
Y	21.58	13.91	14.91	26.38	15.44	51.31	15.03	13.87	57.72	77.35	55.45	93.20
U	0.63	0.19	0.33	0.95	1.67	0.97	1.70	8.50	0.73	0.07	0.55	0.71
Th	4.76	2.55	7.08	8.57	9.60	6.57	11.28	12.34	4.06	6.96	5.66	0.50

TABLE (IV.6) Continued...

No.	13 P8-142	14 P8-147	15 P8-148	16 P8-149	17 P8-154	18 P8-114	19 P8-117	20 P8-118	21 P8-121	22 P8-139	23 P8-140
Rb	25.24	66.33	43.53	54.69	34.03	26.29	81.92	118.27	94.25	123.95	54.49
Sr	103.02	30.16	71.81	59.68	109.93	3.09	15.52	14.66	11.75	18.98	21.6
Ba	659.15	414.69	688.68	792.15	892.71	532.80	777.45	635.80	520.96	459.97	301.28
Cs	0.29	0.42	0.46	0.36	0.35	0.46	0.31	0.54	0.36	0.36	0.33
Cr	64.85	99.40	73.85	47.93	41.58	58.89	34.90	35.59	47.93	118.47	137.77
Sc	7.32	0.45	3.71	6.26	7.82	0.67	2.20	0.73	6.26	1.38	1.59
Co	3.50	1.57	2.97	4.17	4.21	1.73	1.34	1.20	4.17	1.45	1.52
Zr	292.00	741.44	712.02	546.18	407.08	249.53	1120.60	686.32	573.75	290.44	329.34
Hf	7.47	18.98	19.08	14.57	11.21	29.30	28.83	30.35	14.57	9.82	10.50
Ta	0.79	2.37	2.87	1.54	1.10	4.47	3.28	6.16	1.54	1.70	1.68
Y	76.76	123.77	141.50	118.84	97.86	99.63	219.45	330.82	158.84	105.83	97.99
U	0.95	0.56	0.15	0.14	0.22	0.49	2.26	5.36	2.63	2.21	2.97
Th	0.77	6.19	5.90	3.90	1.96	1.77	19.37	25.13	14.66	18.30	15.29

Samples from Abu-Kharif complex

from 1 to 3 syntectonic granodiorites
4 to 8 late-tectonic calc-alkaline granite
9 to 11 post-tectonic alkaline granite

Samples from Deloro pluto

From 12 to 17 calcic syenite-granite
18 to 21 peralkaline granite
22 to 23 granophyric granite

Figure (IV.9) shows the variation of Ba versus Sr and Rb versus Cs. It is obvious that Abu-Kharif granites show a wide variation in Ba, Sr, Rb and Cs concentrations. It is also clear that the syntectonic granodiorites have the highest Sr and the lowest Rb and Cs contents. The calcic syenite-granite of the Deloro pluton behaves similarly to the Abu-Kharif granodiorites in his granitic series (i.e., it has the highest Ba, Sr and the lowest Rb and Cs contents).

From Figure (IV.9b), it is also seen that the Abu-Kharif granitic rocks display a relative increase in their Rb contents with increasing Cs from the granodiorites through the alkaline granites to the calc-alkaline granites which possess the highest Rb and Cs contents. Meanwhile, the Deloro granitic rocks have a relatively constant Cs values. Figure (IV.10) shows the variation of D.I. against Sr, Rb and other elements. The curves show a gradual increase in Rb with increasing values of D.I. in the studied granites, while Sr decreases. The Egyptian alkaline granite lies below the general trend as it is depleted in Sr. In 1973, Sayyah *et al*. reported Sr values as low as 8 ppm. in some Egyptian younger granites.

Figure (IV. 11) shows the variation of Ba and Sr with K. The plots of Abu-Kharif and Deloro granitic rocks indicate that both Ba and Sr contents decrease with increasing K values. Gindy *et al*. (1979) also showed that Ba and Sr behave in a similar substitional way with respect to K.

Fig.(IV.9a); Ba-Sr variation diagram for the analysed rocks

Fig.(IV.9b); Rb-Cs variation diagram for the studied granites.
Symbols as in fig.(IV.1)

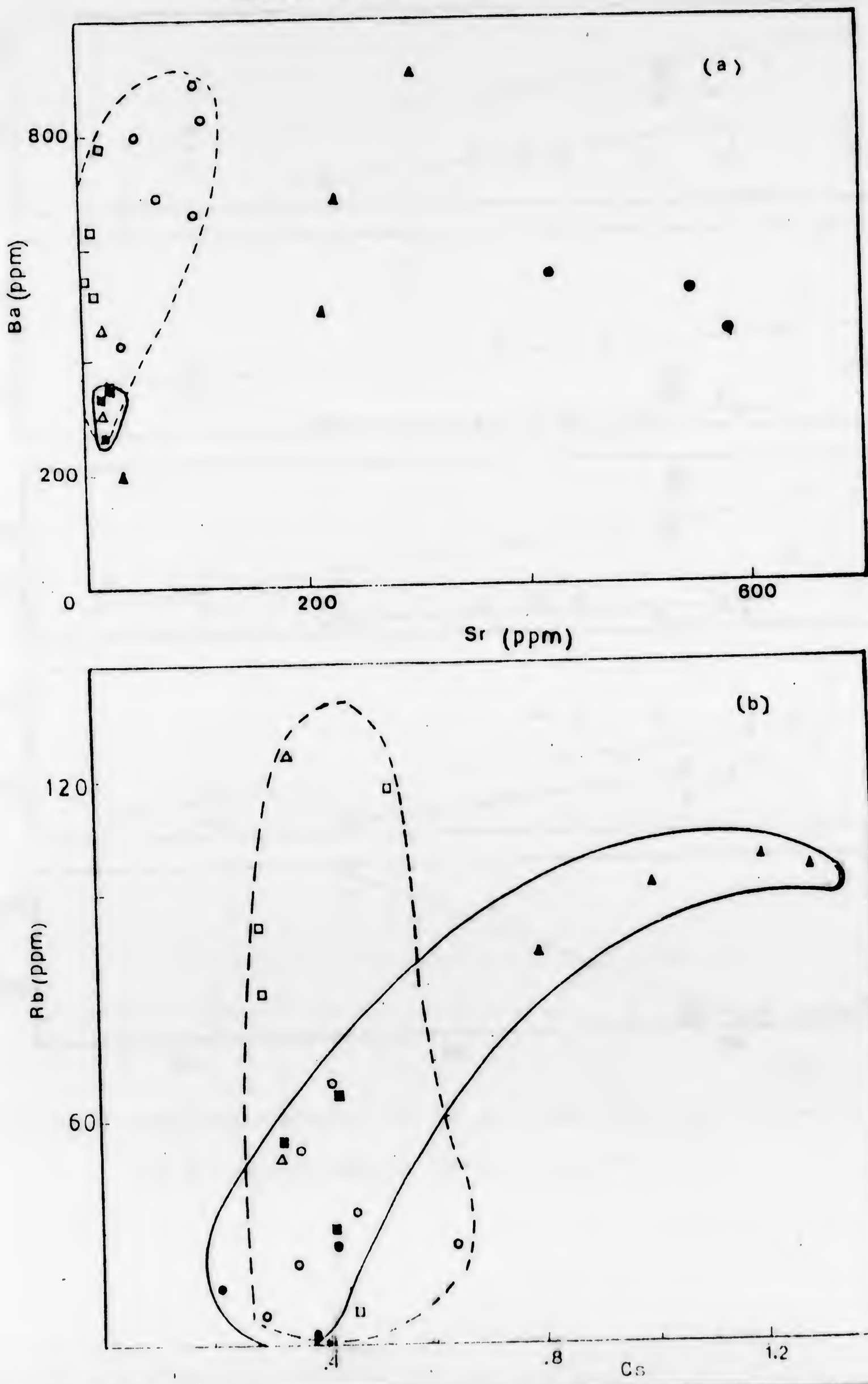

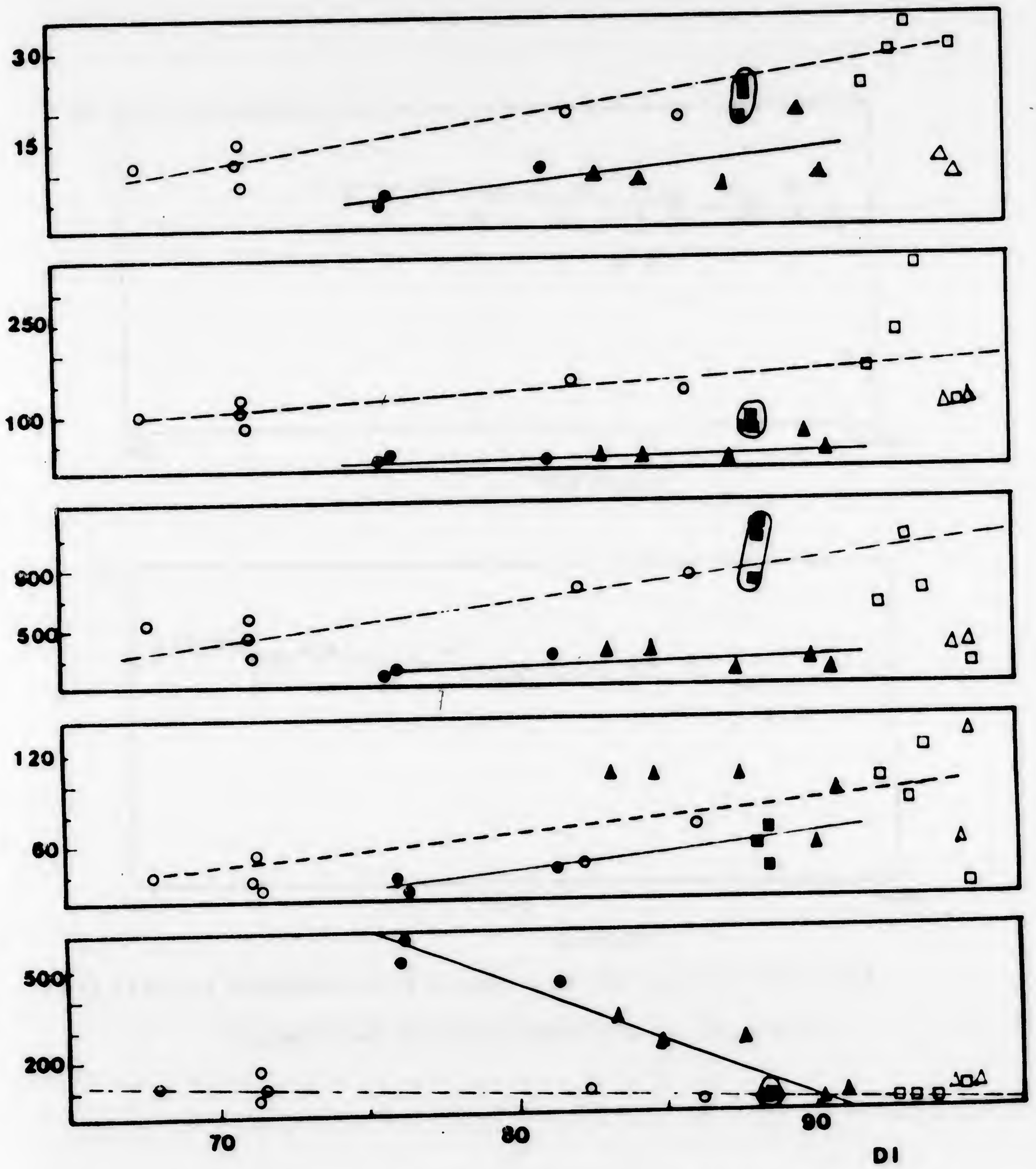

Fig.(IV.10); Variation diagram of Sr, Rb, Zr, Y and Hf (in ppm), versus D.I. for the studied samples. Symbols as in fig.(IV.1).

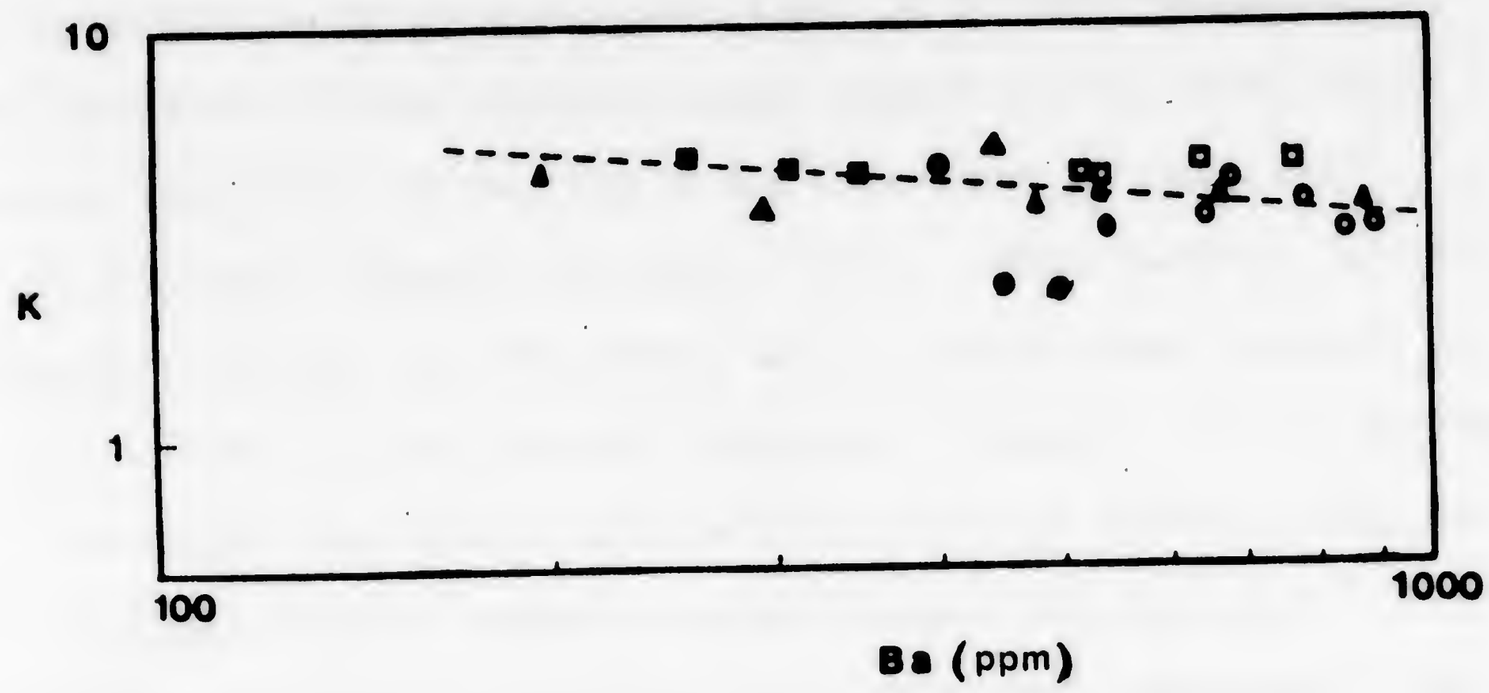

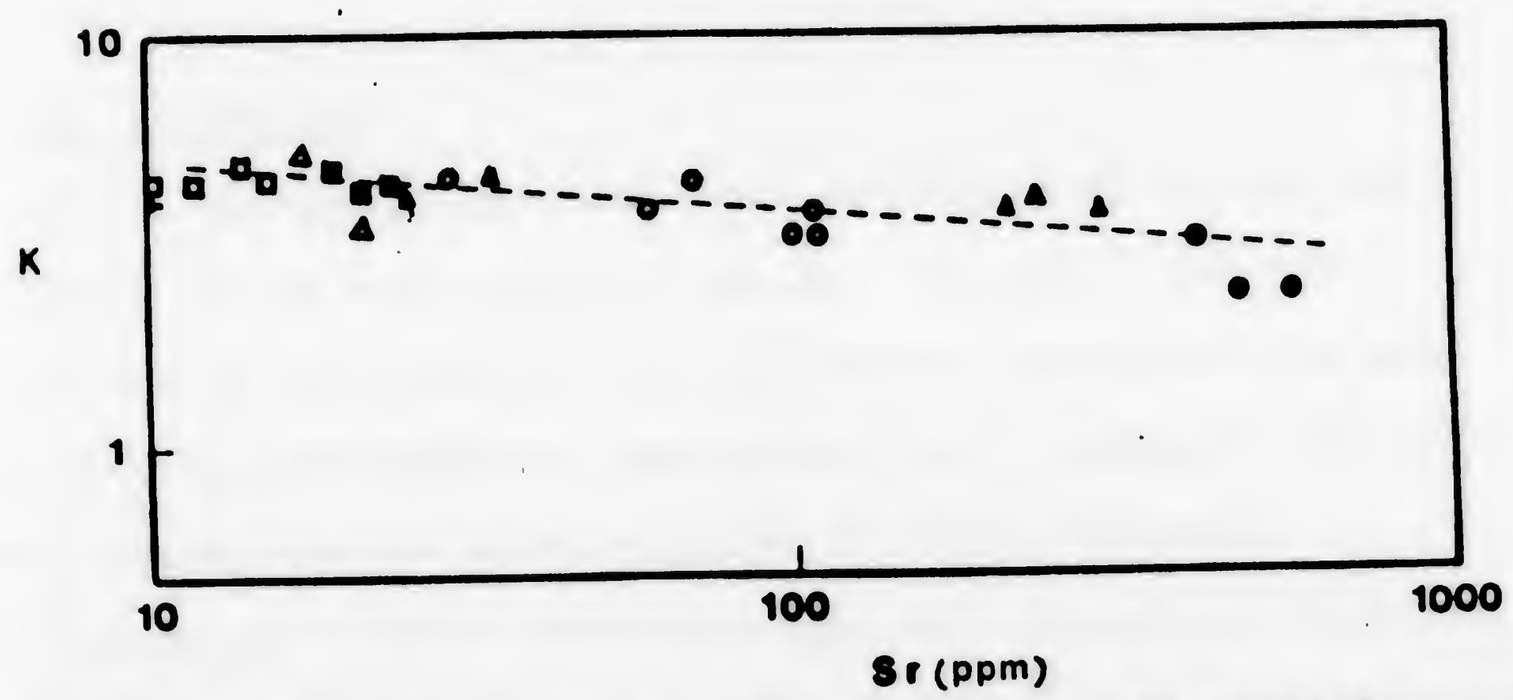

Fig.(IV.11); Variation of Sr contents and Ba contents with K for the examined granites. Symbols as in fig.(IV.1).

The maximum concentration of Sr in the granitic rock series would occur earlier than that of Ba and consequently the depletion of the crystallizing magmas in Sr would start earlier than that in Ba, while Rb increases in the late potash feldspar phases (El-Gaby, 1975). This feature is well displayed in Fig. (IV.12) where the relative distribution of Sr, Ba and Rb in the studied granites is shown. It is obvious that both the Abu-Kharif and Deloro granites exhibit more or less similar trends, namely convex toward the Ba apex. Meanwhile, the Deloro granites are relatively enriched in Ba.

2. Cr, Sc and Co

Cr, Sc and Co are much more concentrated in the basic varieties of the two granitic series. Maximum concentrations for Sc and Co are found in the Abu-Kharif granodiorites and in Deloro syenite-granite (see Table IV.6), however, the more acidic varieties are less enriched in these elements. Fourcade et al. (1981) concluded that all transition elements are much more concentrated in mafic rocks than in granodiorites.

Figure (IV.13) shows the variation of Cr, Sc, and Co versus the differentiation index. It is obvious that Sc and Co show a continuous decrease with increase of the differentiation index. Chromium displays a similar trend in the Abu-Kharif rocks, but it shows no apparent relationship in Deloro granitic series. The slope difference in the trend of Abu-Kharif and Deloro granitic rocks is due to the

Fig.(IV.12); Ternary diagram showing relative distribution of Sr, Ba and Rb in the studied granites.
Symbols as in fig.(IV.1).

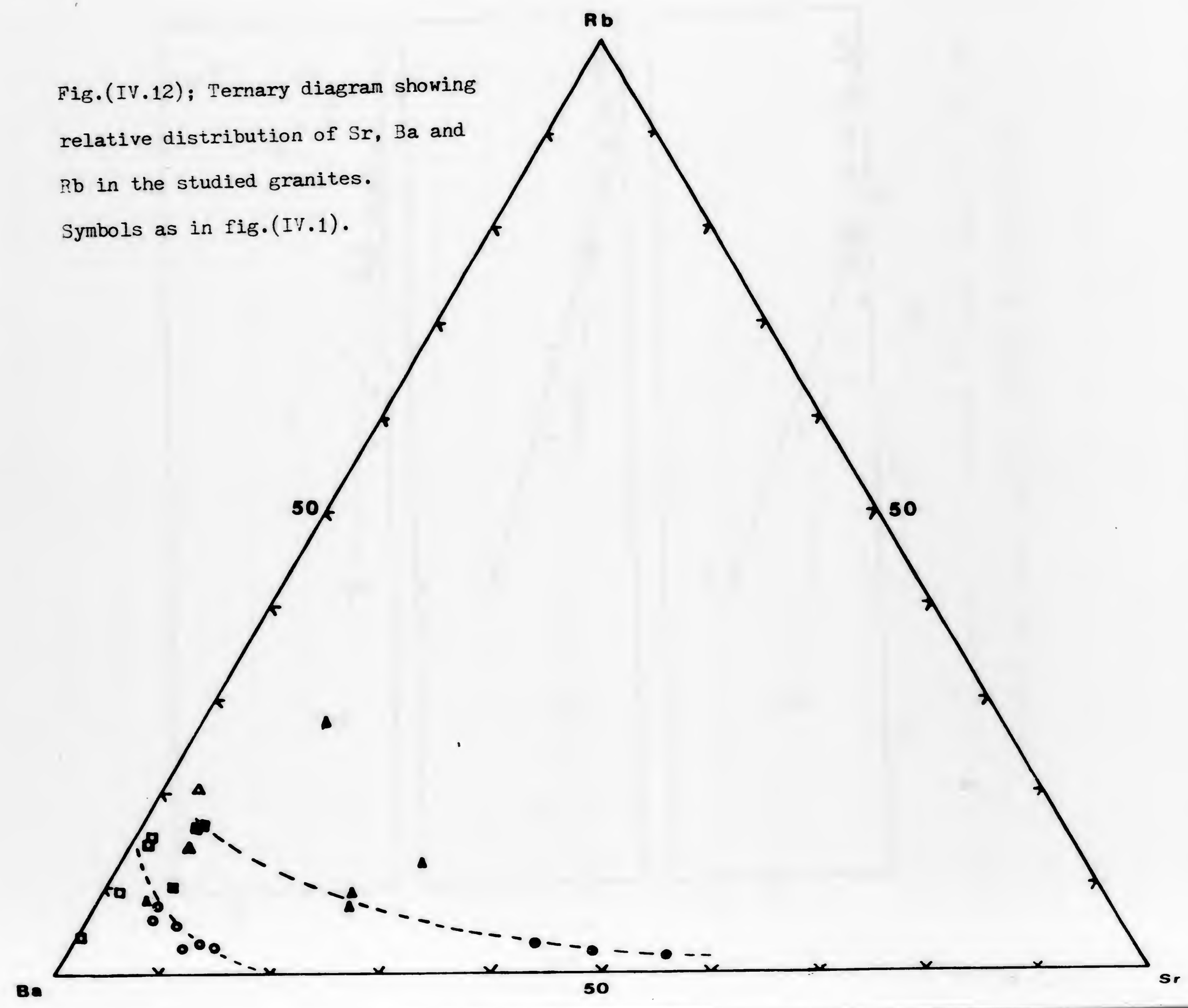

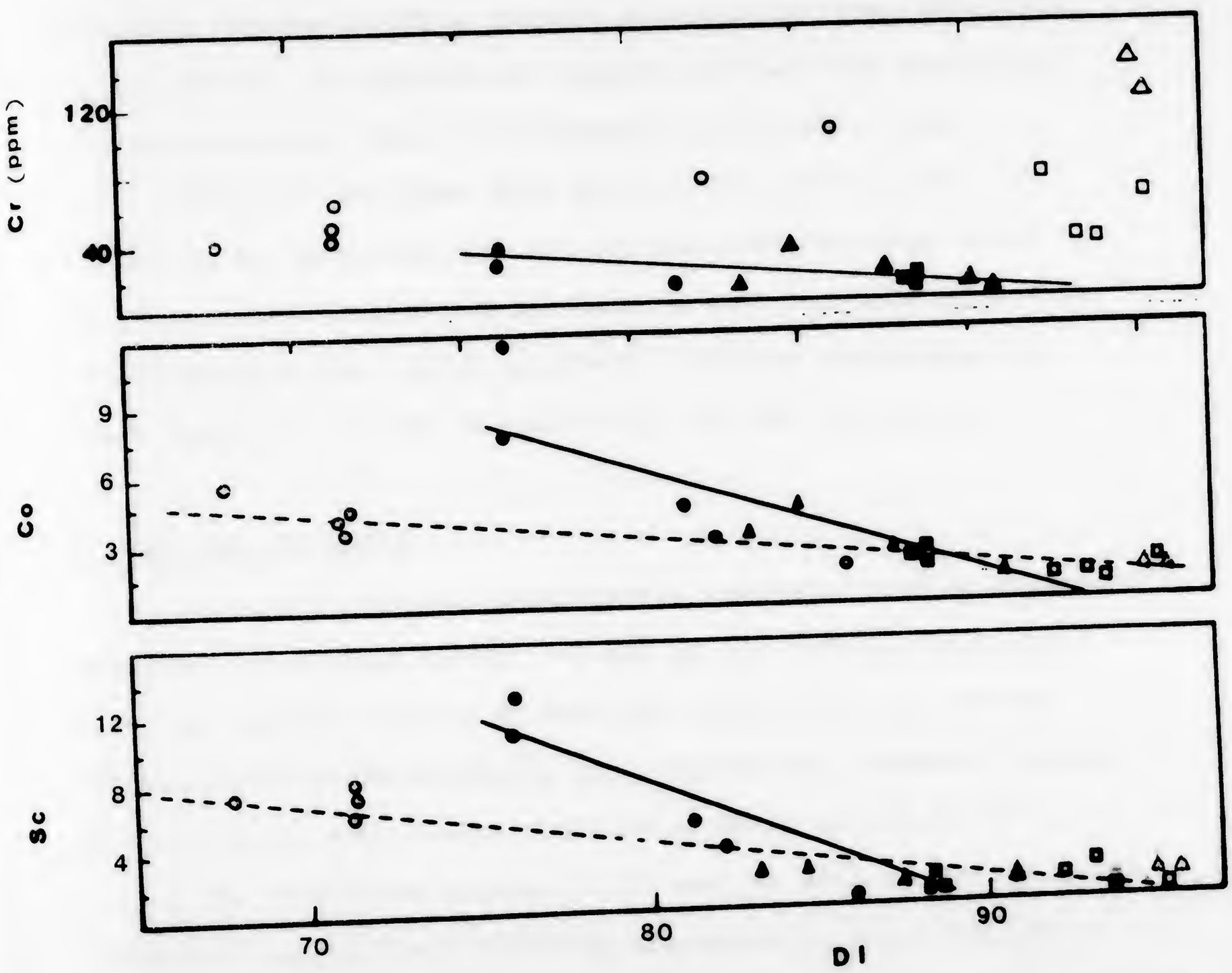

Fig.(IV.13); Variation diagram of Sc, Co and Cr (in ppm), versus D.I. for the Abu-Kharif and Deloro granites. Symbols as in fig.(IV.1).

relative enrichment of Sc and Co in Abu-Kharif granodiorites (average of 9.6 ppm. and 7.5 ppm. respectively). Cr, Sc and Co are broadly decreasing with decreasing Mg and Ca contents and with increasing SiO_2 content in granodiorites (Fourcade et al.(1981). Sc abundances usually reflect the abundance of mafic minerals which concentrate Sc (Vlasov, 1966).

Thus, it is clear that Mg, Ca, Fe, Sc, Co and Cr behave in the same general way in both the Abu-Kharif and Deloro granitic rocks and decrease toward the more acid end. Nockolds and Allen (1953) reached a similar conclusion in their study of Hamadat intrusion of the Red Sea hills.

3. Zr, Hf, Ta and Y

Zr and Ta form a pronouncedly coherent pair of elements (Rankama and Sahama, 1952). Gindy et al. (1979) concluded that, in igneous rocks, Zr does not enter into any of the common rock-forming minerals but remains as a separate phase, usually Zircon which also contains a small amount of Hf.

The relations between Zr, Y and Hf with differentiation index for the examined granites are shown in Fig. (IV.10). The diagram generally reflects a steady increase in Zr, Hf and Y contents with increasing differentiation is occurring in the Deloro granitic rocks suggesting that there is a continuous granitic series. The Abu-Kharif alkaline granites have a relative higher Zr, Hf, Y and Ta contents. As a result, the plots of the Abu-Kharif alkaline granites lie above the granodiorite, calc-alkaline granitic trend.

Figure (IV.14 a and b) show the relation between Zr and Y contents and between Ta and Hf contents in the studied granitic rocks. From the diagram, it is obvious that Zr increase with increasing Y in both the Deloro and Abu-Kharif granites. Meanwhile, Hf and Ta display a similar relation (Hf increases with increasing Ta). It is also noticeable that the Deloro granites are relatively enriched in Y and Hf contents comparable to Abu-Kharif granites. In both complexes, the alkali amphibole granites have a similar, higher Ta and Zr values, as they are enriched also in Hf and Y.

El-Gaby (1975) demonstrated that the peralkaline varieties contain outstanding high Zr amounts. He added, these granites with alkaline to peralkaline tendency are almost always those provisionally separated on the basis of the distribution of the REE.

In Fig. (IV.15) Zr is plotted against Ba and Sr for the studied granitic samples. From that figure, the plots of the Deloro pluton seem to have a common field, while those of the Abu-Kharif granitic complex occupy two separate fields. The latter observation is due to the fact that the Egyptian alkaline granite is highly enriched in zirconium and depleted in both Ba and Sr. Accordingly, it occupies a separate field, leading to the conclusion that this younger granitic phase is not a part of the granodiorite - calc alkaline granitic series.

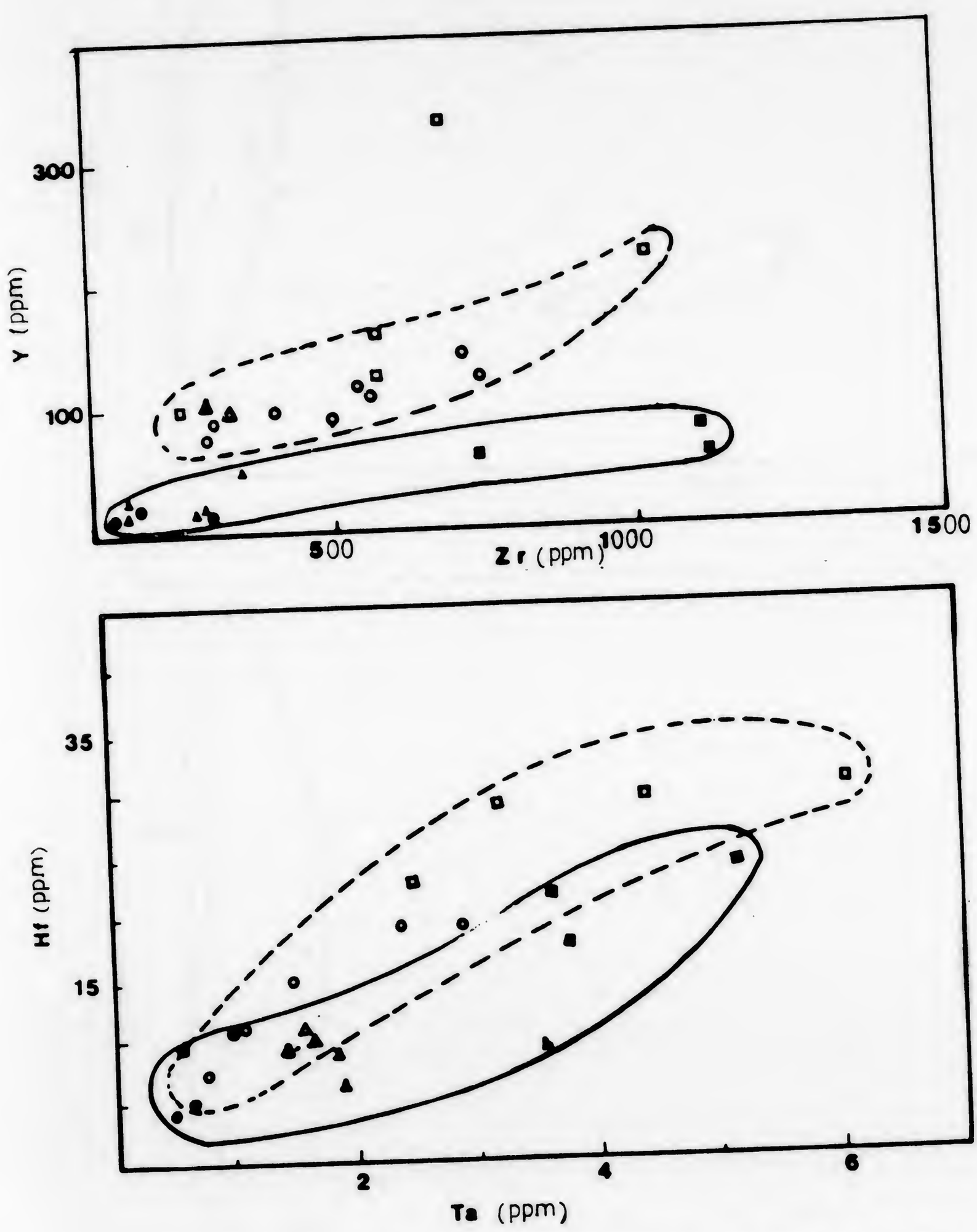

Fig.(IV.14); Y-Zr variation diagram and Hf-Ta variation diagram for the Abu-Kharif and Deloro granitic rocks.

Symbols as in fig.(IV.1)

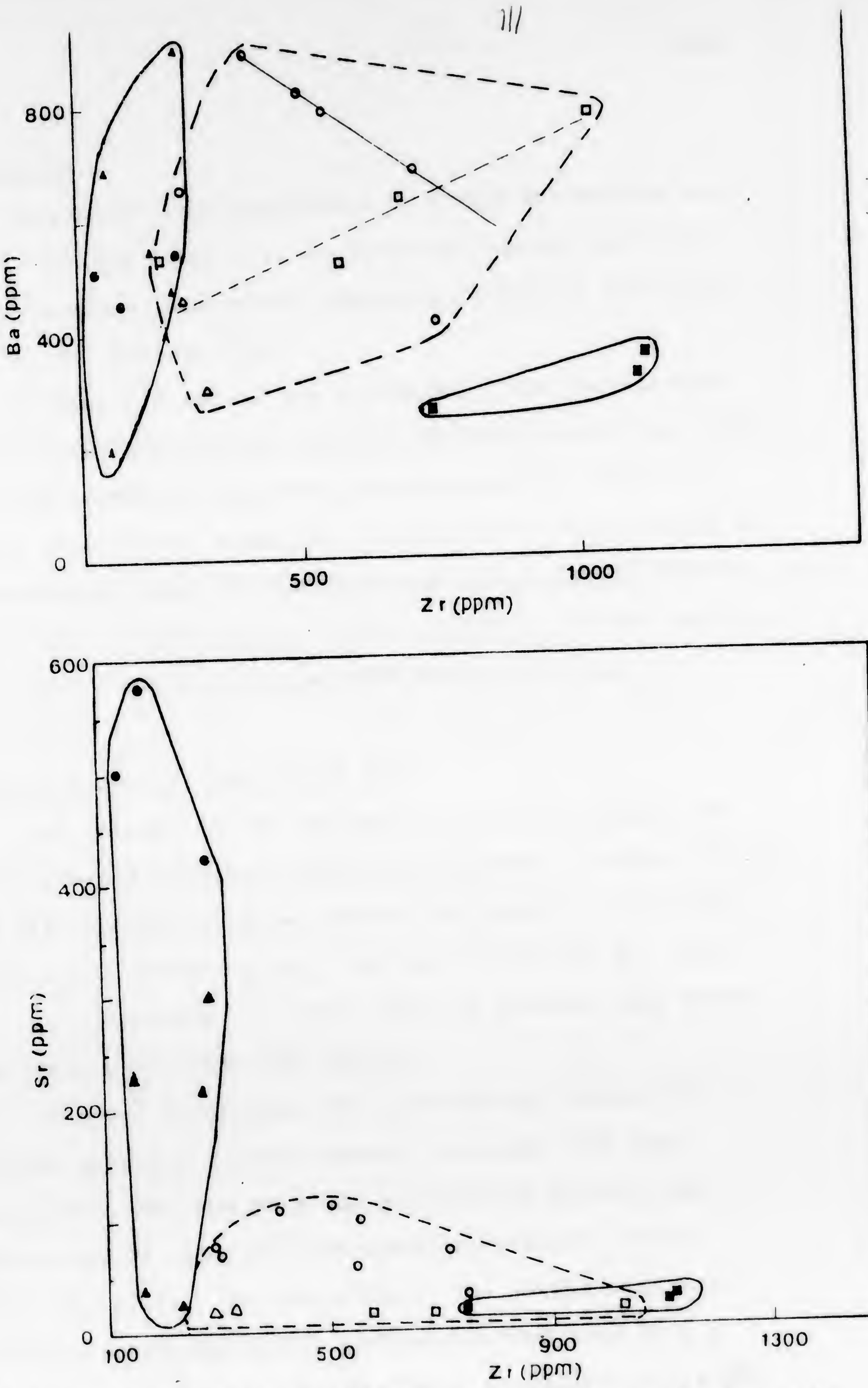

Fig.(IV.15); Ba-Zr and Sr-Zr interelement relationships for the Abu-Kharif and Delony granitic rocks. Same symbols as in fig.(IV.1)

4. U and Th

In general, the abundances of U and Th increase from basic to silicic rocks. It is also well-established that there is a close geochemical coherence between K and U and Th (Heier and Rogers, 1963).

In Fig. (IV.16), U and Th contents for the studied granitic rocks are plotted against the differentiation index. Beside the anomalous Egyptian alkaline granite, which is markedly depleted in U and Th, a sympathetic relationship is obtained where U and Th increase with increasing differentiation index. Gindy et al. (1979) reached a similar conclusion, that U and Th increase with differentiation.

5. Presentation of Rare Earth data

The results of the analyses on the REE composition of the examined granitic rocks are presented in Table (IV.7), which also include average results of granitic rocks from several areas (Tindle et al. 1981 and Strong et al. 1982).

In comparison, it seems that the present data match rather well with other REE results.

In order to discuss REE distribution within the different granitic phases, several diagrams have been constructed. The sum of 8 REE are plotted against the differentiation index for the examined granitic rocks (Figure IV. 17.a). In that Figure, the alkali amphibole granites of both Abu-Kharif and Deloro complexes show a relatively high REE enrichment. With increasing D.I., the

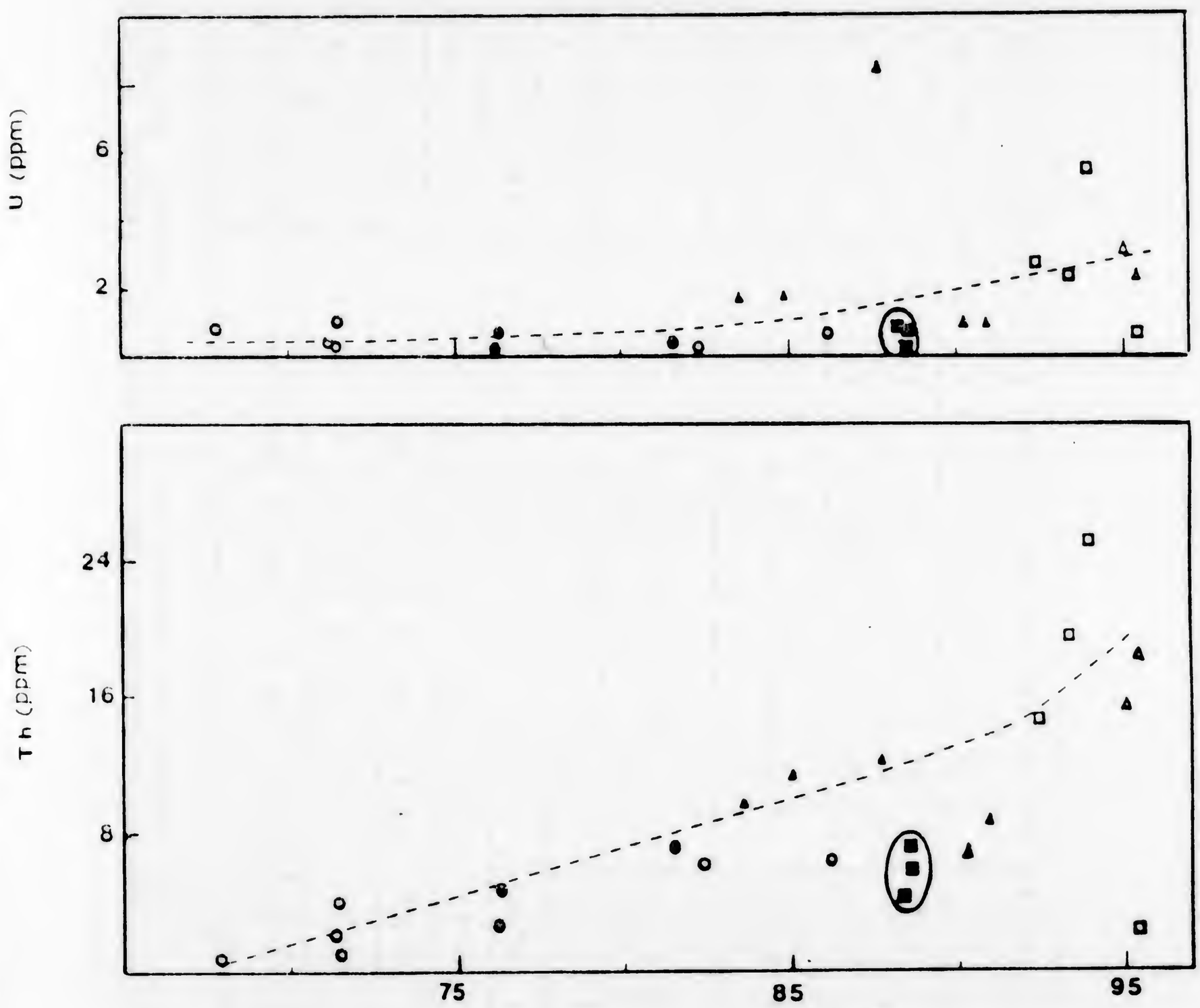

Fig.(IV.16); Variation diagram of Th and U versus D.I. for the analysed granitic rocks. Symbols as in fig.(IV.1).

TABLE (IV.7) REE concentrations (ppm) in whole rock samples from the Abu-Kharif and Deloro granitic rocks as well as from other areas.

No.	1 AK 26	2 AK 66	3 AK 40	4 AK 80	5 AK 99	6 AK 33	7 AK 108	8 P8-141	9 P8-142	10 P8-147	11 P8-148	12 P8-149
La	27.45	36.95	39.23	37.96	33.47	152.50	93.28	37.12	30.33	45.89	37.70	43.53
Ce	56.20	76.72	68.64	66.47	66.68	333.00	209.90	97.08	74.86	125.74	103.14	116.94
Nd	21.92	30.54	26.16	23.07	25.83	137.43	91.04	61.37	46.70	75.08	67.18	77.98
Sm	4.72	4.87	5.36	4.60	5.01	22.54	18.21	16.70	12.24	20.42	17.90	17.88
Eu	1.21	1.05	0.95	0.78	0.87	2.09	2.01	4.13	2.92	1.89	2.82	3.49
Tb	0.49	0.46	0.49	0.38	0.54	2.25	2.50	2.77	1.87	3.02	3.22	2.75
Ho	0.94	1.69	1.66	1.47	1.45	2.98	3.17	3.40	3.59	6.68	5.12	4.94
Yb	1.14	2.11	2.20	1.81	1.77	7.55	9.52	11.77	9.30	20.00	21.16	14.92
Lu	0.24	0.37	0.28	0.37	0.24	1.2	1.40	1.91	1.52	3.33	3.20	2.32
Ce/Yb	49.30	47.95	31.24	36.80	37.67	44.10	24.12	8.25	8.05	6.29	4.87	7.80
Eu/Yb	1.34	0.67	0.46	0.42	0.44	0.24	0.17	0.32	0.32	0.09	0.12	0.20
ΣLu+Yb+Tb	1.87	2.94	2.97	2.56	2.55	11.00	13.42	16.46	12.68	26.36	27.58	19.99
Σ8REE	113.39	153.00	143.38	135.46	134.42	658.49	427.84	232.88	179.60	295.35	256.37	279.78

TABLE (IV.7) Continued..

No.	13 P8-154	14 P8-114	15 P8-117	16 P8-118	17 P8-121	18 P8-144	19 P8-139	20 P8-140	21 CD-65	22 CD-67	23 288	24 242
La	41.52	109.77	155.30	150.50	97.30	118.82	62.30	41.70	18.09	22.80	31.0	52.7
Ce	100.88	255.10	386.95	338.64	186.54	295.42	140.75	96.67	47.15	51.21	64.4	82.2
Nd	62.37	123.88	196.10	147.40	97.47	160.31	56.75	46.74	23.24	20.66	25.8	38.3
Sm	16.37	29.42	43.33	34.70	22.04	39.69	14.70	11.75	5.49	4.58	4.9	7.0
Eu	3.38	1.76	2.48	2.04	1.52	3.07	1.03	1.11	0.28	0.53	0.97	0.89
Tb	2.44	5.62	6.66	6.45	3.71	6.91	2.46	2.88	-	-	0.57	0.84
Ho	4.63	9.91	9.05	10.10	8.13	13.10	4.31	3.54	-	-	-	-
Yb	12.29	31.69	26.90	36.58	20.23	38.64	12.71	12.69	3.56	2.86	1.78	1.77
Lu	1.89	4.48	3.84	4.94	2.95	5.30	0.17	1.89	-	-	0.13	n.d
Ce/Yb	8.20	8.05	14.38	9.25	9.22	7.63	11.07	7.62	13.24	17.91	36.18	46.44
Eu/Yb	0.29	0.05	0.08	0.05	0.06	0.08	0.07	0.06	0.07	0.18	0.54	0.50
ΣLu+Yb+Tb	16.63	41.79	37.40	47.97	26.89	50.86	15.35	17.46	3.56	2.86	2.48	2.61
Σ8REE	241.18	561.77	821.60	721.28	431.72	668.1	290.94	215.46	97.81	102.64	129.6	183.7

Samples of the Abu-Kharif Complex
From 1 to 2, syntectonic granodiorite
3 to 5, late-tectonic calc-alkaline granite
6 to 7, post-tectonic alkaline granite

Samples of the Deloro pluton
From 8 to 13, calcic syenite granite
14 to 18, peralkaline granite
19 to 20, granophyric granite

From 21 to 22, granites from Newfoundland, Canada, Strong et al. (1982)
From 23 to 24, granodiorite and granite from England, Tindle et al. (1981)

REE displayed a constant figure between the other granitic varieties. The sum of HREE (Lu, Yb and Tb) are plotted against D.I. in Figure (IV.17.b). From the diagram, a continuous increase in HREE within the Deloro granitic rocks is seen. The Abu-Kharif alkaline granite is relatively enriched in HREE and lying above the general trend of the other two varieties. Fig. (IV. 18) illustrates the relationship of the LREE contents (in ppm) of the investigated granites as a function of index of differentiation. Agian, the alkaline granite in both complexes possesses relatively high La, Ce and Nd concentrations. With increase of differentiation, the LREE either remain constant or display a slight increase within the other granitic varieties.

In order to visualize some of the trace element results, the ratio, Ce/Yb is plotted against the ratio Eu/Yb (Fig. IV.19). From that diagram, it is obvious that the Egyptian granitic rocks possesses high ratios of the Ce/Yb and Eu/Yb compared to the granitic rocks of the Deloro pluton. The latter is relatively enriched in Yb. With increasing ratio Ce/Yb, the ratio Eu/Yb gradually increases in all the investigated granitic rocks.

Noteworthy is the fact that the more acidic varieties (the alkali amphibole granite) occupies a separate field displaying a sudden or sharp increase in the ratio Ce/Yb, with the increase of the ratio Eu/Yb. That observation could be explained by the presence of a big negative Eu anomaly

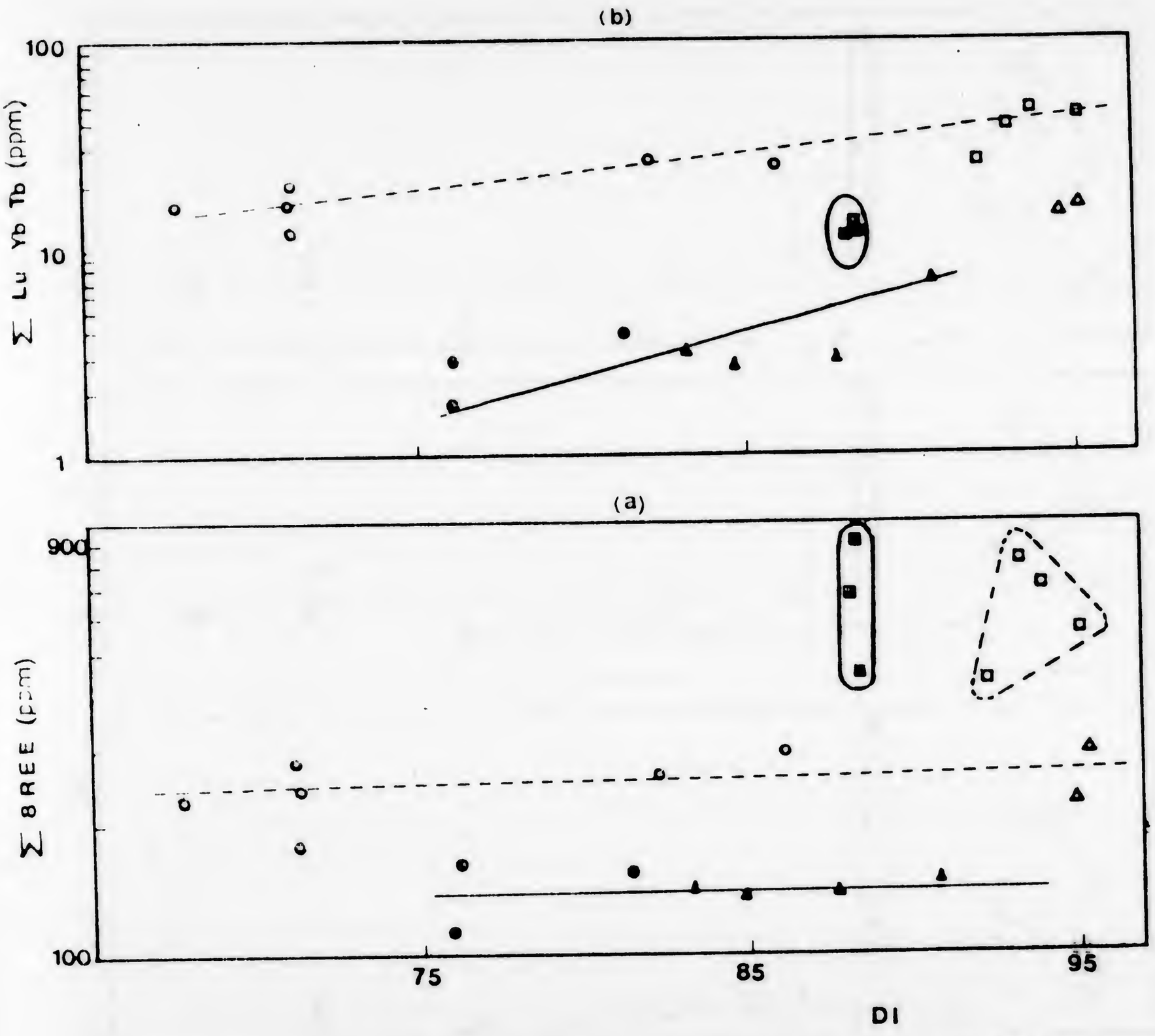

Fig.(IV.17); a) Variation diagram of the sums of 8REE versus D.I. for the analysed granites.

b) Variation diagram of the sums of Lu+Yb+Tb versus D.I. for the studied granitic rocks. Symbols as in Fig.(IV.1).

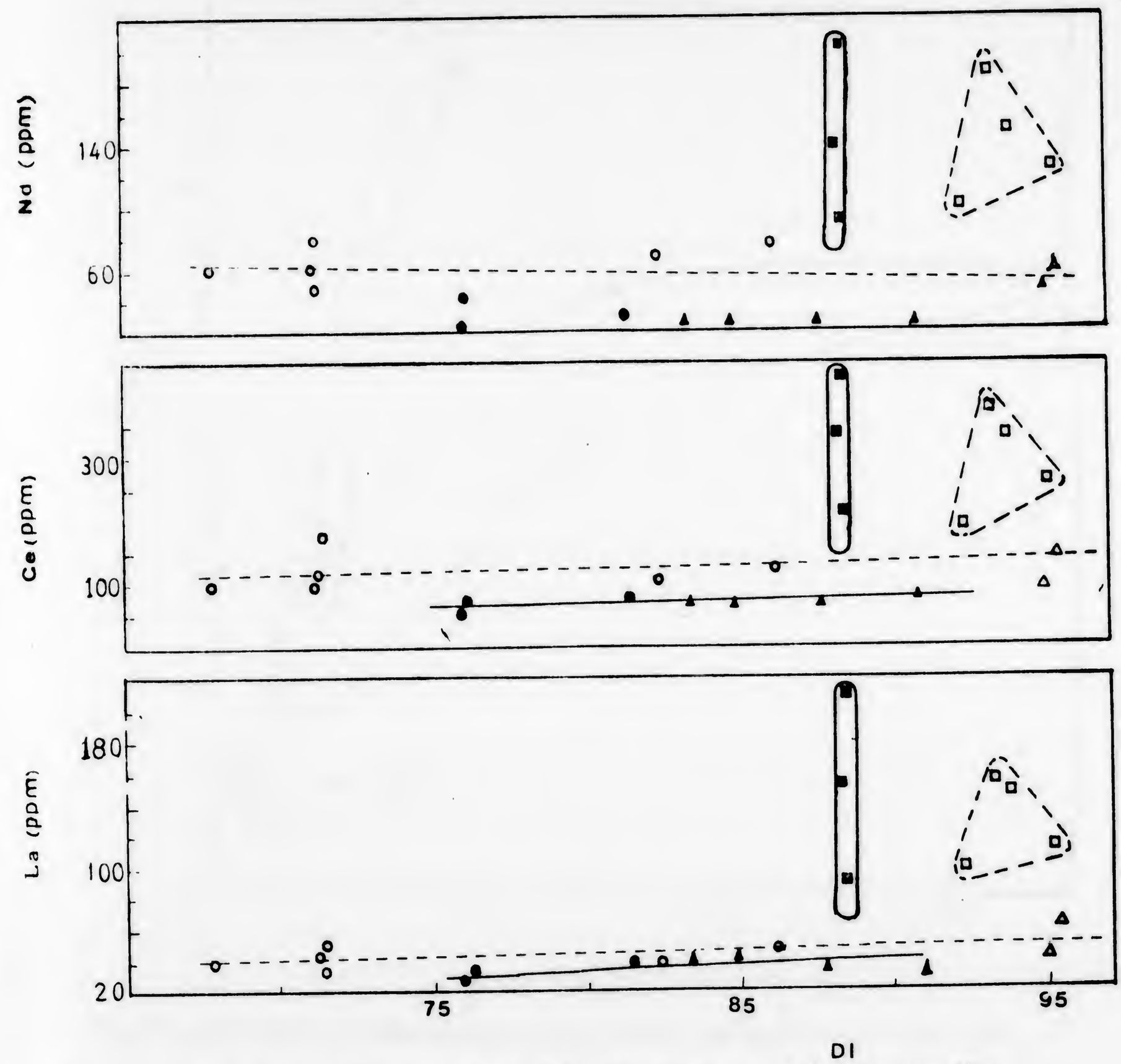

Fig.(IV.18); Variation diagrams of La, Ce, and Nd versus D.I. for the Abu-Kharif and Deloro granites. Symbols as in fig.(IV.1).

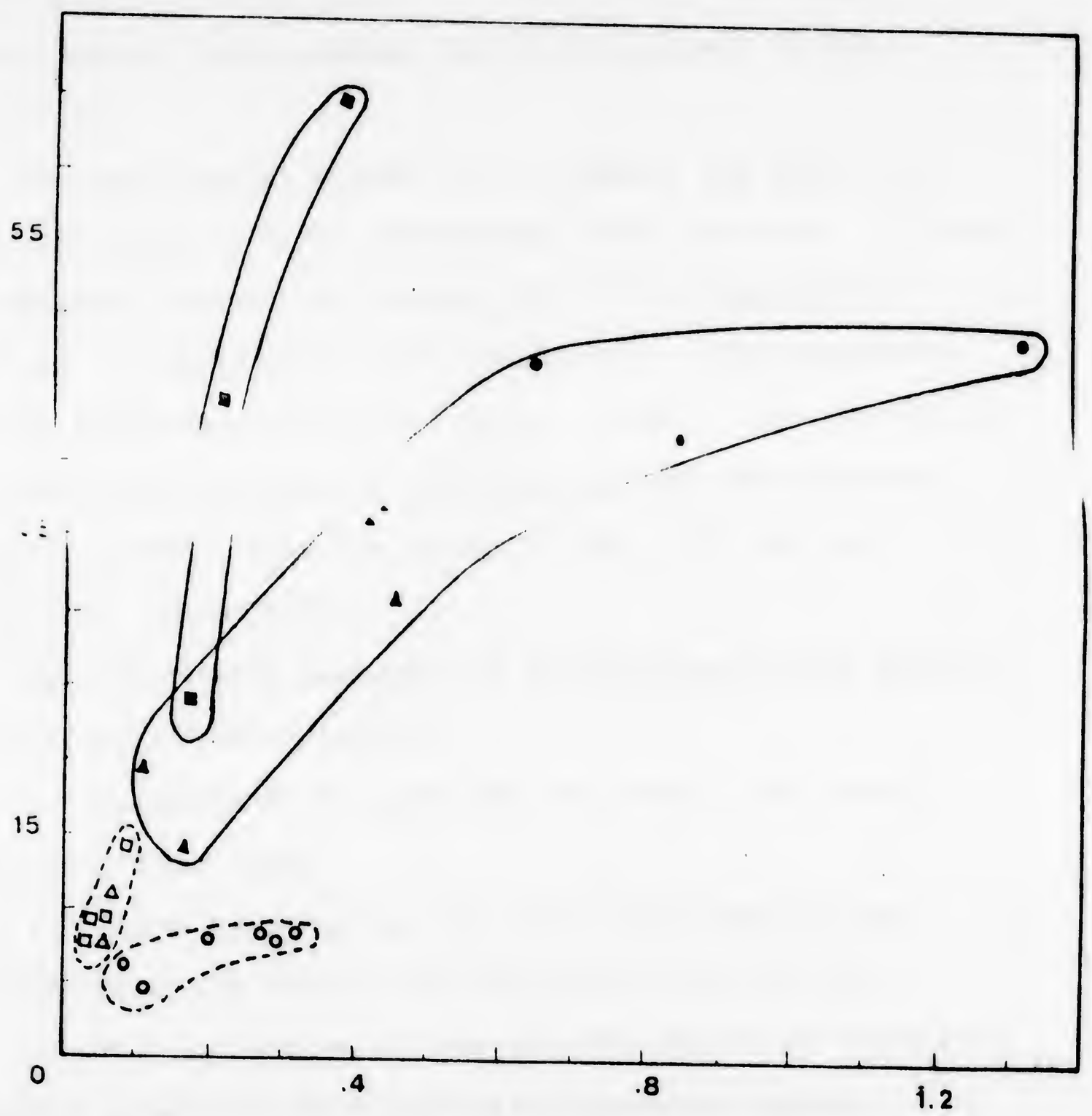

Fig.(IV.19); Plots of the Ce/Yb ratios versus the Eu/Yb ratios for the Abu-Kharif and Deloro granitic rocks. Symbols as in fig.(IV.1).

(see Fig. IV.20 and 21), between the alkali amphibole granitic phases of both granitic complexes. The other varieties show a more gradual increase in their Ce/Yb - Eu/Yb ratios.

The most useful method is to compare the REE data relative to chondritic or sedimentary rock patterns, dividing the abundances element by element, by the corresponding chondritic or sedimentary rock abundances. This procedure was first suggested by Coryell et al. (1963). The chondrite-normalized distributions in the Egyptian and the Canadian examined granitic rocks are given in Fig. (IV. 20) and Fig. (IV.21) respectively.

The lanthanide patterns of the examined rocks exhibit some constant characteristics:

1. Enrichment of light REE over heavy REE in all investigated rock types.

2. Light Rare Earths are more fractionated than heavy REE which are weakly fractionated or not at all.

3. The enrichment of REE and the important negative Eu anomaly appears in the late differentiated phases.

Some of these features have been observed in many other granitic complexes (see for example Fourcade and Allegra, 1981). The three features described above, if not characteristic of the other granitic complexes, seem to be well represented in the Abu-Kharif and Deloro granitic complexes.

Fig.(IV.20); Chondrite normalized REE patterns in whole rocks from the Abu-Kharif granitic complex, Egypt.

Symbols as in fig.(IV.1).

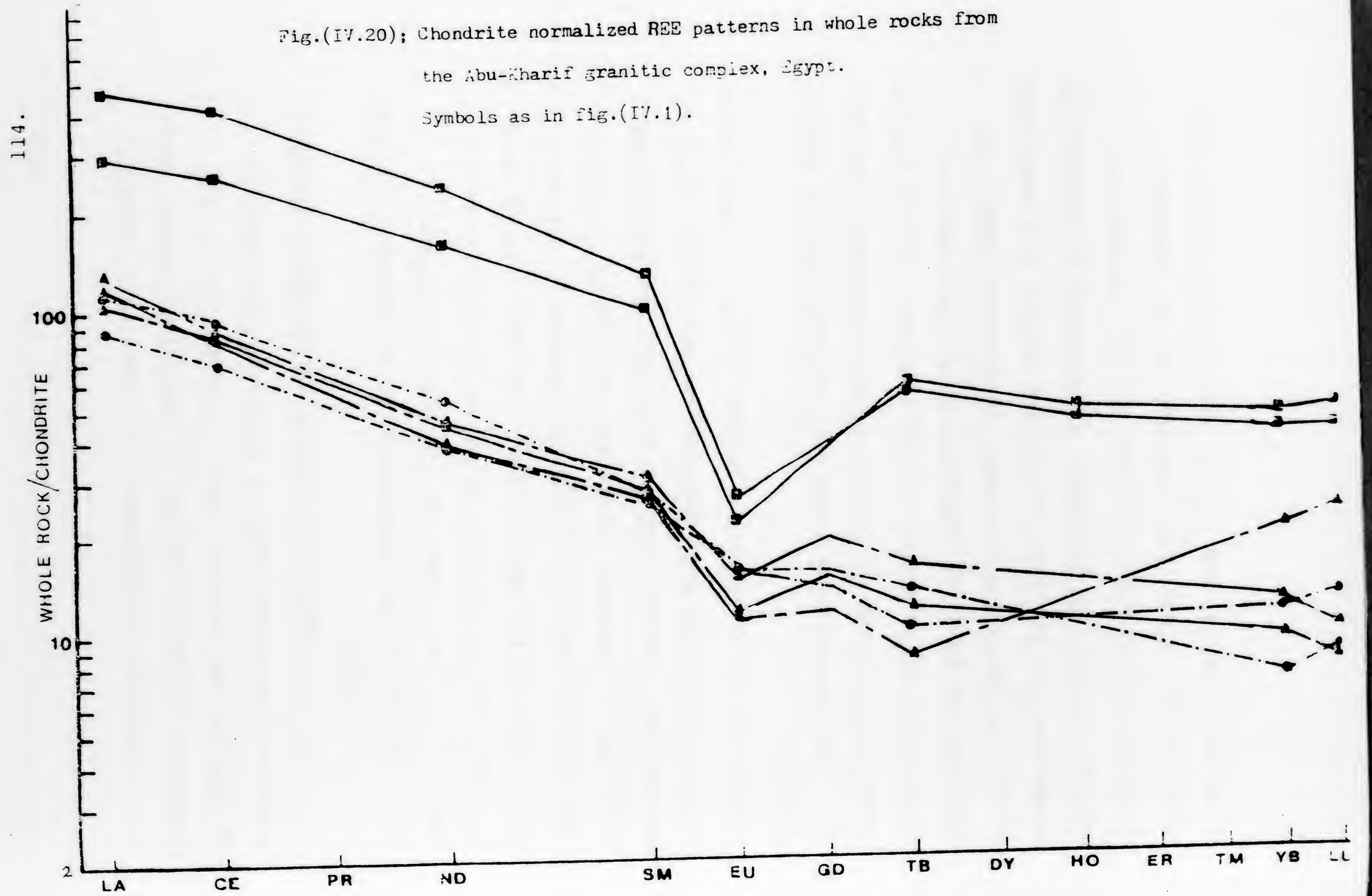

According to character-3, it seems that lanthanide abundances increase as Mg and Ca contents decreased. From the obtained REE patterns (Figs. IV.20 and 21), we can individualize several types of lanthanide distribution:

(A) Lanthanide distribution of Abu-Kharif granitic rocks

The lanthanide distribution of the Egyptian granitic rocks (Fig. IV.20), shows the following characters:

(i) Both the calc-alklaine granites and granodiorites display a very similar REE patterns. The well differentiated LREE, the very small Eu anomaly and the poorly differentiated HREE are the main lanthanide features of the granodiorites and the calc-alkaline granites. The lack of REE differentiation has been explained by Buma et al. (1971) as a result of the occlusion of trapped liquids in crystallizing minerals.

(ii) The more differentiated post-tectonic alkaline garnite shows a distinctive REE pattern which is different from the other previously mentioned granitic phases. The REE patterns show that the Egyptian alkaline granites are relatively enriched in REE and display well fractionated HREE. The presence of an important Eu negative anomaly is a remarkable feature in their REE patterns. The presence of negative Eu anomalies in late stage granites has been explained by Towell et al. (1965), who concluded that Eu suffered a systematic removal from the REE from the more acidic rocks

during magmatic crystallization. In (1978), Hanson pointed out that the negative Eu anomaly in the melt results from plagioclase in the residue. Our petrographic studies reveal that the alkaline granites are of hypersolvus nature in which perthites are the predominant feldspar minerals with the lack of any discrete plagioclases.

In conclusion, the Egyptian granitic rocks display two main different REE patterns. Both the granodiorites and the calc-alkaline granites possess very similar or homogeneous REE patterns, while the alkaline granite exhibits a different and characteristic REE pattern, suggesting that the studied Egyptian granitic rocks are possibly derived from two different magmas. Fourcade and Allegra (1981), concluded that lanthanide patterns seem to be homogeneous inside a given magmatic unit and can be used to characterize each unit of a composite intrusion. Accordingly, both the granodiorites and the calc-alkaline granites can be considered as one magmatic unit, however, the post-tectonic alkaline granite, probably represents another magmatic unit and can be considered as a separate granitic phase.

That conclusion is in agreement with our field observations and with the other geochemical interpretations. Khalil et al. (1978) reached a similar conclusion when they pointed out that the wide variation in the content of the REE in the pluton suggests that the Holterkolen granitic rocks at Norway, could probably be derived from at least two different magmas.

(B) Lanthanide distribution of Deloro granitic rocks

The REE patterns of the Deloro granitic rocks (Fig. IV.21) show the following characteristics:

(i) The peralkaline riebeckite granite possesses the highest REE contents.

(ii) The presence of important negative Eu anomaly in the late stages (granophyric granites and riebeckite granites).

(iii) High enrichment in the heavy REE in all the granitic phases of the Deloro pluton, which is a very primitive feature.

(iv) The different granitic phases show a very similar or subparallel REE patterns characterized by enrichment in their HREE.

The presence of a negative Eu anomaly in the late stages within the Deloro granites could probably be due to the high oxidation state of the magma. Kuehnbaum (1973) in his study of the stability fields of Na-Fe amphiboles pointed out that the high Fe^{+3}/Fe^{+2} ratios of the Deloro riebeckites confirm the presence of relatively high oxidation, he added, both oxygen fugacities (FO_2) and temperature will be higher than estimations in the simple hydrous system. The presence of ilmenite as a predominant accessory mineral (achieved by petrographic studies and electron microprobe analysis), reflect the high oxidation state of the Deloro magma.

Fig.(IV.21); Chondrite normalized REE patterns in whole rocks from the Deloro Pluton, Canada. Symbols as in fig.(iv.1).

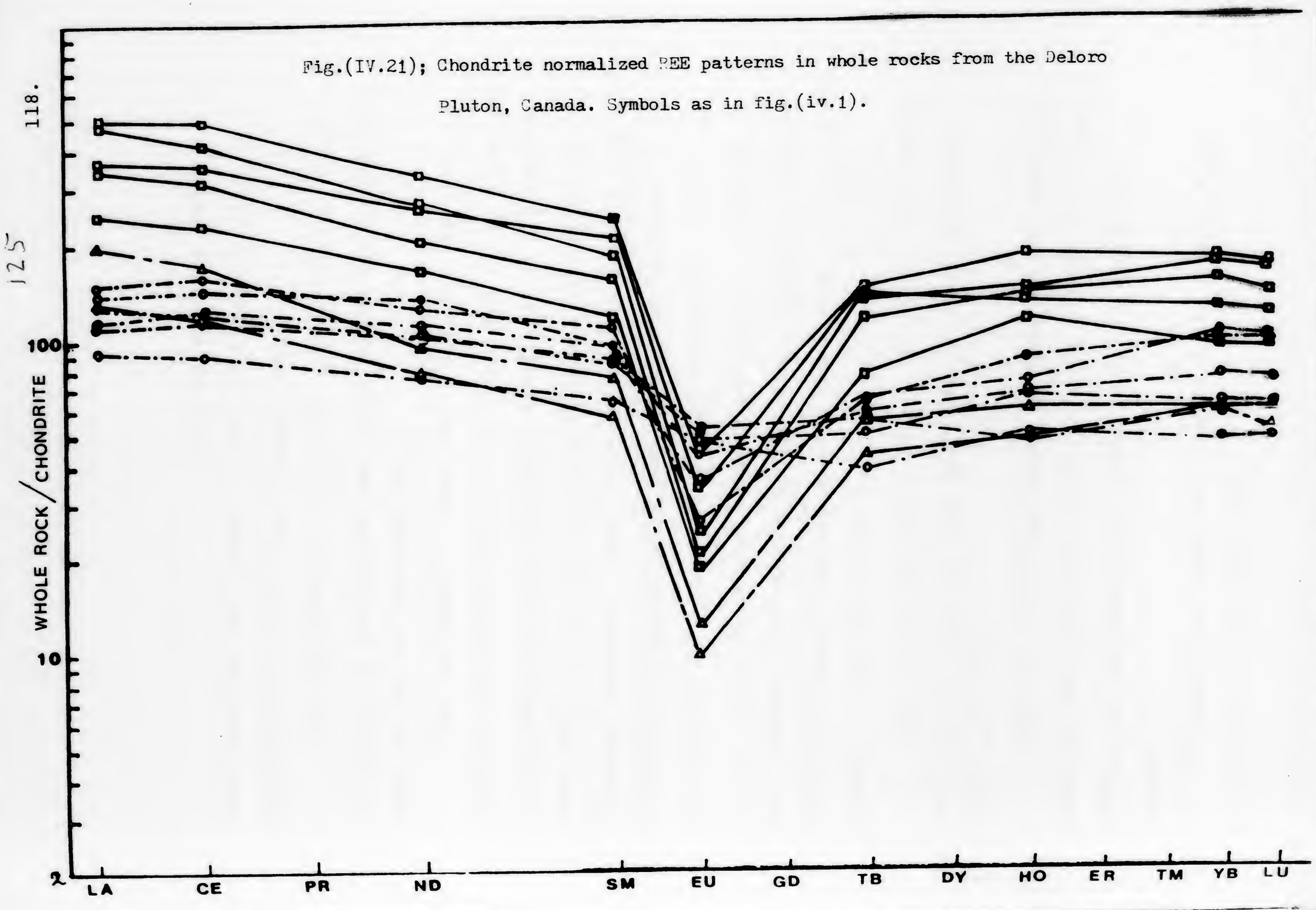

Zielinski and Frey (1970, concluded that multi-stage fractional crystallization processes can cause large Eu depletions.

The hypothesis of fractional crystallization could be applied to demonstrate the origin of the Deloro granitic rocks as will be discussed below.

The enrichment in heavy REE within all the granitic phases of the Deloro pluton is probably due to the presence of the amphiboles and the alkali amphiboles as predominant mafic minerals and the presence of Zircon and garnet as accessory minerals. That interpretation is based on the conclusion of Hanson (1978) who stated that the heavy REE are retained to a greater extent by hornblende, garnet and zircon. Our petrographic studies and that of Kuehnbaum (1973) showed that amphiboles and alkali amphiboles are the sole mafic minerals within most of the Deloro granitic rocks, however, zircon and garnet occur as accessory minerals.

Both zircon and garnet have a very large distribution coefficients (Kd's) for the heavy REE as stated by Hanson (1978) and (1980).

From the geochemical point of view, we can generally point out that the Deloro granitic magma had the following geochemical characteristics relative to the Abu-Kharif magmas:

(i) The magma was highly enriched in femic oxides, K_2O, Na_2O, Cr, Hf, Y and heavy REE.

(ii) It was also depleted in Al_2O_3, MgO and Sr.

It must also be noted that, within the Abu-Kharif granitic complex itself, the alkaline granitic magma was enriched in Na_2O, K_2O, femic oxides, Zr, Y, Hf, Ta and REE, and depleted in Al_2O_3, CaO, Sr, U and Th comparable to the granodiorite-calc alkaline magma.

(C) Petrogenesis of the granitic rocks

The use of trace elements in petrogenetic problems has been marked in the last decade. Several workers emphasized that a significant degree of relative fractionation can be observed among the REE. Between them, Haskin et al. (1966) and Strong et al. (1982) observed that fractionation among the REE is very common in igneous rocks.

In (1969), Kosterin suggested that, since the heavy REE form more stable complexes than the light REE, the former would become enriched in solutions and dominate late stage deposits. From the previous REE characteristics, it seems that the REE patterns of the Deloro granitic complex are homogeneous and that there is a continuous variation in their REE from the calcic syenite-granite to the granophyric and the riebeckite granites. That may permit us to consider that the Deloro granitic rocks could probably form a one granitic series and they are possibley derived from a more basic magma by extensive differentiation. Buma et al. (1971) concluded that the presence of syenites with granites, Eu depletion, low water fugacity, lack of pegmatites and dense rocks at depth, all agree with derivation of the "New England" alkaline

granites by extensive differentiation of a more basic magma.

In conclusion, the hypothesis that the entire series of the Deloro granitic rocks could be the result of crystal/liquid fractionation processes, starting from one parent magma is suggested by the smooth variation of both major and trace elements against the D.I. as well as by the homogeneity in their REE patterns. In (1981), Bellieni et al. has reached a similar conclusion applied to a plutonic complex at Italy.

The Egyptian granitic rocks display two main different REE patterns. The alkaline granites possesses different and characteristic REE patterns comparable to the REE patterns of both the granodiorites and calc-alkaline granites which are very similar ot homogeneous. As the lanthanide patterns seem to be homogeneous inside a given magmatic unit, the Egyptian granitic rocks, accordingly, are possibly derived from two different magmas. The post-tectonic alkaline granite probably represent a separate magmatic unit.

The lanthanide patterns of both the Egyptian and the Canadian granitic rocks are plotted together in Fig. (IV.22). In comparison, the REE patterns of the studied granitic rocks of both complexes reveal two main features:

(i) a remarkable enrichment in heavy REE within all the granitic units of the Deloro pluton comparable to the Egyptian granitic complex (Gebel Abu-Kharif).

Fig.(IV.22); Chondrite normalized REE patterns of the Abu-Kharif (A), and the Deloro (D), granitic complexes. Symbols as in fig.(IV.1).

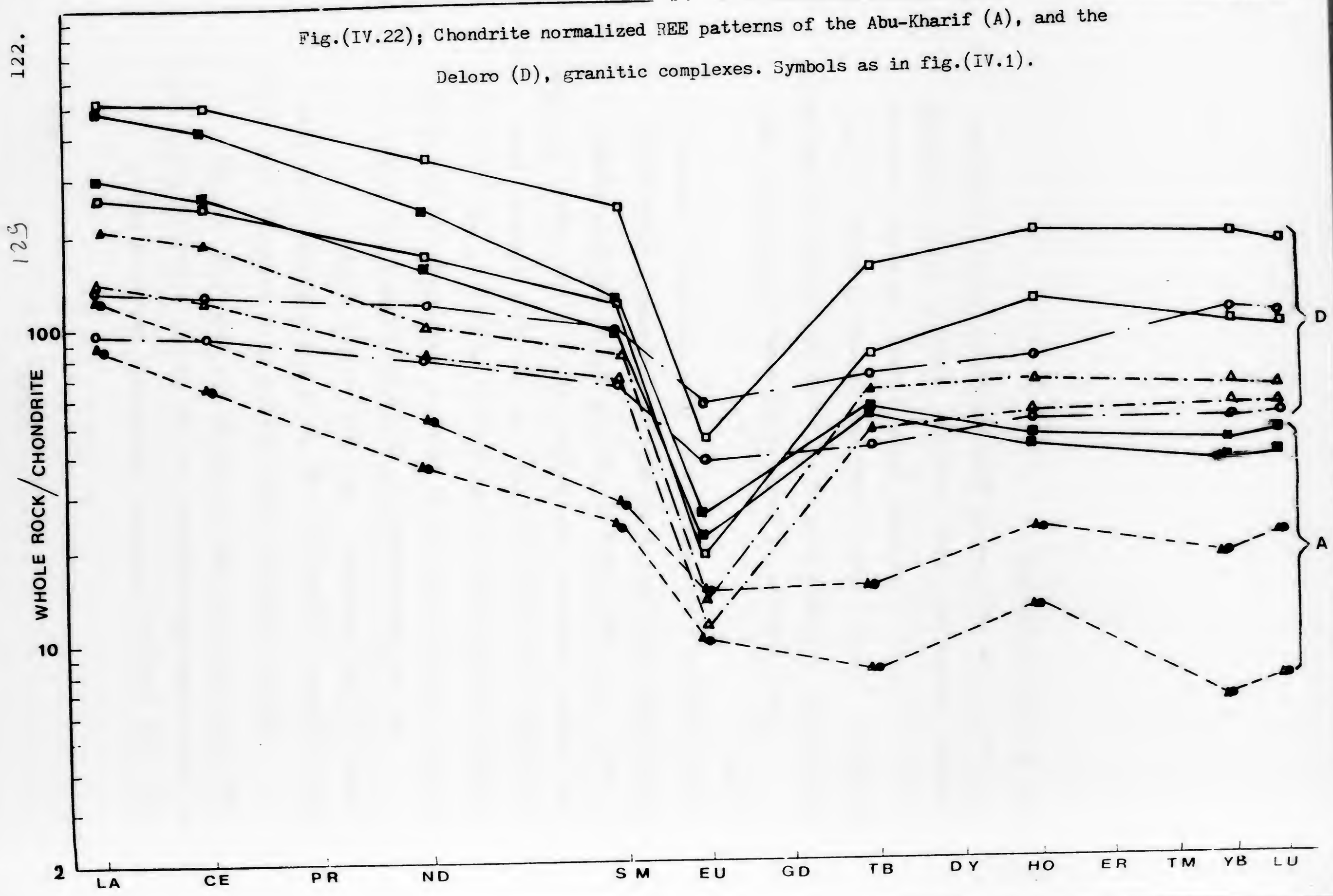

(ii) The granitic rocks of Abu-Kharif exhibits more differentiated REE relative to the Deloro granites which have less differentiated REE or not at all (see Fig. IV.22).

Several Russian investigators have observed late heavy REE enrichment resulting from heavy REE complexing by metasomatic fluids (Mineyev, 1963 and Vlasov, 1966).

As has been suggested by Hanson (1980) the trace element concentration of a melt is dependent on the trace element concentration of the parent, extent of melting and processes of melting involved. We may thus presume that the parental magma of the Deloro granites was highly enriched in heavy REE comparable to that of the Abu-Kharif magmas. Gast (1968) concluded that melting processes fractionate trace elements more efficiently than fractional crystallization.

The processes of partial melting, accordingly, may have acted successively in relating the origin of Abu-Kharif granites. Rather than fractional crystallization, zircon could have been a residual phase during fractional melting. Because zircon is likely in lower crustal rocks, a crustal origin for the Abu-Kharif post-tectonic alkaline granite may also be suggested.

CHAPTER V

GEOCHEMISTRY OF THE ABU-KHARIF AND DELORO MAFIC MINERALS

CHAPTER V

GEOCHEMISTRY OF THE ABU-KHARIF AND DELORO MAFIC MINERALS

Introduction

Prior to the present work, mafic minerals including alkali amphiboles, of granitic rocks have received some attention. Most of the published literature deals with the mineralogy, geochemistry and the classification of such minerals in granitic rocks from different localities.

To study the geochemistry and classification of some of the mineral phases, biotites, amphiboles and alkali-amphiboles of the investigated granitic rocks have been analysed using the ARL electron microprobe at the University of Toronto.

The distribution and behaviour of the trace elements (including the REE), has been determined by neutron activation analysis of 12 new mineral separates. Particular attention was paid to the purity of mineral separates.

The mineral phases analysed are represented by biotites, amphiboles and alkali amphiboles from the Abu-Kharif and Deloro granitic complexes.

Analytical Techniques

1) Heavy liquid separation

Mineral separations using heavy liquids usually require that the density of the liquid is such that the wanted mineral either sinks or floats in the liquid while the unwanted

minerals react in the reverse manner (Zussman, 1967). Most of the liquids used for making separations have low surface tensions and high wetting coefficients. Bromoform, Tetra-bromoethane and Methylene iodide are the heavy liquids most widely used for that purpose. These liquids may be diluted to lower densities with a number of miscible organic solvents.

The heavy liquid separation was applied to 12 new samples from the Abu-Kharif and Deloro granitic rocks. Biotites, amphiboles and alkali amphiboles are the minerals of interest.

The heavy liquid separation of the examined sample powders,(mesh size of 80), were done using the Tetrabromo-ethane (density of 2.964). The ferromagnesisn minerals sank and separated as heavy fractions while the feldspathic minerals floated and separated as light fractions. This process was repeated until the desired separation was accomplished. Finally, the fractions were washed in acetone and dried.

The particular ferromagnesian minearls to be separated were chosen on the basis of our petrographic studies of the petrographic varieties in which they represent the sole mafic minerals. The purity of the mineral separates was carefully tested under the Binocular microscope. The separated minerals were purified further by using the electromagnetic separator.

2) Magnetic separation

Magnetic separation is based on the magnetic susceptibility of the different minerals. For purpose of separation, minerals may be classed as highly magnetic, moderately magnetic, weakly magnetic and almost non-magnetic. Highly magnetic minerals are readily separated by using any suitable permanent magnet of the bar or horse-shoe type.

For the very much larger group of less magnetic minerals, the iso-dynamic type of electromagnetic separator, originally due to Frantz is now widely used. The electromagnet is universally mounted and may be tilted to any position both transversely and longitudinally. The latter to assist material transport along the chute. By suitably balancing the gravitational and magnetic forces, separation can be obtained between minerals with very close susceptibilities (Zussman, 1967).

The examined samples were purified by using Frantz isodynamic magnetic separator. The more magnetic ferromagnesian minerals were moved against the chute slope and eventually discharging into one of two small collector buckets, while the less magnetic ones were discharged into the other collector bucket. Generally speaking, the purity of the analysed samples was mostly greater than 95%.

3) Electron Microprobe Analysis

The data obtained for this thesis were obtained using polished thin sections of the precambrian granitic rocks from the Abu-Kharif and Deloro complexes.

The polished specimen surface was vacuum coated with carbon. The electron microprobe analysis was applied to analyse alkali amphiboles, amphiboles and biotites as well as feldspars, ilmenites and magnetites for the different granitic phases. The analyses of the examined samples were done on the basis of the Energy Dispersive spectrometer of the ARL electron microprobe facilities at the University of Toronto.

To make the results applicable to energy dispersive analysis on the ARL microprobe, all runs were done using the standard energy dispervise operating conditions. The accelerating potential was maintained at 20 Kv and the beam current was set by adjusting the condenser lens (count rate of approximately 3500 cps for Willemite). The X-ray detector is a piece of highly purified Si, with a controlled amount of Li added to compensate for the very small amount of unavoidable impurities (Rucklidge, 1976). Once this was attacined, the required beam current (approximately 0.155 μA), was maintained over the run period. To minimise alkali loss in some minerals, the electron beam was partially defocussed.

The Willemite-Cobalt standards were used for energy and intensity calibrations respectively. Several standards for biotite, amphibole, alkali amphibole, feldspar, ilmenite

and magnetite, extensively used at U of T, were used to calibrate the correction factors for the various elements in these minerals. The EDA spectra of the minerals analysed were converted to oxide analyses using the correction programme PEST. Structural formulae for the minerals were derived through the U of T programme RECALC, which also assigns Fe^{2+} + Fe^{3+} on the basis of assumed mineral stoichiometry.

4) Neutron activation analyses

The neutron activation analyses of 12 new mineral separates represented by biotites, amphiboles and alkali amphiboles from the studied granitic complexes were done using the Slowpoke-2 nuclear reactor at the U of T.

The description of the technique and the operating conditions have already been given in Chapter IV.

Analytical Results on Separated Minerals

The chemistry and classification of the biotites, amphiboles and alkali amphiboles of the different granitic phases from the Abu-Kharif and Deloro granitic complexes will be discussed below.

1) Biotite

The data from 21 new microprobe analyses of biotites from the Abu-Kharif and the Deloro granites are listed in Table (V.1). Biotite analyses from other localities (Deer et al. 1967 and Kabesh et al. 1977) are also given for purpose of comparison. It can be seen that the Abu-Kharif biotites are quite similar compositionally to magnesian rich, ferrous-iron poor varieties from other localities and recovered from calc-alkaline plutonic rocks, while the biotites of the Deloro pluton are iron rich varieties (Table V.1).

In general, the Egyptian biotites are enriched in Mg and depleted in ferrous iron comparable to the biotites of the Deloro granites.

Gross comparison of the composition of biotites of igneous and metamorphic rocks was attempted by Heinrich (1946) and compiled by Engel and Engel (1960). The data of the analysed biotites of the Abu-Kharif and Deloro rocks are plotted in Fig. (V.1). The Abu-Kharif biotites fall

Table(V.1); Microprobe analyses of biotites from the Abu-Kharif and Deloro granitic rocks.

WEIGHT PERCENT	1	2	3	4	5	6	7	8	9	
SIO2	36.96	37.35	37.41	37.95	37.17	37.86	37.49	36.68	37.34	SIO2
AL203	13.56	13.58	13.68	12.42	12.87	13.18	12.99	13.58	13.41	AL203
TIO2	3.66	3.23	3.13	2.91	2.85	3.71	4.16	3.87	3.75	TIO2
FE203										FE203
FEO	18.77	18.74	18.98	17.14	16.95	17.32	17.34	17.28	18.92	FEO
MGO	14.25	13.69	13.43	14.96	15.28	14.48	13.83	13.51	13.19	MGO
MNO	0.24		0.22	0.58	0.53	0.57	0.71	0.55		MNO
CAO	0.14		0.17						0.15	CAO
NA20		0.01								NA20
K20	8.42	9.68	9.24	9.58	9.26	9.98	10.00	9.84	9.89	K20
H20	3.98	3.97	3.97	3.96	3.94	4.01	3.99	3.93	3.97	H20
SUM	99.98	100.17	100.07	99.42	98.85	100.95	100.51	99.88	99.82	SUM
ATOMIC PROPORTIONS										
SI	5.567	5.640	5.638	5.741	5.651	5.656	5.637	5.583	5.647	SI
AL	2.407	2.462	2.422	2.215	2.307	2.387	2.382	2.427	2.390	AL
TI	0.414	0.367	0.355	0.331	0.326	0.417	0.470	0.444	0.427	TI
FE3+										FE3+
FE2+	2.364	2.366	2.387	2.169	2.155	2.164	2.181	2.284	2.393	FE2+
MG	3.200	3.082	3.024	3.374	3.464	3.287	3.100	3.072	2.974	MG
MN	0.038		0.029	0.074	0.068	0.072	0.090	0.071		MN
CA	0.023		0.028						0.024	CA
NA		0.003								NA
K	1.617	1.863	1.780	1.824	1.795	1.982	1.918	1.915	1.754	K
OH	4.000	4.000	4.000	4.000	4.000	4.000	4.000	4.000	4.000	OH
O	20.000	20.000	20.000	20.000	20.000	20.000	20.000	20.000	20.000	O
CATSUM	19.624	19.726	19.674	19.737	19.757	19.725	19.780	19.717	19.688	CATSUM

Table(V.1); Continued ..

WEIGHT PERCENT	10	11	12	13	14	15	16	
SIO2	34.77	35.31	35.42	35.57	34.59	34.16	33.75	SIO2
AL2O3	19.95	12.45	12.55	12.58	18.83	18.68	18.79	AL2O3
TIO2	2.03	1.71	1.52	1.48	1.69	1.84	1.81	TIO2
FE2O3						0.31	1.16	FE2O3
FEO	34.96	31.97	32.83	31.79	35.38	35.82	35.23	FEO
MGO	3.32	4.84	4.68	4.93	3.83	3.85	3.81	MGO
MNO	0.31	0.31	0.25	0.31	0.37	0.26	0.24	MNO
CAO								CAO
NA2O								NA2O
K2O	9.39	9.31	9.59	9.29	9.28	9.26	9.31	K2O
H2O	3.61	3.69	3.69	3.78	3.61	3.69	3.68	H2O
SUM	99.34	99.59	99.69	99.74	99.51	99.83	99.79	SUM
ATOMIC PROPORTIONS								
SI	5.778	5.739	5.756	5.763	5.758	5.686	5.638	SI
AL	2.145	2.385	2.404	2.462	2.123	2.835	2.121	AL
TI	0.254	0.209	0.186	0.183	0.211	0.231	0.228	TI
FE3+						0.038	0.145	FE3+
FE2+	4.859	4.345	4.349	4.383	4.967	4.937	4.914	FE2+
MG	0.822	1.172	1.133	1.262	0.949	0.959	0.948	MG
MN	0.044	0.043	0.035	0.043	0.052	0.037	0.034	MN
CA								CA
NA								NA
K	1.991	1.930	1.908	1.921	1.969	1.967	1.981	K
OH	4.000	4.000	4.000	4.000	4.000	4.000	4.000	OH
O	20.000	20.000	20.000	20.000	20.000	20.000	20.000	O
CATSUM	19.892	19.824	19.850	19.817	19.962	20.000	20.000	CATSUM

Table(V.1); Continued

WEIGHT PERCENT	17	18	19	20	21	22	23	24
SIO2	35.74	34.65	35.51	35.39	35.45	40.95	49.80	37.60
AL203	11.52	12.15	11.62	13.70	14.13	17.28	25.56	15.43
TIO2	1.01	3.24	3.28	0.50	0.45	.82	0.00	0.60
						.43	0.08	4.03
FEO	33.59	35.00	34.47	31.91	31.69	2.38	0.00	26.01
MGO	2.27	2.86	3.82	4.63	4.78	22.95	0.22	1.93
MNO		0.45	0.39	0.41	0.23	tr	0.38	0.95
						0.00	0.00	0.32
						0.16	0.40	1.01
K20	8.66	7.34	7.11	9.27	9.26	9.80	9.67	8.13
H20	3.55	3.66	3.70	3.70	3.72	4.71	0.88	3.23
SUM	96.35	99.36	99.90	99.50	99.72	99.51	96.11	99.24
ATOMIC PROPORTIONS								
SI	6.031	5.678	5.748	5.741	5.722	5.72	5.97	6.00
AL	2.292	2.347	2.218	2.620	2.689	2.84	2.76	2.95
TI	0.128	0.400	0.399	0.061	0.055	0.08	0.40	0.07
						0.34	0.45	0.50
FE2+	4.741	4.796	4.668	4.331	4.277	0.28	3.61	3.52
MG	0.570	0.699	0.921	1.120	1.150	4.77	1.01	0.46
MN		0.063	0.054	0.056	0.032	---	---	0.13
						---	0.03	0.06
						0.03	0.05	0.31
K	1.865	1.534	1.468	1.919	1.907	1.75	1.69	1.78
OH	4.000	4.000	4.000	4.000	4.000	3.95	1.45	2.96
O	20.000	20.000	20.000	20.000	20.000			
CATSUM	19.627	19.516	19.477	19.847	19.832			

1 to 9 , Samples of the Abu-Kharif granitic complex,(Phlogopites).

10 to 21 , Samples of the Deloro granitic complex,(Annites).

22 , Phlogopite (Deer, Howie and Zussman 1967).

23 , Biotite (Deer,Howie and Zussman 1967).

24 , Biotite (Kabesh et al. 1977).

between the fields of granites and gneisses while the Deloro biotites fall within the field of pegmatites.

To bring out the interdependence of the chemical composition of biotite and the nature of the associated ferromagnesian minerals occuring along with in that rock, the chemical data of the investigated biotites have been plotted on the variation diagrams of Nockolds (1947) in Fig. (V.2).

The diagram is divided into three fields according to the paragenesis of the biotites:

1. Biotites associated with muscovite and aluminous minerals such as topaz and spodumene, field (I).
2. Biotites unaccompanied by other ferromagnesian minerals, field (II).
3. Biotites associated with hornblende and pyroxene or olivine, field (III).

From Figure (V.2), it is clear that the analysed biotites of both the Abu-Kharif and Deloro complexes fall within field (III). Our petrographic studies have shown that the mafic minerals associated with the biotite in the analysed granitic phases are amphiboles or alkali amphiboles, which is in agreement with the interpretation suggested by the diagram.

Another way of looking at the distribution of the Eqyptian and the Canadian biotites is by plotting them in the system siderophyllite-eastonite-phlogopite-annite of Deer et al., 1967 (Fig. V.3). The biotites from the Deloro pluton plot close together in the annite-rich portion

Fig.(V. 1)

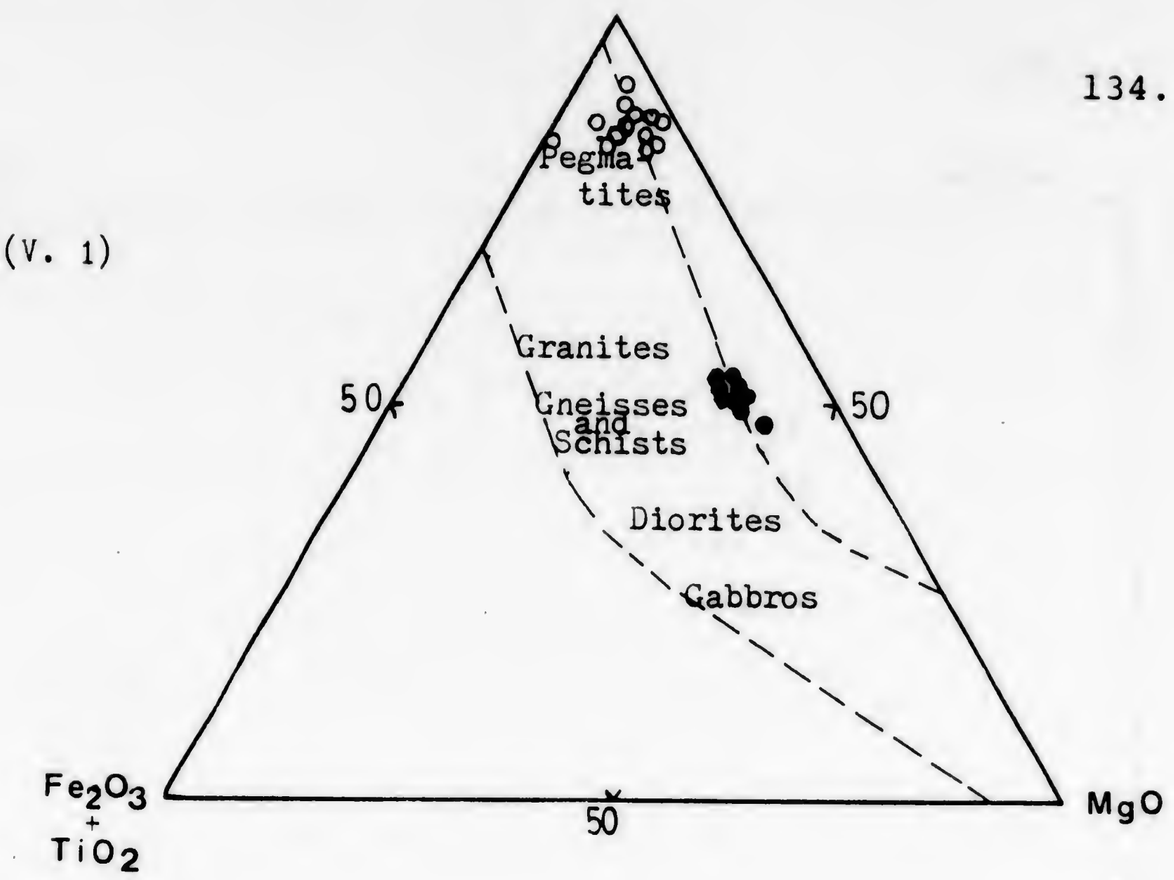

Fig.(V. 2)

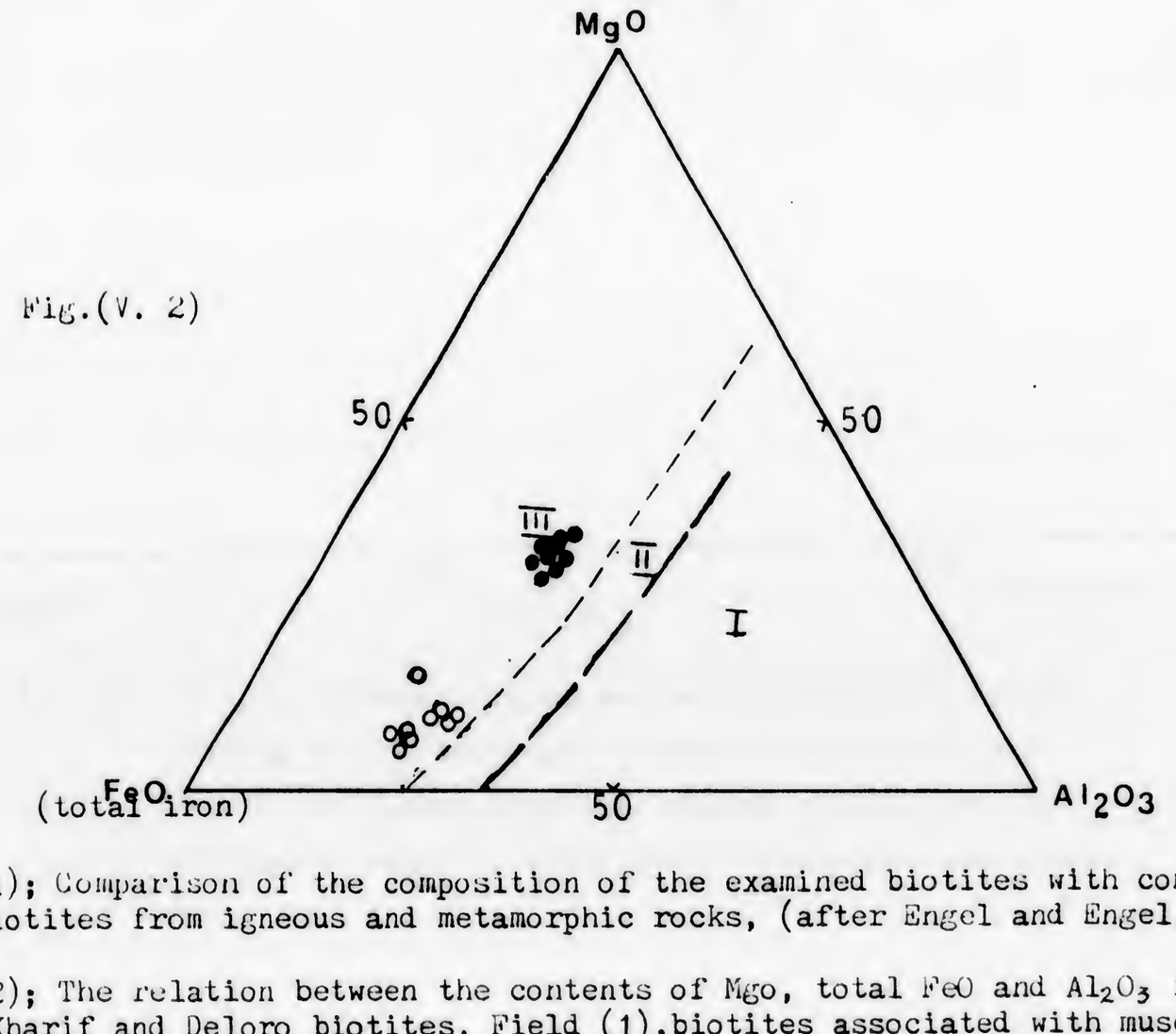

Fig.(V. 1); Comparison of the composition of the examined biotites with composition of biotites from igneous and metamorphic rocks, (after Engel and Engel, 1960).

Fig.(V. 2); The relation between the contents of Mgo, total FeO and Al_2O_3 from the Abu-Kharif and Deloro biotites. Field (1),biotites associated with muscovite. (II), biotites unaccompanied by other ferromagnesian minerals. (III), biotites associated with hornblende, pyroxene or olivine.

Symbols:

Closed circles are the Abu-Kharif biotites

Open circles are the Deloro biotites.

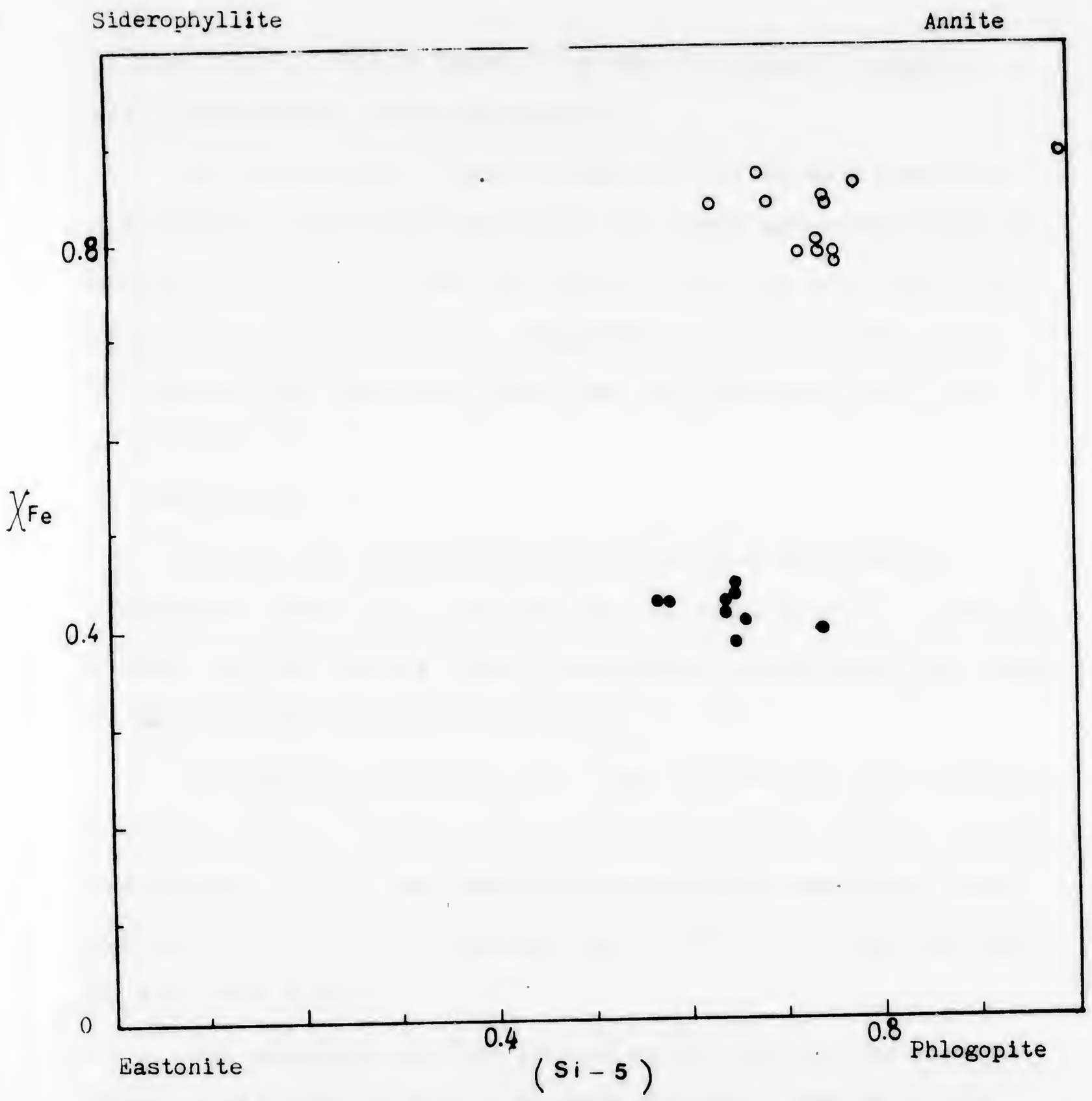

Fig.(V. 3); The join siderophyllite-eastonite-phlogopite-annite showing the distribution of biotites from the Abu-Kharif and Deloro granites. Filled circles are the Abu-Kharif samples, while open circles are the Deloro ones.

of the field. While those from the Abu-Kharif complex are considerably more phlogopitic.

In conclusion, the biotites of the Deloro granites are ferrous-iron-rich varieties and they are classified as Annite (Fig. V.3). The Abu-Kharif biotites are magnesian rich, iron poor varieties comparable to the Deloro ones. The Abu-Kharif biotites plot near the phlogopitic field (Fiv. V.3).

2) Amphibole

Due to the complexity of the Deloro amphiboles, Kuehnbaum (1973) has studied them in some detail. However, within the Abu-Kharif granitic phases, hornblende was found to be the only amphibole variety.

Microprobe analyses of 11 new amphiboles are presented in Table (V.2). Some of the analyses of the Deloro amphiboles (Kuehnbaum, 1973) and some other amphibole analyses from different localities (Deer et al., 1967) are also included in the same Table.

The analyses of the investigated amphiboles compare rather well with those of Kuehnbaum (1973) and they are also similar to the ferrohastingsite of Deer et al., 1967 (see Table V.2).

The distribution of the amphiboles from the Deloro complex is illustrated in Fig. (V.4). In that figure, the mg values

$$\left(mg = \frac{Mg}{Fe^{2+} + Fe^{3+} + Mn + Mg} \right)$$

Table(V.2); Microprobe analyses of calcic amphiboles from the Deloro granites

	1	2	3	4	5
SiO_2	39.01	40.31	39.44	43.26	38.76
TiO_2	0.11	0.30	0.32	1.33	0.35
Al_2O_3	10.83	8.77	8.99	8.40	12.23
ΣFe=FeO	28.02	30.94	33.02	23.08	24.99
MnO	1.23	1.15	0.57	0.46	0.42
MgO	3.93	2.28	1.70	7.16	5.03
CaO	10.78	10.14	10.05	11.29	11.24
Na_2O	1.44	1.53	1.69	1.83	1.71
K_2O	2.34	2.38	2.36	1.14	2.30
H_2O*	1.85	1.83	1.82	1.93	1.87
Total	99.54	99.65	99.95	99.88	98.90
Structural formulae based on 23 oxygens.					
Si	6.314	6.589	6.490	6.708	6.208
Al	1.686	1.411	1.510	1.292	1.792
	8.00	8.00	8.00	8.00	8.00
Al	0.380	0.279	0.232	0.242	0.517
Ti	0.013	0.037	0.040	0.155	0.043
Fe	3.79?	4.230	4.543	2.994	3.347
Mn	0.169	0.159	0.079	0.060	0.057
Mg	0.947	0.557	0.416	1.654	1.201
	5.30	5.26	5.31	5.11	5.16
Ca	1.869	1.776	1.772	1.875	1.930
Na	0.451	0.484	0.540	0.549	0.531
K	0.484	0.496	0.494	0.226	0.496
	2.80	2.76	2.81	2.64	2.93

Table(V.2); Continued

	6	7	8	9	10	11
SiO_2	40.56	38.49	37.12	36.58	36.55	37.40
TiO_2	0.12	0.21	0.23	0.14	0.36	0.24
Al_2O_3	9.94	11.66	11.20	10.65	11.13	10.73
$\Sigma Fe=FeO$	28.21	28.98	32.94	33.50	33.98	32.65
MnO	0.89	0.87	1.46	0.64	0.83	0.44
MgO	4.19	3.21	0.13	0.56	0.29	1.34
CaO	10.84	10.87	10.46	10.48	10.43	10.64
Na_2O	1.36	1.35	1.31	1.44	1.26	1.49
K_2O	1.57	2.20	2.65	2.98	3.14	2.61
H_2O*	1.87	1.85	1.79	1.77	1.79	1.80
Total	99.56	99.67	99.30	98.74	99.78	99.35

Structural formulae based on 23 oxygens.

Si	6.505	6.234	6.207	6.181	6.122	6.219
Al	1.495	1.766	1.793	1.819	1.878	1.781
	8.00	8.00	8.00	8.00	8.00	8.00
Al	0.384	0.459	0.415	0.303	0.321	0.322
Ti	0.014	0.025	0.029	0.018	0.046	0.030
Fe	3.783	3.925	4.607	4.734	4.761	4.540
Mn	0.121	0.119	0.207	0.092	0.117	0.062
Mg	1.001	0.775	0.032	0.141	0.073	0.331
	5.30	5.30	5.29	5.29	5.32	5.29
Ca	1.863	1.886	1.874	1.897	1 873	1.896
Na	0.424	0.423	0.425	0.471	0.410	0.480
K	0.321	0.454	0.566	0.641	0.672	0.554
	2.61	2.76	2.87	3.01	2.96	2.93

Table(V.2); Continued

WEIGHT PERCENT	12	13	14	15	16	17	18	19	
SIO2	44.65	47.09	43.08	42.58	45.87	46.44	45.48	45.75	SIO2
AL203	4.57	4.26	6.65	5.99	3.70	4.35	4.00	4.41	AL203
TIO2	1.89	0.09	0.17	0.16	0.21	0.69	1.21	1.15	TIO2
FE203	6.77	3.55	6.03	5.33	5.57	4.52	5.74	5.08	FE203
FEO	24.87	27.77	26.32	27.37	26.01	26.52	24.38	25.25	FEO
MGO	2.77	3.55	1.98	1.84	3.01	3.18	4.08	3.66	MGO
MNO	0.59	0.75	0.53	0.62	0.67	0.67	0.68	0.67	MNO
CAO	8.65	10.26	9.19	9.16	8.94	9.02	8.68	8.91	CAO
NA2O	1.16	0.93	0.98	1.23	1.01	1.26	1.53	1.33	NA2O
K2O	0.74	0.93	2.07	2.06	1.16	1.12	1.14	1.11	K2O
H2O	1.88	1.92	1.86	1.83	1.86	1.90	1.89	1.90	H2O
SUM	98.54	101.19	98.86	98.18	98.01	99.67	98.80	99.22	SUM
ATOMIC PROPORTIONS									
SI	7.124	7.343	6.952	6.971	7.378	7.326	7.229	7.235	SI
AL	0.859	0.783	1.265	1.156	0.782	0.809	0.748	0.822	AL
TI	0.227	0.011	0.021	0.020	0.025	0.082	0.144	0.137	TI
FE3+	0.813	0.416	0.732	0.657	0.674	0.537	0.686	0.685	FE3+
FE2+	3.318	3.622	3.553	3.748	3.499	3.499	3.236	3.339	FE2+
MG	0.659	0.825	0.476	0.449	0.722	0.748	0.966	0.863	MG
MN	0.080	0.099	0.072	0.086	0.091	0.090	0.091	0.090	MN
CA	1.479	1.714	1.589	1.607	1.541	1.525	1.476	1.510	CA
NA	0.359	0.281	0.307	0.390	0.315	0.385	0.471	0.408	NA
K	0.151	0.185	0.426	0.430	0.238	0.225	0.231	0.224	K
OH	2.000	2.000	2.000	2.000	2.000	2.000	2.000	2.000	OH
O	22.000	22.000	22.000	22.000	22.000	22.000	22.000	22.000	O
CATSUM	17.068	17.288	17.395	17.514	17.185	17.225	17.270	17.231	CATSUM

Table(V.2); COntinued

WEIGHT PERCENT	20	21	22	23
SIO2	45.10	45.76	44.63	37.49
AL2O3	3.28	3.01	5.41	10.81
TIO2	2.75	1.23		0.86
FE2O3	6.83	6.01	5.89	7.52
FEO	23.84	26.22	26.99	25.14
MGO	4.09	3.09	2.34	1.34
MNO	0.85	0.61	0.61	0.95
CAO	8.27	9.11	9.29	9.77
NA2O	1.42	0.91	1.11	2.06
K2O	0.95	1.02	1.74	1.91
H2O	1.90	1.88	1.88	2.01
SUM	99.27	98.85	99.89	99.86
ATOMIC PROPORTIONS				
SI	7.132	7.318	7.119	6.07
AL	0.611	0.567	1.017	2.06
TI	0.327	0.148		0.11
FE3+	0.813	0.724	0.707	0.92
FE2+	3.153	3.507	3.608	3.41
MG	0.964	0.737	0.556	0.32
MN	0.114	0.083	0.082	0.13
CA	1.401	1.561	1.588	1.70
NA	0.435	0.282	0.343	0.65
K	0.192	0.208	0.354	0.40
OH	2.000	2.000	2.000	2.17
O	22.000	22.000	22.000	
CATSUM	17.142	17.134	17.368	

23 ; Ferrohastingsite (Deer, Howie and Zussman 1967).

(a) Ca + Na + K < 2.5

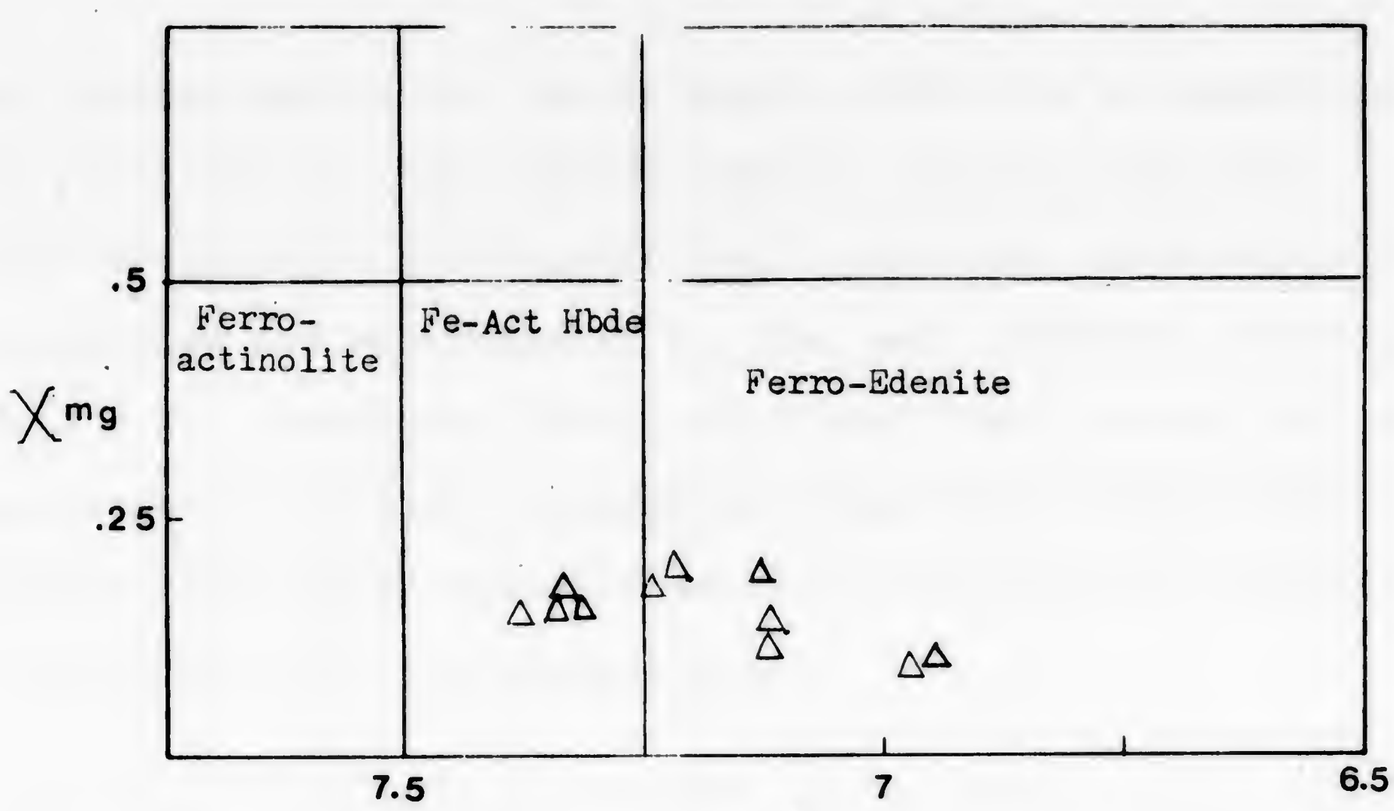

(b) Ca + Na + K > 2.5

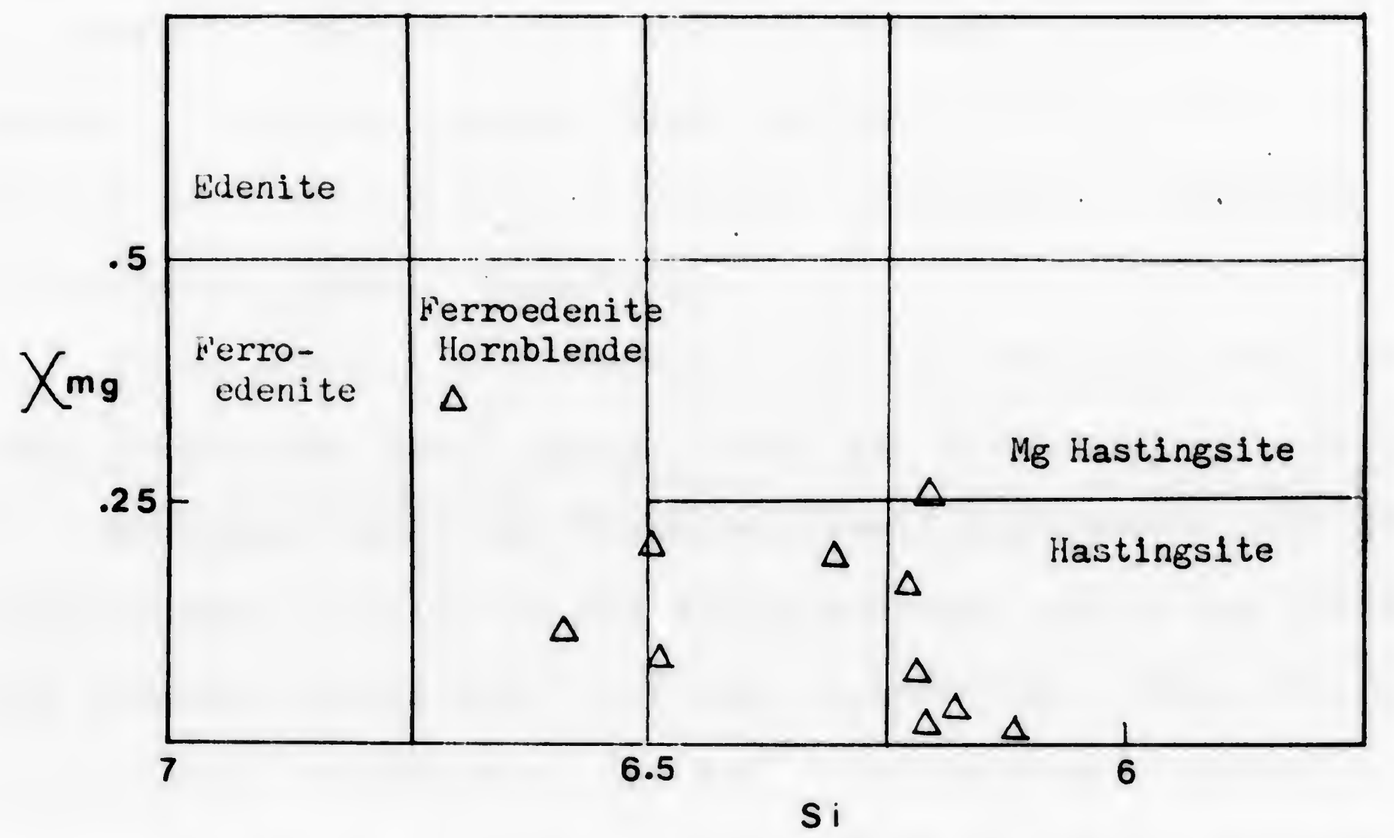

Fig.(V. 4); A portion of Leakes (1968) amphibole classification diagram, showing the distribution of amphiboles from the Deloro granites.

are plotted against si (after Leake, 1968) for 22 amphiboles. The plots of the investigated samples indicate that the ferro-actinolitic hornblendes, ferro-edinites, ferro-edinitic hornblendes and hastingsites are the main amphibole varieties (Fig. V.2). Kuehnbaum (1973) has found that the main mafic constituents are calcic amphiboles covering a broad compositional range from ferro-actinolite to hastingsite, which is in agreement with the present data.

3) Alkali amphiboles

The data from 24 new microprobe analyses of alkali amphiboles from the Abu-Kharif and Deloro granitic rocks are listed in Table (V.3). The alkali amphiboles of the Abu-Kharif complex possess high contents of TiO_2, FeO, CaO and K_2O and less of Fe_2O_3 and Na_2O, (Table V.3), compared to the Deloro alkali amphiboles.

These results are compared with the analyses from some other localities (Deer et al., 1967 and Refaat et al., 1980).

In comparison, the Egyptian alkali amphiboles, are compositionally very similar to the arfvedsonites, while the Canadian ones compare rather well with the riebeckites. Some of the Deloro alkali amphiboles,(the Fe^{2+} rich ones)are similar, compositionally, to arfvedsonites. The classification of alkali amphiboles listed in the older literature is unreliable for the following reasons (De Keyser, 1966).

Table(V.3); Microprobe analyses of alkali amphiboles from the Abu-Kharif and Deloro granitic rocks.

WEIGHT PERCENT	1	2	3	4	5	6	7	8	
SIO2	49.36	49.07	51.81	50.56	46.92	46.49	45.26	48.68	SIO2
AL2O3	0.69	1.12	0.36	3.46	1.49	1.53	1.35	1.84	AL2O3
TIO2	0.92	0.84	0.37	0.19	1.34	1.76	1.62	0.99	TIO2
FE2O3	7.68	7.05	0.08		4.64			2.55	FE2O3
FEO	28.86	29.19	33.74	31.14	32.19	32.30	33.43	32.93	FEO
MGO	0.63	0.63	0.71	0.95		0.26			MGO
MNO	0.71	0.72	0.76	0.79	0.75	0.85	0.91	1.02	MNO
CAO	4.10	4.49	5.02	5.39	4.97	6.12	6.05	6.26	CAO
NA2O	3.89	3.85	4.00	3.73	4.60	7.87	8.31	2.60	NA2O
K2O	1.17	1.02	1.15	1.80	1.01	0.91	1.07	1.24	K2O
H2O	1.88	1.88	1.89	1.91	1.85	1.84	1.82	1.87	H2O
SUM	99.88	99.88	99.89	99.91	99.75	99.94	99.82	99.97	SUM
ATOMIC PROPORTIONS									
SI	7.852	7.810	8.228	7.955	7.615	7.571	7.473	7.808	SI
AL	0.130	0.210	0.067	0.641	0.285	0.295	0.263	0.347	AL
TI	0.110	0.101	0.044	0.022	0.163	0.215	0.202	0.120	TI
FE3+	0.919	0.845	0.009		0.566			0.307	FE3+
FE2+	3.840	3.896	4.482	4.097	4.370	4.399	4.616	4.417	FE2+
MG	0.149	0.149	0.169	0.222		0.064			MG
MN	0.096	0.098	0.102	0.106	0.103	0.118	0.127	0.138	MN
CA	0.698	0.766	0.854	0.909	0.864	1.068	1.071	1.076	CA
NA	1.200	1.189	1.233	1.137	1.448	2.484	2.660	0.808	NA
K	0.237	0.208	0.233	0.362	0.210	0.190	0.225	0.254	K
OH	2.000	2.000	2.000	2.000	2.000	2.000	2.000	2.000	OH
O	22.000	22.000	22.000	22.000	22.000	22.000	22.000	22.000	O
CATSUM	17.232	17.260	17.423	17.451	17.625	18.404	18.637	17.275	CATSUM

Table(V.3); Continued

WEIGHT PERCENT	9	10	11	12	13	14	15	16	17
SIO2	48.07	49.17	48.71	48.09	52.57	52.36	51.82	50.60	49.43
AL203	1.77	1.12	1.28	1.65	1.18	1.24	1.54	0.45	0.85
TIO2	1.62	0.84	0.84	0.81	0.04	0.04	0.01		0.76
FE203	2.11	7.07	3.66	5.42	8.91	10.80	10.11	13.33	7.10
FEO	33.01	29.25	32.69	31.05	27.24	25.42	26.05	25.51	29.52
MGO		0.63		0.28		0.45	0.35		0.34
MNO	1.19	0.73	1.06	1.07	0.46	0.43	0.51	0.22	0.58
CAO	5.83	4.50	6.75	6.69	0.38	0.20	0.41		2.45
NA20	2.78	3.86	2.22	1.97	6.70	6.81	6.84	6.84	6.31
K20	1.43	1.02	0.79	1.07	0.42	0.28	0.37	1.18	0.60
H20	1.86	1.89	1.87	1.87	1.93	1.94	1.93	1.90	1.88
SUM	99.66	100.09	99.87	99.97	99.82	99.97	99.93	100.03	99.75
ATOMIC PROPORTIONS									
SI	7.756	7.810	7.823	7.709	8.187	8.112	8.063	7.974	7.880
AL	0.337	0.210	0.243	0.312	0.216	0.226	0.282	0.084	0.160
TI	0.197	0.101	0.102	0.097	0.005	0.005	0.001		0.091
FE3+	0.256	0.845	0.442	0.654	1.044	1.259	1.183	1.581	0.852
FE2+	4.455	3.886	4.391	4.162	3.548	3.294	3.390	3.362	3.936
MG		0.149		0.066		0.103	0.080		0.081
MN	0.162	0.098	0.144	0.146	0.061	0.056	0.068	0.029	0.067
CA	1.007	0.766	1.161	1.149	0.064	0.033	0.078		0.419
NA	0.868	1.189	0.693	0.612	2.024	2.047	2.062	2.091	1.952
K	0.294	0.208	0.162	0.220	0.083	0.056	0.073	0.238	0.122
OH	2.000	2.000	2.000	2.000	2.000	2.000	2.000	2.000	2.000
O	22.000	22.000	22.000	22.000	22.000	22.000	22.000	22.000	22.000
CATSUM	17.333	17.260	17.160	17.127	17.232	17.192	17.271	17.358	17.560

Table(V.3); Continued

WEIGHT PERCENT	18	19	20	21	22	23	24	
SIO2	50.12	51.28	51.25	51.21	51.91	51.03	50.27	SIO2
AL2O3	0.34	0.48	0.68	0.31		0.44	0.52	AL2O3
TIO2	0.61	0.45	0.64			0.19	0.91	TIO2
FE2O3	10.14	12.24	11.03	12.65	12.35	13.84	11.85	FE2O3
FEO	26.99	25.79	26.40	25.75	26.03	24.75	25.32	FEO
MGO	0.69						0.80	MGO
MNO	0.47	0.37	0.55	0.27	0.25	0.27	0.48	MNO
CAO	1.07	0.30					0.87	CAO
NA2O	6.67	6.48	6.88	7.02	6.92	6.41	6.17	NA2O
K2O	1.00	0.62	0.56	0.59	0.55	0.97	1.11	K2O
H2O	1.90	1.91	1.91	1.91	1.91	1.91	1.91	H2O
SUM	100.00	99.91	99.91	99.71	99.91	99.81	100.21	SUM
ATOMIC PROPORTIONS								
SI	7.925	8.036	8.036	8.057	8.133	8.011	7.886	SI
AL	0.064	0.089	0.126	0.057		0.082	0.097	AL
TI	0.072	0.053	0.075			0.022	0.107	TI
FE3+	1.207	1.443	1.301	1.497	1.456	1.635	1.399	FE3+
FE2+	3.569	3.380	3.462	3.389	3.411	3.249	3.322	FE2+
MG	0.163						0.188	MG
MN	0.063	0.050	0.073	0.036	0.033	0.036	0.064	MN
CA	0.181	0.050					0.146	CA
NA	2.045	1.968	2.092	2.143	2.102	1.950	1.876	NA
K	0.202	0.124	0.113	0.118	0.110	0.125	0.222	K
OH	2.000	2.000	2.000	2.000	2.000	2.000	2.000	OH
O	22.000	22.000	22.000	22.000	22.000	22.000	22.000	O
CATSUM	17.491	17.192	17.278	17.296	17.244	17.181	17.307	CATSUM

Table(V.3); Continued

WEIGHT PERCENT	25	26	27	28	
SIO2	52.41	48.41	45.61	50.81	SIO2
AL203	0.61	1.81	3.03	1.79	AL203
TIO2	0.45	1.32	1.21	1.02	TIO2
FE203	14.37	11.25	9.54	13.17	FE203
FEO	14.82	23.81	26.01	20.61	FEO
MGO	5.07	0.06	0.52	0.28	MGO
MNO	1.46	0.75	0.40	0.33	MNO
CAO	1.33	1.18	2.91	1.09	CAO
NA2O	4.94	7.37	5.36	7.22	NA2O
K2O	2.10	1.52	2.11	1.19	K2O
H2O	2.12	1.07	1.88	1.57	H2O
SUM	99.68	98.55	98.58	98.98	SUM
ATOMIC PROPORTIONS					
SI	7.92	7.62	7.07	7.55	SI
AL	0.11	0.33	0.55	0.31	AL
TI	0.05	0.16	0.14	0.11	TI
FE3+	1.63	1.33	1.11	1.33	FE3+
FE2+	1.87	3.13	3.37	2.56	FE2+
MG	1.14	0.01	0.12	0.06	MG
MN	0.19	0.10	0.05	0.04	MN
CA	0.22	0.20	0.48	0.17	CA
NA	1.45	2.25	1.61	2.08	NA
K	0.41	0.30	0.41	0.22	K
OH	2.04	0.99	1.94	1.55	OH

1 to 12 , Samples of the Abu-Kharif granitic complex,(Arfvedsonites)
13 to 24, Samples of the Deloro granitic complex,(Riebeckites)
25& 26 , Riebeckite and Arfvedsonite (Deer, Howie and Zussman 1967).
27 & 28 , Arfvedsonite and Riebeckite (Refaat, et al. 1980),

(i) A complex formula easily results due to the ion-substition in the sodic amphiboles (Borley, 1963).
(ii) The identification and description of the sodic amphiboles in the previous literature have mostly been mistaken views (Miyashiro, 1957).
(iii) The analytical errors of water content are believed to be common, causing defect on the calculated structural formula (Philips, 1963).

Many classification schemes have been made to clarify the different varieties of sodic amphiboles by Miyashiro (1957), Kaufmann (1963) and Brock et al. (1964).

In Figure (V.5), the Abu-Kharif and Deloro alkali amphiboles are plotted in the Miyashiro scheme which is graphically represented by Si against R^{3+} (Al + Fe^{3+}). It is evident that the Deloro alkali amphiboles fall in the riebeckite and arfvedsonite fields, while the Abu-Kharif ones fall within the arfvedsonite and the sodatremolite fields.

The values of Na + K are plotted against Fe^{3+} values in Fig. (V.6), which is considered a classification scheme for alkali amphiboles (Lyons, 1976). The diagram indicates that the Egyptian alkali amphiboles fall within the arfvedsonite field, while the Canadian ones, again, fall into the categories of both riebeckite and arfvedsonite.

The relation between (Na + K) and Ca for the studied alkali amphiboles is illustrated in Fig. (V.7), after Thompson (1976). In that diagram, the composition of the

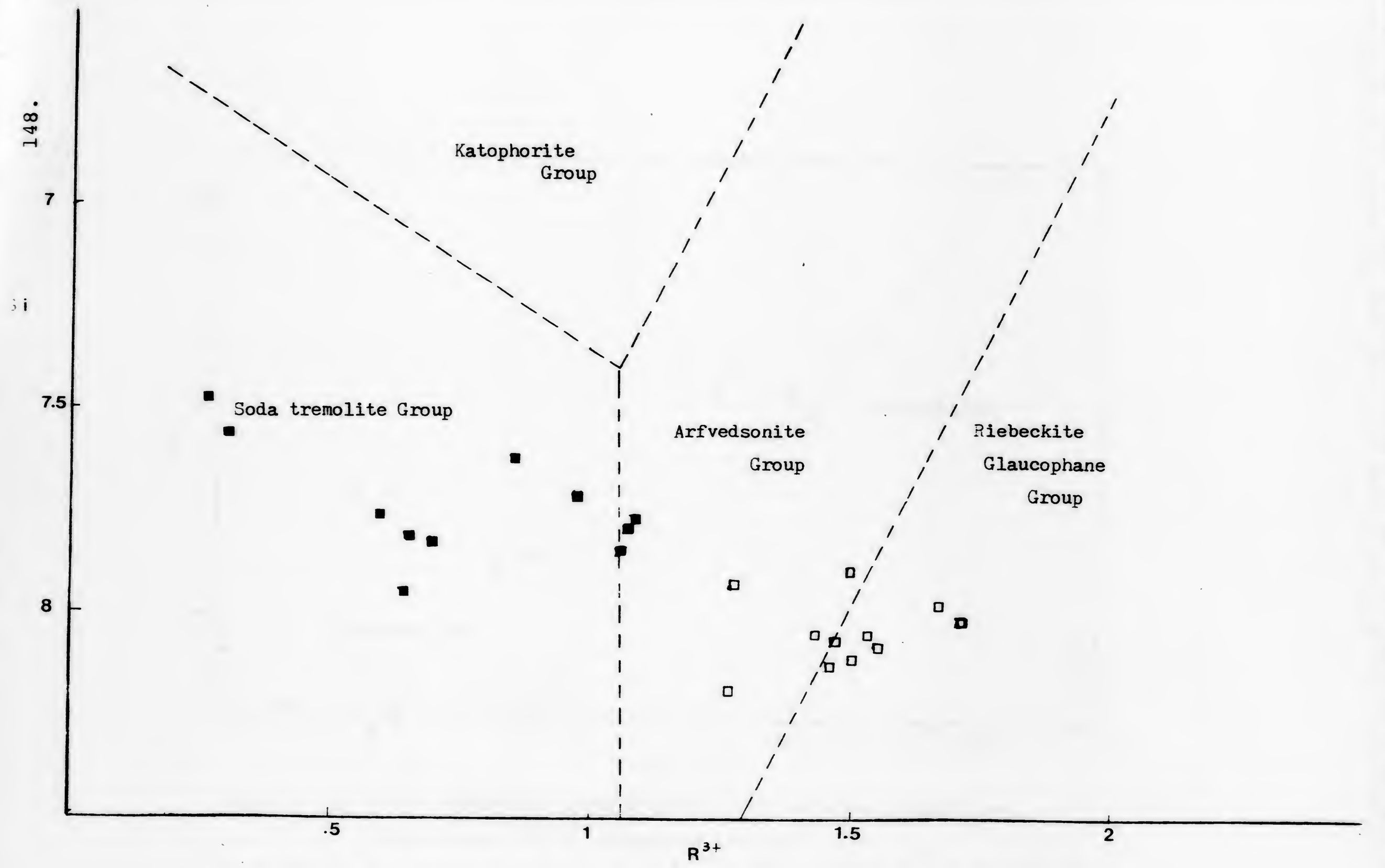

Fig.(V. 5); Atomic variation in Si with R^{3+} (where $R^{3+}=Al+Fe^{3+}$) in the Abu-Kharif and Deloro alkali amphiboles. Filled squares are the Abu-Kharif samples and open squares are the Deloro samples.

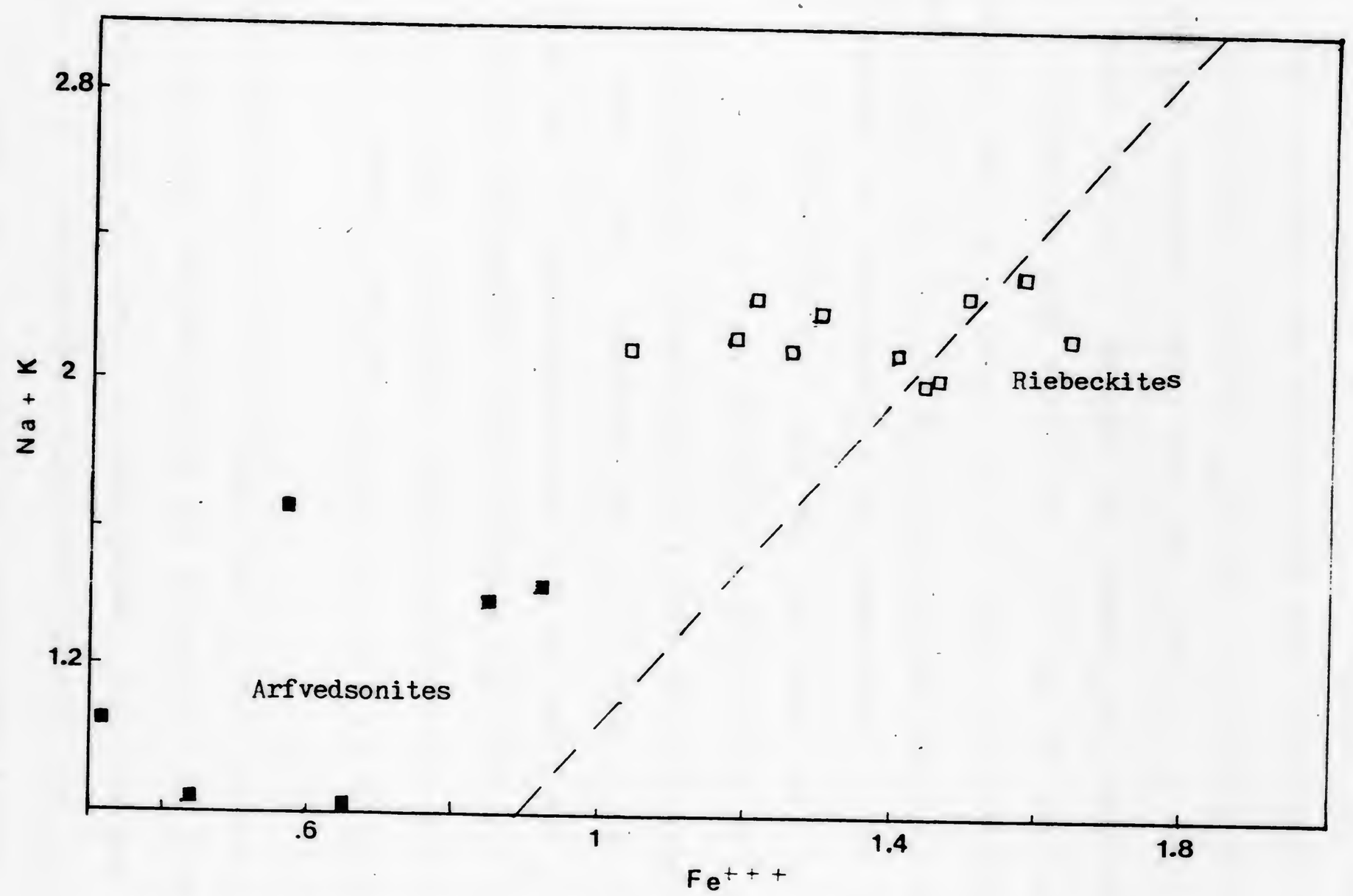

Fig.(V. 6); Atomic variations in Na+K with Fe^{3+} in the alkali amphiboles (after Lyons, 1976). Symbols as in Fig.(V. 5).

examined alkali amphiboles are compared to the three end members and the naturally projected amphiboles. It is evident that the Deloro alkali amphiboles lie near the projected compositions of riebeckite and arfvedsonite, while the Abu-Kharif ones are close to the composition of the ferrorichterite (Fig. V.7).

Values of Ca + Al are plotted against values of Na + K + Si + Ti for the examined alkali amphiboles (Fig. V. 8). It is obvious that the studied alkali amphiboles of the Abu-Kharif granites are in close relationship to the natural arfvedsonite (at point 2 of the diagram). While those of Deloro pluton lie far from the theoretical arfvedsonite but nearer to the theoretical riebeckite (Fig. V. 8).

It is also observed that (Ca + Al) decreases as (Na + K + Si + Ti)increase from arfvedsonite to riebeckite.

The relation between Fe^{2+} and Fe^{3+} in the investigated alkali amphiboles is shown in Fig. (V.9). In 1980, Refaat et al. pointed out that Fe^{3+} increases from arfvedsonite to riebeckite while Fe^{2+} shows the opposite relation. From Figure (V.9), it is clear that the Deloro samples fall in the field of high Fe^{3+} - low Fe^{2+} contents (riebeckite), while the Abu-Kharif ones plot within the field of high Fe^{2+} - low Fe^{3+} values.

The investigated riebeckites and arfvedsonites are, in general, characterized by higher values of Fe^{2+} than Fe^{3+}, but there is little difference between ferric

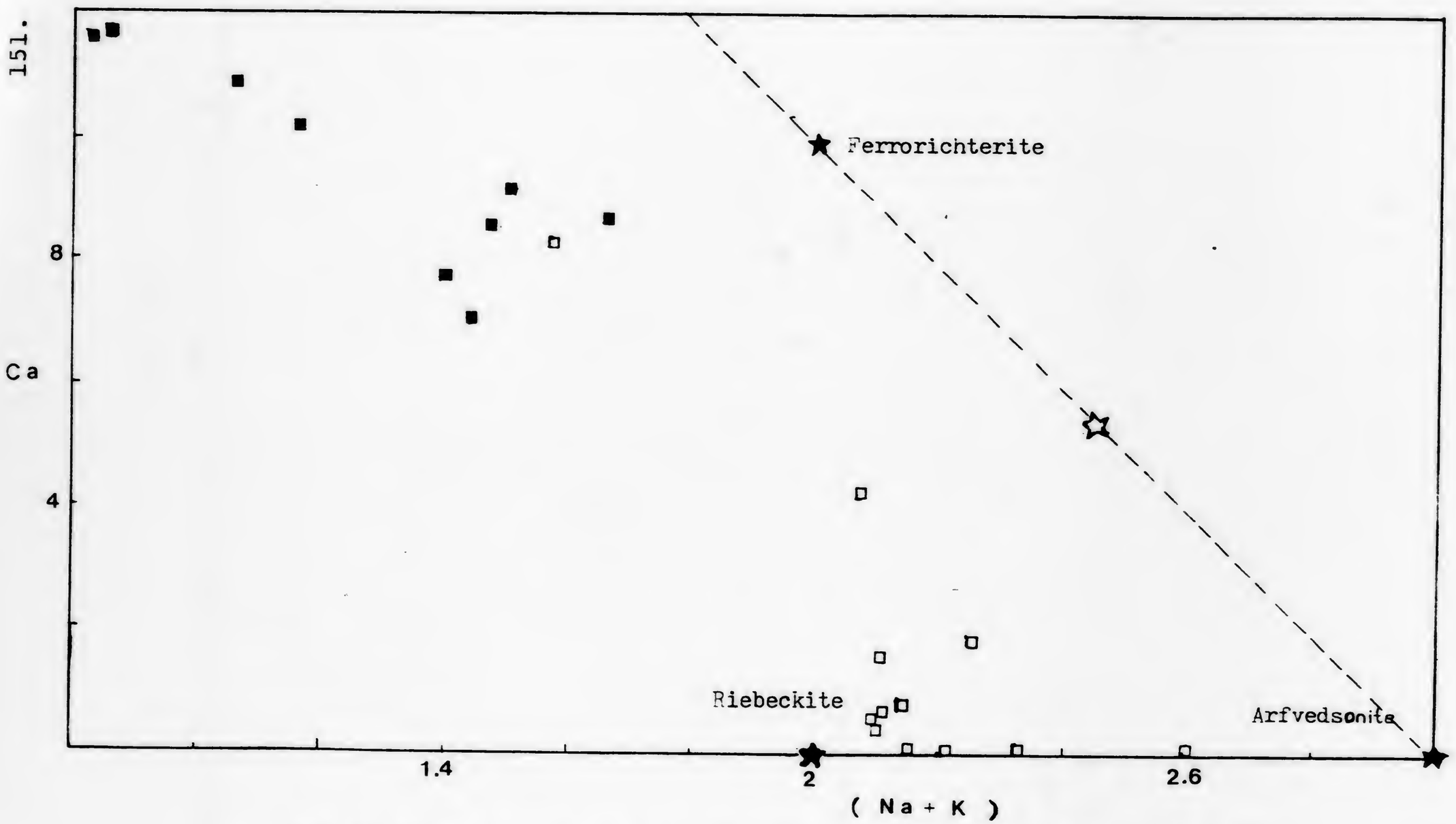

Fig.(V. 7); Ca versus Na+K for the Abu-Kharif and Deloro alkali amphiboles.
Filled stars indicate Fe-amphibole end members as labelled.
The open star is arfvedsonite formula suggested by Miyashiro, (1957),-after Thompson, 1976- .
Symbols as in Fig.(V. 5).

Fig.(V. 8); Atomic variation in Ca+Al with Na+K+R++ (where R++=Si+Ti). Closed circles are; (1) =end member arfvedsonite (after Sundius, 1964).
(2) =natural arfvedsonite (after Miyashiro,1957).
(3) =end member riebeckite (after Borley, 1963).
Symbols as in Fig.(V. 5)

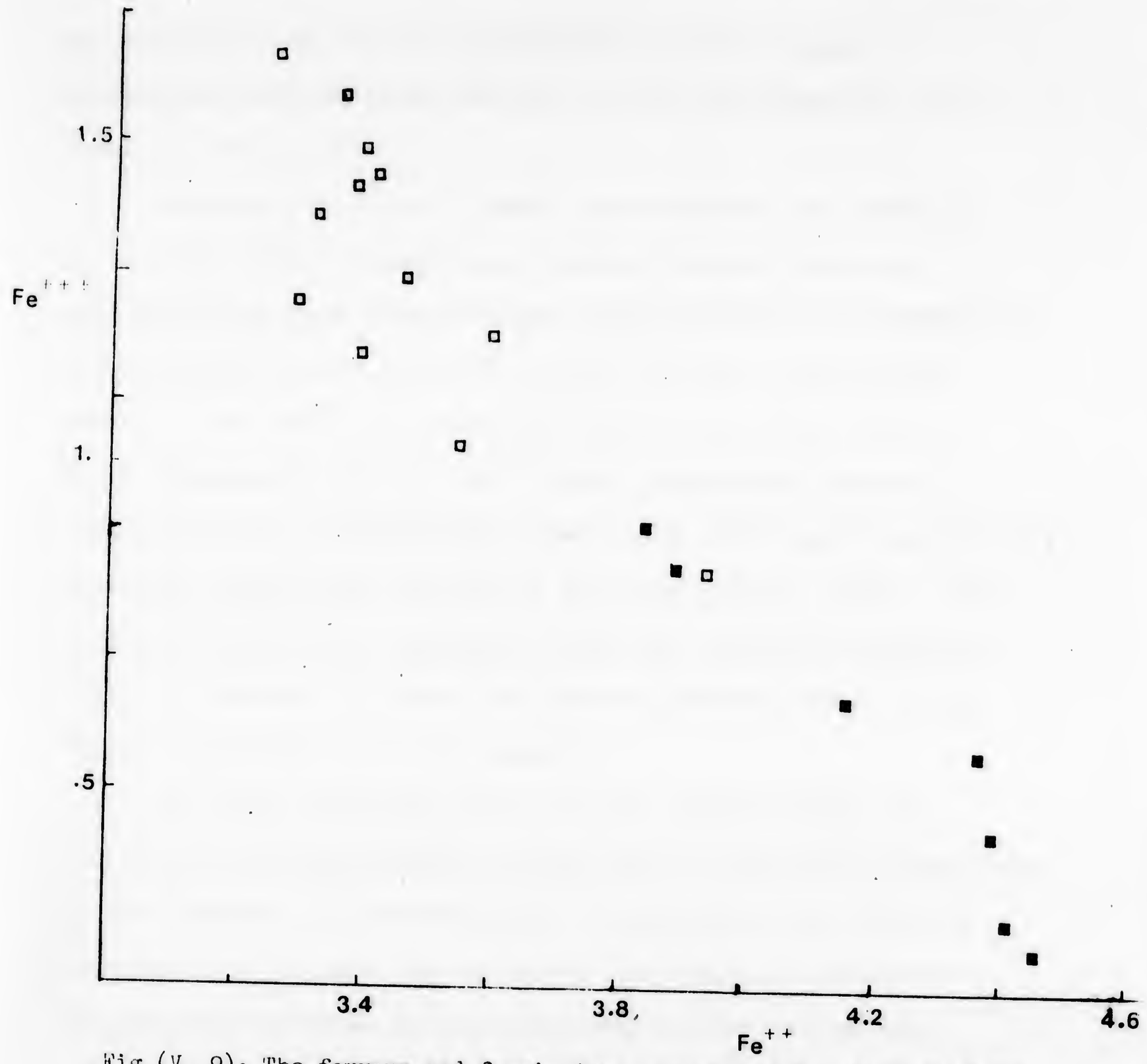

Fig.(V. 9); The ferrous and ferric iron content of the Abu-Kharif and Deloro alkali amphiboles. Symbols as in Fig.(V. 5).

and ferrous iron in the riebeckites, while a great difference between both cations in the arfvedsonites are observed (Table V.3).

According to Ernst (1968), who studied the behavior of iron in alkali amphiboles, we may suggest that the arfvedsonites were crystallized from arfvedsonite-riebeckite discontinuous solid solution series at high temperature (mainly over 500°C) in reducing conditions given rise to sodic amphiboles rich in Fe^{2+} while riebeckites began to crystallize at a temperature lower than 500°C under relatively oxidizing conditions causing a decrease in Fe^{2+} ions. That interpretation is in agreement with our previous interpretation in Chapter IV about the high oxidation state of the Deloro riebeckite granitic magma.

The high oxidation state of the Deloro magma in addition to its deficiency in Mg, help to develop riebeckites at the expense of arfvedsonites. Meanwhile, the relative enrichment of Mg and the relative low oxidation state of the Abu-Kharif magma play an important role during the arfvedsonite crystallization.

It is also evident that Si atomic proportions in the alkali amphiboles increased from arfvedsonite to riebeckite as the iron became more oxidized, i.e. oxygen fugacity increased.

The previous discussions and descriptions of the different variation diagrams lead us to the conclusion that the Egyptian alkali amphiboles, according to Miyashiro (1957), Borley (1963) and Lyons (1976), are considered to be arfvedsonites. However, the Canadian alkali amphiboles are mainly represented by riebeckites with a few arfvedsonites.

Trace Elements

Trace elements, including the REE, were determined for 12 mineral separates representing biotites, amphiboles and alkali amphiboles of the different granitic phases from the Abu-Kharif and Deloro complexes.

The data from the analyses of the mineral fractions are tabulated in Table (V.4). The Rare Earth Elements have been normalized to whole-rock values in Figs. (V.10 and V.11).

The elemental abundances and the behavior of the determined (15) trace elements willbe considered under the following groups:

1) Cr, Sc and Co

Within the Abu-Kharif granites, it is observed that hornblende has the highest Cr, Sc and Co concentrations, followed by biotites, while alkali amphiboles (arfvedsonites) possess the lowest values. In the Deloro mafic minerals, the calcic amphiboles are enriched in both Sc and Co relative to the alkali amphiboles. However, the latter are slightly enriched in Cr (average of 58.8 ppm) compared to the calcic amphiboles (average of 24.4 ppm).

2) Ba and Cs

The Abu-Kharif alkali amphiboles have the highest Ba contents, followed by the biotites, while hornblendes have the lowest Ba contents. In the same granitic complex, the

TABLE (V.4): Trace element concentrations (ppm) of some mineral separates from the Abu-Kharif and Deloro granitic rocks.

	Abu-Kharif Samples					Deloro Samples						
	Hbd	Biot	Biot	Arf	Arf	Amph	Amph	Amph	Reb	Reb	Reb	Reb
La	35.65	400.88	430.2	853.24	1432.10	127.11	100.39	65.18	704.6	598.4	1378.0	722.4
Ce	111.57	1067.7	1128.91	1913.3	3166.3	364.73	338.19	169.93	1550.2	1486.3	3226.27	1740.03
Nd	75.4	452.78	626.76	636.44	1174.4	311.14	297.08	212.56	783.97	661.19	1185.42	817.31
Sm	15.3	94.19	82.89	149.85	182.5	57.94	61.60	31.75	192.87	178.16	266.1	245.0
Eu	2.00	10.63	8.80	11.62	17.5	6.03	5.26	8.38	10.18	10.28	13.64	14.45
Tb	1.71	9.32	8.84	16.53	14.16	9.80	11.99	5.62	29.39	30.57	34.24	44.44
Ho	2.68	16.86	19.69	25.70	21.26	12.67	19.03	8.00	54.05	60.31	50.72	81.85
Yb	5.16	30.18	28.80	55.6	48.08	33.78	88.18	24.41	120.25	164.92	155.26	221.91
Lu	0.89	4.55	4.9	10.23	9.20	5.05	15.63	3.79	19.95	27.55	25.19	34.86
Cr	129.65	85.62	107.73	42.35	12.19	34.05	30.20	8.91	39.15	53.48	61.45	81.19
Sc	43.08	33.48	29.52	7.78	7.71	34.18	2.05	22.91	19.87	15.64	15.74	15.24
Co	41.48	26.96	29.04	5.06	3.38	13.30	2.45	9.73	3.06	3.07	3.14	4.02
Ba	783.8	1280.3	1257.5	1623.13	1812.7	1416.3	1315.73	900.08	2733.4	3511.0	3200.7	4051.5
Cs	1.16	6.86	6.26	0.67	0.81	2.08	0.56	0.45	0.89	0.75	0.65	0.32
Hf	9.25	40.51	51.14	78.38	92.76	31.45	42.22	18.26	185.78	234.76	200.32	415.71

investigated biotites possess the highest Cs contents (6.56 ppm) relative to the other mafic minerals. Meanwhile, the Deloro alkali amphiboles are enriched in both Ba and Cs relative to the calcic amphiboles (see Table V.4).

3) Hf

Among the Abu-Kharif mafic minerals, the alkali amphiboles are highly enriched in Hf (average of 80 ppm), relative to biotites (45.8 ppm), while hornblendes have the lowest values (9.3 ppm).

In the Deloro mineral separates, the alkali amphiboles are highly enirched in Hf (average of 259 ppm) relative to the amphiboles (average of 30.6 ppm).

4) Rare Earth Elements

Considering the lanthanides, the concentrations in the different mineral phases cover a wide range, some very enriched (alkali amphiboles) and some depleted (Abu-Kharif hornblende). Biotite in the Abu-Kharif calc-alkaline granites appears rather rich in lanthanides (Table V.4). Fourcade et al. (1981) in his case study of the "Pyrenees" granites in France has reported that biotite enrichment in the lanthanides may be due to inclusions of apatite needles which were not completely removed in the separation.

It is significant that the Abu-Kharif and Deloro mafic minerals all have REE distributions very similar to the whole-

rock distirubion, but not surprising.

The REE patterns of both plutons (Figs. V.10 and V.11) show that the alkali amphiboles of both complexes are highly enriched in REE.

In comparison, it is noted from the slopes of the plots that the REE's are highly fractionated within the Abu-Kharif minerals, while they are poorly fractionated within the Deloro ones. It is also noteworthy that the Egyptian ferromagnesian minerals are highly depleted in heavy REE relative to the Deloro minerals. The heavy REE depletion in the Abu-Kharif studied mineral phases probably reflects the depletion in the melt resulting from zircon crystallization. Buma et al. (1971) reached a similar conclusion.

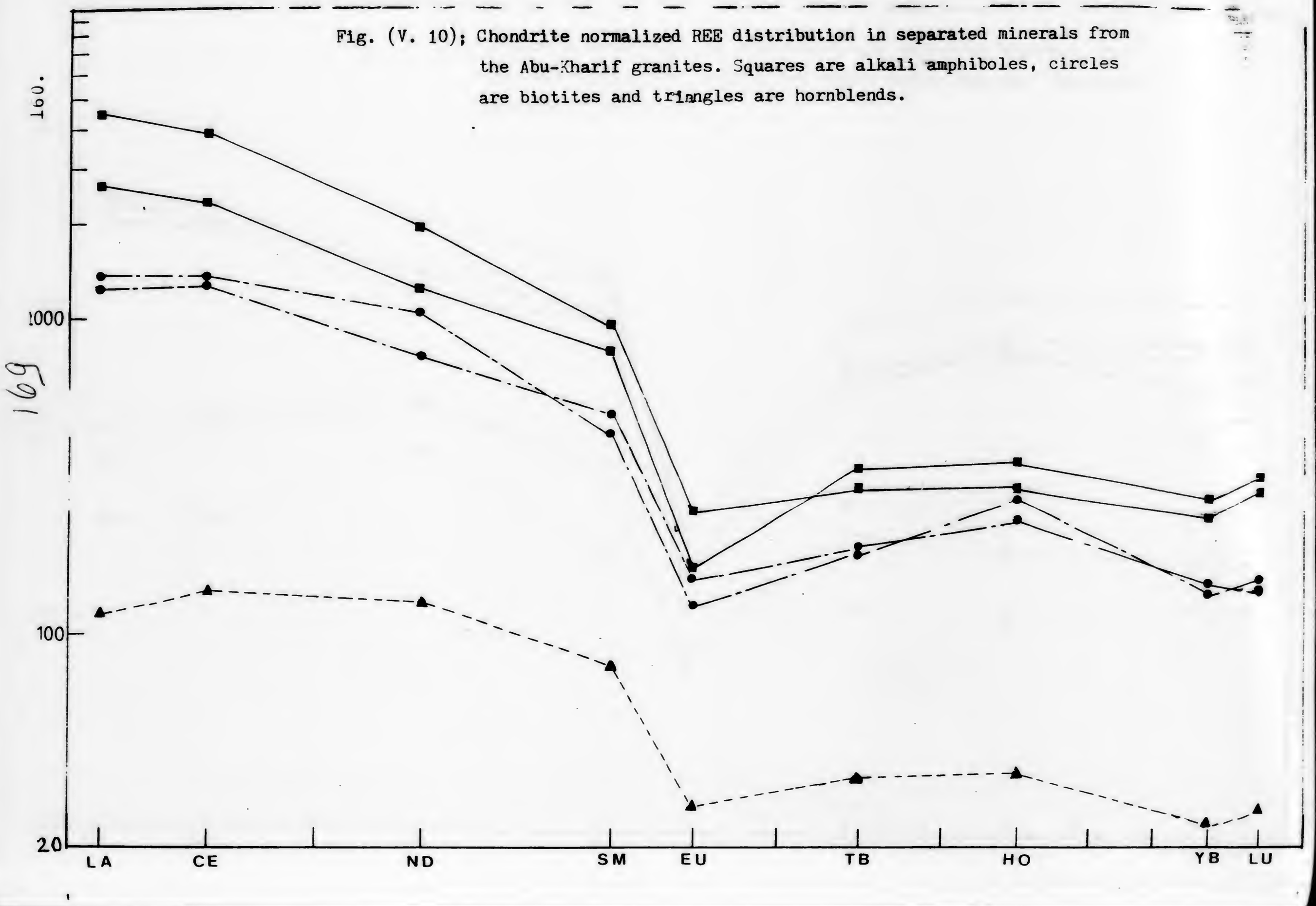

Fig. (V. 10); Chondrite normalized REE distribution in separated minerals from the Abu-Kharif granites. Squares are alkali amphiboles, circles are biotites and triangles are hornblends.

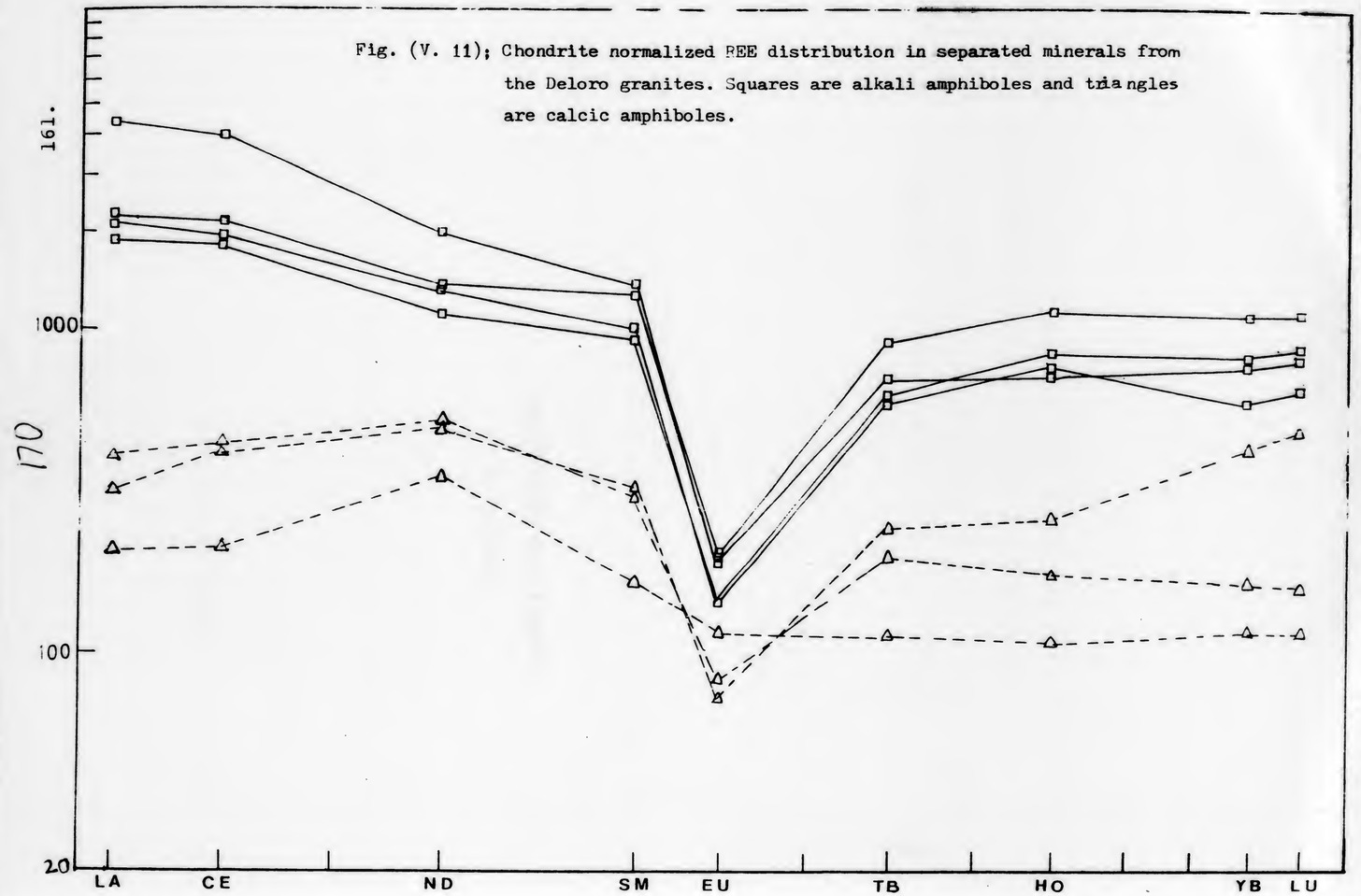

Fig. (V. 11); Chondrite normalized REE distribution in separated minerals from the Deloro granites. Squares are alkali amphiboles and triangles are calcic amphiboles.

CHAPTER VI

SUMMARY AND CONCLUSIONS

CHAPTER VI

SUMMARY AND CONCLUSIONS

The Abu-Kharif granitic complex mainly consists of syntectonic grey granodiorites, late tectonic pink calc-alkaline granites and a still younger phase of alkaline granites. The granodiorites and the calc-alkaline granites are traversed by acidic, intermediate and basic dykes, the so-called post-granitic dykes. Our field observations show that the post-tectonic alkaline granites intrude the dykes. Consequently, they represent a separate granitic phase, chronologically emplaced after the dyke intrusion.

The Deloro granitic pluton mainly consists of calcic syenite-granite, peralkaline riebeckite granite and granophyric granite. The sequence of emplacement of the Deloro pluton was as follows: intrusion of gabbroic rocks, intrusion and fractionation <u>in situ</u> of the calcic suite (calcic syenite-granite), diapiric intrusion of the relatively dry peralkaline magma and finally the high level intrusion of granophyric granites.

Petrographic studies reveal that the Abu-Kharif granites include several petrographic varieties in each granitic field type. Among the syntectonic granodiorites, hornblende, biotite hornblende, biotite and leucocratic granites are recognized. Among the late-tectonic stage; biotite hornblende, biotite, biotite muscovite and leucocratic granites are distinguished. The alkali amphiboles of the alkaline,

post-tectonic granites, are optically and chemically found to be arfvedsonites. The arfvedsonite biotite, arfvedsonite and leucocratic granites are the main petrographic varieties among the post-tectonic alkaline granites.

Several petrographic varieties are also recorded in each granitic phase of the Deloro pluton. Among the calcic syenite-granite; Aenigmatite-bearing varieties have been recognized beside the ferroedenite actinolitic-hornblende and hastingsite varieties. Among the peralkaline stage, riebeckite, riebeckite biotite and leucocratic granites are recognized. Granophyric granite is the only variety in this stage.

The detailed petrogarphic studies reveal the following:

1. Within the Abu-Kharif granites, the feldspars of the syntectonic granodiorites, compositionally, are predominantly plagioclases with subordinate amounts of alkalifeldspars. Among the late-tectonic pink calc-alkaline granites, alkali-feldspar predominates over plagioclase. In the post-tectonic alkaline granites, the alkalifeldspars are exclusive.
2. Among the Deloro granites, the feldspars of the three different granitic phases are predominantly alkalifeldspars with some thin rims of secondary albite which developed along perthite margins.
3. The alkalifeldspars of the alkali amphibole granites of both granitic complexes are predominantly perthites, displaying the hypersolvus nature of such granitic rocks. The perthite crystals are occasionally twinned on both Baveno and Carlsbad laws.

4. The occurrence of albite outer zones, the concentration of albite inclusions around the cleavage planes and the occurrence of unevenly distributed macro perthite bands in some perthite crystals, all indicate the presence of replacement perthite. That phenomenon is frequently observed in the alkali amphibole granites of both the Abu-Kharif and Deloro complexes.

5. The occurrence of perthite crystals enclosing corroded previously crystallized perthites indicates two phases of perthite development separated by a period of magmatic corrosion.

6. Within the Deloro pluton, the main mafic constituents of the syenite-granitic phase are calcic amphiboles cover a broad compositional range extending from ferro-actinolite to hastingsite.

The study of the petrochemistry and geochemistry of the examined granitic phases included the study of the major and trace elements variation as well as their REE patterns. In addition, the chemical data were processed into several petrochemical parameters such as molecular norms, Niggli values, Rittmann's Suite index and differentiation index.

The plots of the normative minerals, albite-orthoclase and quartz on the ternary diagram of Tuttle and Bowen (1958) indicate magmatic origin for the different granitic field types of the Abu-Kharif and Deloro complexes.

Among the Abu-Kharif granitic rocks, the calculated Niggli values indicate that the granodiorites and the calc-alkaline granites are characterized by alk lower than al. Samples of the post-tectonic alkaline granites show alk higher than al. Meanwhile, the Deloro peralkaline riebeckite granites show a similar relation.

The Niggli-values of the Deloro granites show a continuous variation in composition from the calcic syenite-granite to the peralkaline and granophyric granites. The plots of the Egyptian rocks, apart from the separate alkaline granite, display a continuous variation from the syntectonic granodiorites through the calc-alkaline granites. These results are in harmony with the field observations.

The study of the differentiation trends in the Deloro samples reveals that the plots of the different granitic phases are located on one differentiation trend. Among the Abu-Kharif granitic rocks, the plots of both syntectonic granodiorites and calc-alkaline granites are located on one differentiation trend, while the latter group (the alkaline granites) represents a different, more differentiated stage. It is also evident that the post-tectonic alkaline granites are either located above or below this trend.

Study of the major oxides of both the Abu-Kharif and Deloro granitic rocks shows that the alkaline and peralkaline granites have higher values of Na_2O accompanied with low

Al_2O_3. The enrichment of sodium may account for the occurrence of the alkali amphiboles (arfvedsonites and/or riebeckites) among these rocks.

Study of the trace elements reveal the follwoing facts:

1) Considering the trace elements (Ba, Sr, Rb and Cs), it is found that the more basic varieties of the Abu-Kharif and Deloro graitic complexes (the granodiorites and calcic syenite-granites respectively) have in general, higher Sr and Ba concentrations and lower Rb and Cs contents than the more differentiated granitic varieties.

2) The maximum concentration for Cr, Sc and Co are found in the more basic varieties (Abu-Kharif granodiorites and Deloro syenite-granite). However, the more acidic varieties are less enirched in those elements.

3) Among the investigated Egyptian and Canadian granitic rocks, it is noted that the alkali amphibole granites have a higher Ta, Zr, Hf and Y contents relative to the other granitic phases. The plots of Zr, Hf and Y against the D.I. show a continuous variation throughout the Deloro granitic phases, suggesting a single continuous granitic series. Within the Abu-Kharif granites, the plots of the alkaline granite lie above the granodiorite, calc-alkaline granitic trend.

4) From the distribution of U and Th, it is clear that U and Th increase from basic to silicic rocks in both the

Abu-Kharif and Deloro granitic complexes. Apart from the separate, Egyptian alkaline granites, a sympathic relation is obtained where U and Th increase with increasing differentiation index among the other granitic phases.

The lanthanide distribution among both the Abu-Kharif and Deloro granitic rocks indicates that the alkali amphibole granites of both complexes are highly enriched in REE and exhibit an important negative Eu anomaly comparable to the other granitic phases.

In comparison, the REE patterns of the different granitic rocks of both the Abu-Kharif and Deloro complexes reveal two main features:

a) The Egyptian granites exhibit a more differentiated REE relative to the Canadian granitic rocks in which REE are less differentiated or not at all.

b) A remarkable enrichment in heavy REE wihtin the Deloro granites comparable to the Abu-Kharif granites.

The REE results show that the Egyptian granitic rocks display two main different REE patterns, both the granodiorites and the calc-alkaline granites possesses a very similar or homogeneous REE patterns, while the alkaline granites exhibit a different and a characteristic REE patterns, suggesting that those granitic rocks are possibly derived from two different magmas. The alkaline granitic phase probably represents a separate magmatic unit. The homogeneity

between the REE patterns of the different granitic phases of the Deloro pluton may permit us to consider that the Deloro granitic rocks could probably be derived from a more basic magma by extensive differentiation and they possibly form a single continuous granitic series. These results are in strong agreement with the field observations.

From the geochemical point of view, it can generally be seen that the Deloro granitic magma was highly enriched in femic oxides, K_2O, Na_2O, Cr, Hf, Y and heavy REE and depleted in Al_2O_3, MgO and Sr compared to the Abu-Kharif magmas.

According to the sympathetic relation among their major and trace elements variation and the homogeneity in their REE patterns, the different granitic phases of the Deloro pluton are possibly forming a single continuous granitic series from the calcic syenite-granite to the peralkaline granite throughout the granophyric granite. Among the Abu-Kharif granitic rocks, it is found that the syntectonic granodiorites and the late tectonic calc-alkaline granites exhibit a smooth variation and a continuous evolution in their major and trace elements. However, the younger, post-tectonic alkaline granitic phase usually lie above or below the previous evolution trend leading to the conclusion that this younger alkaline granitic phase is not a part of the granodiorite-calc alkaline granitic series, and should be considered as a separate magmatic unit.

Our geochemical studies of the Abu-Kharif and Deloro ferromagnesian mineral phases reveal the following:

1. The Abu-Kharif biotites, compositionally, are magnesian rich, ferrous iron-poor varieties relative to the Deloro biotites which are ferrous iron rich varieties.

2. The biotites are plotted in the system siderophyllite-eastonite-phlogopite-annite. The Canadian biotites plot close together in the annite-rich portion of the field. While the Egyptian biotites are considerably more phlogopitic.

3. Hornblende found is to be the only amphibole variety in the Abu-Kharif granitic complex. The Deloro calcic-amphiboles are classified (according to Leake, 1968) as ferro-actinolitic hornblendes and hastingsites.

4. The alkali amphiboles of the Abu-Kharif granites are enriched in FeO, CaO, K_2O and TiO_2 and depleted in Fe_2O_3 and Na_2O compared to the Deloro alkali amphiboles.

5. From the relation between (Na+K) and Ca, it is found that the Deloro alkali amphiboles lie near the projected compositions of riebeckite and arfvedsonite.

6. According to Miyashiro (1957), Borly (1963) and Lyons (1976), the Egyptian alkali amphiboles should be classified as arfvedsonites. However, the Canadian ones are mainly represented by riebeckites with some few arfvedsonites.

7. It is noted that the Deloro alkali amphiboles fall in the field of high Fe^{3+}-low Fe^{2+} contents (riebeckites), while the Abu-Kharif ones plot within the field of high Fe^{2+}-low Fe^{3+} values.

8. It is also observed that the Si atomic proportions increase from the Egyptian alkali amphiboles (arfvedsonites) to the Deloro alkali amphiboles (riebeckites) as the iron becomes more oxidized.

9. The (Ca+Al) is found to decrease as the (Na + K + Si + Ti) increases from the Egyptian alkali amphiboles (arfvedsonites) to the Canadian ones (riebeckites).

10. The trace element distribution among the investigated ferromagnesian mineral separates of both the Abu-Kharif and Deloro granitic rocks indicates that the alkali amphiboles are generally more enriched in Hf, Ba and Cs and depleted in Cr, Sc and Co. However, the amphiboles show the opposite relation.

11. Considering the lanthanides, the alkali amphiboles of the Abu-Kharif and Deloro granites possesses the highest REE contents with respect to the other ferromagnesian minerals.

12. The Deloro mafic minerals possesses high contents of heavy REE compared to those of the Abu-Kharif rocks.

13. In comparison, it is noted that the REE's are highly fractionated within the Abu-Kharif mineral separates while they are poorly fractionated within the Deloro ones.

14. It is significant that the Egyptian and the Canadian mineral phases investigated all have REE distributions very similar to the whole-rock distribution.

REFERENCES

REFERENCES

Abdel-Maksoud, M.A., Sabet, A.H., and Abdel-Rahman, A.M., Some observations on the geology and structures of Abu-Kharif area, and a new phase of granite. Chemie d Der Erde, accepted, 1979.

Abdel-Rahman, A.M., 1979: Geology of the area around Gabal Abu-Kharif, Eastern Desert, Egypt, with special emphasis on the granitic rocks. M.Sc. Thesis, Cairo University, Fac. Sc. 182pp.

Akaad, M.R. and El Ramly, M.F., 1960: Geological history and classification of the basement rocks of the Central Eastern Desert of Egypt. Geol. Surv. Egypt, Paper 9, 24.

Akaad, M.K., 1972: A contemplation and asessment of the 1960-1961 classification of the rocks of the Central Eastern Desert. Annals, Geol. Surv. Egypt, v. II, 19-45.

Amin, M.S., Sabet, A.H. and Mansour, A.O., 1953: Geology of Gabal Atud District. Geol. Survey Egypt, Cairo.

Barth, T.F.W., 1962: Theoretical petrology. Wiley, New York.

Bellieni, G., Peccerillo, A. and Poli, A., 1981: The Vedrette di Ries (Rieserferner) Plutonic Complex: Petrological and Geochemical Data Bearing on its Genesis. Contrib. Mineral. Petrol. 78, 145-156.

Berlin, R., and Henderson, C.M.B., 1969: The distribution of Sr and Ba between alkali feldspar, palgioclase and groundmass phases of porphyrites - Geochim. et Cosmochim. Acta, 33, 247-255.

Blackerby, B.A., 1968: Convolute zoning of plagioclase phenocrysts in Miocene volcanics from the western Santa Monica Mountains, California. Amer. Miner., 33-95.

Buma, G., Frey, F.A., and Wones, D.R., 1971: New England granites: Trace element evidence regarding their origin and differentiation. Contr. Mineral. Petrol. 31, 300-320.

Borley, G.D., 1963: Amphiboles from the younger granites of Nigeria. Part 1. Chemical classification. Mineral. Mag. 33, 260, 358-376.

Brock, P.W.G., Gellatly, D.C. and Knorring, O., 1964: A new sodic amphibole end-member. Mineral. Mag. 33, 267, 1057-1065.

Burri, C. and Niggli, P., 1945: Die jungen Eruptivgesteine des mediterranen. Orogens. I. Publ. Vulkaninstitut Immaneul Friedlaender No. 3.

Coryell, C.D., Chase, J.W., and Winchester, J.W., 1963: A procedure for geochemical interpretation of terres - trial rare earth abundance patterns. J. Geophys. Res., 68, 559-566.

Deer, W.A., Howie, R.A. and Zussman, J., 1967: Rock-forming minerals. Longman. London.

De Keyser, F., 1966: Arfvedsonite in granites of the Ingham District, North Queensland. Contr. Mineral. Petrol., 12, 315-324.

El-Etr, H. and Abdel-Rahman, M.A., 1973: Photogeology of the Esh Mellaha Range, Gulf of Suez District, Egypt. Proc. Egypt. Acad. Sci., v. 26, 37-44.

El Gaby, S., 1975: Petrochemistry and Geochemistry of some granites from Egypt. N. Jb. Miner. 124, H. 2, 147-189.

El-Ramely, M.F., 1972: A new geological map for the basement rocks in the Eastern and South-Western Desert of Egypt. Annals. Geol. Surv. Egypt, v. II, 1-18.

El-Shazly, E.M., 1964: On the classification of the Pre-Cambrian and other rocks of magmatic affiliation in Egypt. Inter. Geol. Congress, India, Sect. 10.

Engel, A.E.J., and Engel, C.G., 1960: Progressive metamorphism and granitization of the major paragneiss, Northwest Adirondack Mountains, New York, Part II, Mineralogy. Geol. Soc. Am. Bull. 71, 1-57.

Ernst, W.G., 1962: Synthesis, stability relations and occurrence of riebeckite and riebeckite-arfvedsonite solid solutions. J. Geol. 70, 689-736.

Ernst, W.G., 1968: Amphiboles. In: Engelhardt, W. von, Hahn, T., and Roy, R. (eds.). Mineral. rocks and inorganic materials. Springer-Verlag. Gottingen, Heidelberg, New York.

Fourcade, S. and Allegre, C.J., 1981: Trace elements behavior in granite genesis: A case study, the calc-alkaline plutonic association from the Querigut complex (Pyrenees, France). Contrib. Mineral. Petrol. 76, 177-195.

Fyson, W.K. and Frith, R.A., 1979: Regional deformations and emplacement of granitoid plutons in the Hackett

River, greenstone belt, Slave province, Northwest Territories. Can. J. Earth Sci., 16, 1187-1195.

Gast, P.W., 1968: Trace element fractionation and the origin of tholeiitic and alkaline magma types. Geochim. Cosmochim. Acta. 32, (10), 1056-1086.

Gindy, A.R., Khalil, S.O. and Arslan, A.I., 1979: Geochemistry of Hamadat granitoid pluton, Southwest of Qoseir, Red. Sea.Chem. Erde, 38, 40-58.

Goldschmidt, V.M., 1954: Geochemistry (edited by A. Muir). Oxford Univ. Press. London.

Hanson, G.N., 1978: The application of trace elements to the petrogenesis of igneous rocks of granitic composition. Earth Planet. Sci. Lett. 38, 26-43.

Hanson, G.N., 1980: Rare Earth Elements in petrogenetic studies of igneous system. Ann. Rev. Earth. Planet. Sci. 8, 371-406.

Haskin, L.A., Frey, F.A., Schmitt, R.A., Smith, R.H., 1966: Meteoritic solar and terrestrial rare-earth distributions. Physics and Chemistry of the Earth, 7, 169-321.

Heier, K.S., and Rogers, J.J.W., 1963: Radiometric determination of thorium, uranium and potassium in basalts and in two magmatic differentiation series. Geochim. Cosmochim. Acta 27, 137-154.

Heinrich, E.W., 1946: Studies in the mica group; the biotite-phlogopite series. Am. J. Sci. 244, 836-848.

Hume, W.F., 1935: Geology of Egypt. Survey of Egypt, Cairo, V. II, Part II.

Jacobson, R.R.E., Macleod, W.N., and Black, R., 1958: Ring complexes in the younger granite province of northern Nigeria. Geol. Soc. Lond. Mem. no. 1, 72pp.

Kabesh, M.L., Abdel-Khalek, M.L. and Heikal, M.A., 1977: The Chemistry of Biotites as a Guide to the Petrogenesis of El Ineigi Granitic Rocks, E.D., Egypt. Chem. Erde, 36, 139-148.

Kaufmann, H., 1963: Some monoclinic amphiboles and relations of their physical properties to chemical composition and crystal structure. Brigham Young Univ. Research Studies, Geol. Ser. 10, 121-158.

Khalil, S.O., Neef, T.A. and Brunfelt, A.O., 1978: Rare Earth Element distribution of the Holterkollen Plutonic complex, Oslo Area, Norway. Chem. Erde, Bd. 37, 125-142.

Kosterin, A.V., 1959: The possible modes of transport of the rare earths by hydrothermal solutions. Geochemistry 4, 381-387.

Kuehnbaum, R.M., 1973: Petrology of the Deloro pluton and associated country rocks, near Madoc, Ontario. M.Sc. thesis, University of Toronto, 173pp.

Leake, B.E., 1968: A catalog of analyzed calciferous and sub-calciferous amphiboles together with their nomenclature and associated minerals. Geol. Am. Spec. Paper, 98, 210pp.

Lumbers, S.B., 1967b: Geology and mineral deposits of the Bancroft Madoc area. In Guidebook, Geology of parts

of Eastern Ontario and Western Quebec, Ann. Mtg. Geol. Assoc. Canada and Min. Assoc. Canada, Kingston, 1967, 13-29.

Lyons, P.C., 1976: The chemistry of riebeckites of Massachusetts and Rhode Island. Mineral. Mag. 40, 473-479.

Martin, R.F., and Bonin, B.,1976: Water and Magma Genesis: The association hypersolvus granite-subsolvus granite. Can. Min., v. 14, 228-237.

Mineyev, D.A., 1963: Geochemical differentiation of the rare earths. Geochemistry 12, 1129-1149.

Miyashiro, A., 1957: The chemistry, optics, and genesis of the alkali-amphiboles. J. Fac. Sci. Univ. Tokyo. Sec. II.11, 57-83.

Morcos, B.M., 1977: Photo-geological studies on the Precambrian rocks of the Central Eastern Desert of Egypt. Ph.D. Thesis, Cairo University, Fac. Sc., 269pp.

Nockolds, S.R., 1947: The relation between chemical composition and paragenesis in the biotite mica of igneous rocks. Am. J. Sci. 245, 401-420.

Nockolds, S.R. and Allen, R., 1953: The geochemistry of some igneous rock series: Part I. - Geochim. et Cosmochim. Acta, 4, 105-142.

Nockolds, S.R., 1954: Average chemical composition of some igneous rocks. Geol. Soc. Am. Bull., 65, 1007-1032.

Niggli, P., 1939; Tabellen Zur petrographic und zum gesteinsbestimmen. Mineralog. Petrogrph. Inst. E. T.H. Zurich (in Streckeisen, 1967).

Phillips, R., 1963: The recalculation of amphibole analyses. Mineral. Mag. 33, 263, 701-711.

Ramberg, H., 1962: Intergranular precipitation of albite formed by unmixing of alkali feldspar. Neues. Jahrb. Mineral., Abhandle., 98, 14-34.

Rankama, K. and Sahama, Th. G., 1952: Geochemistry. The University of Chicago Press, 912p.

Refaat, A.M. and Kabesh, M.L., 1980: The Chemistry of Arfvedsonites and Riebeckites from Sabir Alkali Granites, Taiz Area, Yemen Arab Republic, Chem. Erde, 39, 37-45.

Rittmann, A., 1957: On the serial characters of igneous rocks. Egypt. J. Geol., 1, 1, 23-48.

Rucklidge, J.C., 1976: Electron Microprobe Instrumentation. Can. Min., v. 1, 1-44.

Sabet, A.H., 1961: Geology and mineral deposits of Gabal El-Sibai area, Red Sea hills, Egypt, U.A.R., Ph.D. Thesis, Leiden State University, The Netherlands.

Sabet, A.H., 1972: On the stratigraphy of the basement rocks of Egypt. Annals Geol. Surv. Egypt., v. II, 79-101.

Sabet, A.H., Bessonenko, V.V. and Bykov, B.A., 1976: The intrusive complexes of the Central Eastern Desert of Egypt. Annals, Geol. Surv. Egypt., v. VI, 53-73.

Saha, A.K., 1957: Mode of emplacement of some granitic rocks in southeast Ontario. Ph.D. Thesis, University of Toronto, 212pp.

Sayyah, T.A., Hashad, A.H. and Ibrahim, A.M., 1973: Contribution to the geochemistry of some pink granites, Central Eastern Desert. Egypt. J. Geol., 17, 57-69.

Schürmann, H.M.E., 1966: The Pre-Cambrian along the Gulf of Suez and the northern part of the Red Sea. E.J. Brill, Leiden.

Schwerdtner, W.M., Stone, D., Osadetz, K., Morgan, J. and Stott, G.M., 1979: Granitoid complexes and the Archean tectonic record in the southern part of northwestern Ontario. Can. J. Earth Sci. 16, 1965-1977.

Strong, D.F., and Dupuy, C., 1982: Rare earth elements in the bimodal Mount Peyton batholith: Evidence of crustal anatexis by mantle-derived magma. Can. J. Earth Sci. v. 19, 308-315.

Tauson, L.V., 1967: Geochemical behavior of rare elements during crystallization and differentation of granitic magmas. Geochem. Int. 4, 1067-1075.

Thompson, R.N., 1976: Alkali amphiboles in the Eocene high-level granites of Sky, Scotland. Mineral. Mag. 40, 891-893.

Thornton, C.P., and Tuttle, O.F., 1960: Chemistry of igneous rocks, 1, Differentiation Index. Am. J. Sci., 258, 9, 664-684.

Tindle, A.G., and Pearce, J.A., 1981: Petrogenetic modelling of in situ fractional crystallization in the zoned Loch Doon Pluton, Scotland. Contrib. Mineral. Petrol. 78, 196-207.

Toulmin, P., III, 1960: Composition of feldspars and crystallization history of the granite-syenite complex near Salem, Essex County, Massachusetts, U.S.A., 21st Int. Geol. Cong., Copenhagen, Pt. 13, 275-286.

Towell, D.G., Winchester, J.W. and Spirn, R.V., 1965: Rare earth distribution in some rocks and associated minerals of the batholith of southern California. J. Geophys. Res. 70, 3485-3496.

Tuttle, O.F. and Bowen, N.L., 1958: Origin of granite in the light of experimental studies in the system $NaAlSi_3O_8$ - $KAlSi_3O_8$ - SiO_2 - H_2O. Geol. Soc. Am., Mem. 74.

Tuttle, O.F., 1952: Origin of the contrasting mineralogy of extrusive and plutonic salic rocks. J. Geol., 60, 107-124.

Vlasov, K.A., Ed., 1966: Geochemistry and mineralogy of rare elements and genetic types of their deposits, v. 1, translated from Russian by Israel program for scientific translations. Jerusalem.

Wilson, M.E., 1940: Marmora map sheet 560A, Geol. Surv. Canada.

Zalata, A.A., 1972: Geology of the basement rocks in the northern part of El Shayib and Safaga sheets, Eastern Desert. Ph.D. Thesis, Assiut University. Fac. Sc., 240.

Zielinski, R.A. and Frey, F.A., 1970: Gough Island: Evaluation of a fractional crystallization model. Contr. Mineral. and Petrol. 29, 242-254.

Zussman, J., 1967: Physical Methods in Determinative mineralogy.